

~~CONFIDENTIAL~~

Cleared: December 12th, 1986

Clearing Authority: Air Force Wright Aeronautical Laboratories

(Unclassified)

PRELIMINARY DESIGN AND EXPERIMENTAL INVESTIGATION
OF THE FDL-5A UNMANNED HIGH L/D SPACECRAFT

Part I Summary

J. T. Lloyd

*** Export controls have been removed ***

DOWNGRADED AT 3 YEAR INTERVALS;
DECLASSIFIED AFTER 12 YEARS.
DOD DIR 5200.10

This document is subject to special export controls and each transmittal to foreign governments or foreign nationals may be made only with prior approval of the Air Force Flight Dynamics Laboratory, Wright-Patterson Air Force Base, Ohio 45433.

THIS DOCUMENT CONTAINS INFORMATION AFFECTING THE NATIONAL DEFENSE OF THE UNITED STATES WITHIN THE MEANING OF THE ESPIONAGE LAWS, TITLE 18 U.S.C., SECTIONS 793 AND 794, THE TRANSMISSION OR REVELATION OF WHICH IN ANY MANNER TO AN UNAUTHORIZED PERSON IS PROHIBITED BY LAW

~~CONFIDENTIAL~~

Approved for Public Release

Contracts
UNCLASSIFIED

(U) FOREWORD

(U) This is the final report of work performed under Contract No. AF33(615)-5241, "Preliminary Design of Two Volumetrically Efficient High L/D Unmanned Flight Test Vehicles". This report was prepared under Project 1366, "Aerodynamics and Flight Mechanics", Task 136616, "Synthesis of Hypersonic Vehicles".

(U) The work was sponsored by the Aerospace Vehicle Branch, Flight Mechanics Division Air Force Flight Dynamics Laboratory. The research investigation was performed under the direction of the Air Force Project Engineer Mr. Thomas R. Sieron. Mr. C. J. Cosenza and Mr. A. C. Draper of AFFDL provided overall technical guidance.

(U) The work was accomplished by the Lockheed-California Company, Burbank, California and the report is also identified as LR 21204.

(U) This is Part I of a five part report:

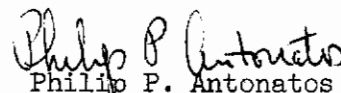
Part I	Summary
Part II	Parametric Configuration Development and Evolution
Part III	Aerodynamics
Part IV	Aerothermodynamics
Part V	Vehicle Design

(U) This manuscript was released by the authors for publication in January 1968.

(U) Mr. J. T. Lloyd of the Spacecraft and Hypersonics Division was the project engineer for the Lockheed-California Company. Special appreciation is given to Mr. G. L. Alexander for his valuable guidance and consultation in the conduct of this program.

(U) The assistance of Flight Dynamics Laboratory personnel including Messrs M. L. Buck, R. D. Neumann, V. Dahlem, P. Lane, and W. H. Goesch contributed significantly to the accomplishments of this program.

(U) This technical report has been reviewed and is approved.


Philip P. Antonatos
Chief, Flight Mechanics Division
Air Force Flight Dynamics Laboratory

UNCLASSIFIED

Approved for Public Release

(U) ABSTRACT

(U) Conceptual design and experimental wind tunnel testing of unmanned entry research vehicles having high hypersonic lift/drag ratio and high volume are described. Analytic parametric data are presented for two lifting body classes designated HLD-35 and FDL-5. The FDL-5 is a unique configuration which is aerodynamically stabilized without outboard fins. Experimental aerodynamic and heat transfer data from the Arnold Engineering Development Center Wind Tunnels A, B, C, and F are compared with analytic data for the FDL-5. Candidate structure and subsystems are selected for performing unmanned hypersonic research with the vehicle.

This report is subject to special export controls and each transmittal to foreign governments or foreign nationals may be made only with prior approval of the Air Force Flight Dynamics Laboratory (FDMS), Wright-Patterson Air Force Base, Ohio 45433.

Contrails

TABLE OF CONTENTS

<u>Section</u>		<u>Page</u>
1	INTRODUCTION	1
2	PARAMETRIC CONFIGURATION DEVELOPMENT AND EVALUATION	3
	2.1 AERODYNAMIC PARAMETRIC ANALYSES	3
	2.2 AEROTHERMODYNAMIC PARAMETRIC ANALYSES	9
	2.3 DESIGN CONSIDERATIONS	9
	2.4 GEOMETRY SELECTION	16
	2.5 CONFIGURATION EVOLUTION	16
3	TEST PROGRAM	31
4	FDL-5 AERODYNAMIC PERFORMANCE SUMMARY	38
5	FDL-5 HEAT TRANSFER SUMMARY	54
6	FDL-5 DESIGN	65
	6.1 STRUCTURES	65
	6.2 SYSTEMS	66
	6.3 WEIGHT	68
7	CONCLUSIONS	84
	7.1 AERODYNAMICS	85
	7.2 AEROTHERMODYNAMICS	85
	7.3 STRUCTURES	86
	7.4 WEIGHT	86
	REFERENCES	87

LIST OF ILLUSTRATIONS

<u>Figure</u>		<u>Page</u>
1	Evolution of High L/D Vehicle Concepts	4
2	F-5 General Arrangement	5
3	Basic Geometry	7
4	Variation of L/D_{\max} with Volume	10
5	Nose Radius Trade	12
6	Effect of Body Side Angle and Yaw Angle on Side Panel Surface Temperatures	13
7	Alternate Recovery Techniques	15
8	Landing Weight Penalty	18
9	HLD-35-1 General Arrangement	21
10	HLD-35-2 General Arrangement	23
11	HLD-35-3 General Arrangement	25
12	General Arrangement - High L/D Lifting Body - 35 ft	27
13	FDL-5 General Arrangement	29
14	20-Inch Steel Force Model for Tunnels A, B, C	33
15	15-Inch Fiber Glass Force Model for Tunnel F	34
16	20-Inch Aluminum Pressure/Heat Transfer Model for Tunnel F (Pressure Plugs Installed)	35
17	20-Inch Steel Pressure Model for Tunnels A and C	36
18	20-Inch Thin Skin Heat Transfer Model for Tunnel C	37
19	FDL-5 Variation of Maximum L/D with \bar{V}^*	40
20	FDL-5 Variation of Maximum L/D	41
21	Comparison of Estimated and Experimental Coefficients - Axial Force Coefficient Variation with Angle of Attack (M = 18.98)	42
22	Comparison of Estimated and Experimental Coefficients - Normal Force Coefficient Variation with Angle of Attack (M = 18.98)	43

LIST OF ILLUSTRATIONS (Continued)

<u>Figure</u>		<u>Page</u>
23	Elevon Effects - Lift/Drag Ratio Variation with Angle of Attack (M = 19.00)	44
24	Comparison of Estimated and Experimental Coefficients - Pitching Moment Coefficient Variation with Angle of Attack (M = 18.98)	45
25	FDL-5 Longitudinal Stability (M = 18.9)	46
26	FDL-5 Flap Effect on Longitudinal Stability at Various Mach Numbers	47
27	Comparison of Estimated and Experimental Coefficients - Yawing Moment Coefficient Variation with Angle of Yaw (M = 19.21)	48
28	Comparison of Estimated and Experimental Coefficients - Rolling Moment Coefficient Variation with Angle of Yaw (M = 19.21)	49
29	FDL-5 Yawing Moment Coefficient Slope Variation with Mach Number	50
30	FDL-5 Rolling Moment Coefficient Slope Variation with Mach Number	51
31	Variation of a Lower Surface Centerline Pressure Coefficient with Mach Number (X/L = .30)	52
32	Variation of a Lower Surface Centerline Pressure Coefficient with Mach Number (X/L = .96)	53
33	Reference Trajectory	56
34	Temperature Histories at Various Vehicle Locations	57
35	Peak Lower Surface Centerline Temperatures	58
36	Effect of Transition Criterion on Peak Lower Surface Centerline Temperatures	59
37	Effect of Wing Loading on Peak Temperatures	60
38	Correlation of Tunnel F Forward Ramp Centerline Heating Data	61
39	Comparison of Predicted and Revised Design Point Radiation Equilibrium Temperature - at 50 and 96 Percent Chord	62
40	Upper Surface Isotherms	63
41	Lower Surface Isotherms	64

LIST OF ILLUSTRATIONS (Concluded)

<u>Figure</u>		<u>Page</u>
42	Study Vehicle (F-5) Structural Arrangement for Design Concept Evaluation	69
43	Design Pressures Flight Test Vehicle	71
44	Comparison of Maximum Flight Structural Load Capabilities	72
45	Thickness Requirements for Lower Surface Panels (L = 25.0 Inches)	74
46	Upper Surface Weight Comparison - Structure and Thermal Protection System for Various Thermo-Structural concepts	75
47	Lower Surface Weight Comparison - Structure and Thermal Protection System for Various Thermo-Structural Concepts	76
48	MV-37 Flight Test Vehicle Structural Arrangement	77
49	BE-1 Systems General Arrangement	79

LIST OF TABLES

<u>Table</u>		<u>Page</u>
1	Aerodynamic Trades	8
2	Aerothermodynamic Sensitivity Summary	11
3	Alternate Landing Systems	15
4	Geometry Trades	19
5	Stability Trades	20
6	Test Summary	32
7	Model Summary	31
8	Minimum Gage for Metallic Materials	73
9	Weight Statement	81
10	Equipment Breakdown	82

SECTION 1

(U) INTRODUCTION

(U) This preliminary design study of two volumetrically efficient high L/D unmanned flight test vehicles is a part of the continuing USAF Flight Dynamics Laboratory program to conduct basic research on hypersonic maneuvering vehicle systems. Use of atmospheric maneuvering has been found to provide operational flexibility and versatility for performing a large variety of potential USAF missions. Technologies for high-performance entry systems have been gradually developing over the past six years. The study reported herein is concerned with unmanned free-flight research vehicles which would be used (1) to obtain broad free-flight hypersonic technology data in aerodynamics, thermodynamics, structures, and propulsion, (2) to demonstrate the maneuver potential of advanced entry vehicle concepts operating in the large-scale entry environment, (3) to demonstrate operational utility of such vehicles, and (4) to demonstrate reusable structure concepts and the adaptability of the airframe to man.

(U) This contract followed an earlier study entitled "Preliminary Design of Hypersonic High L/D Test Vehicles" (Ref. 1). In the earlier study, six high L/D entry vehicles were analyzed to establish the size, weight, and system requirements for conducting free flight research on high performance entry systems from orbital speed to landing.

(U) The present study was focused on improving the hypersonic geometry and properties of a high L/D research vehicle. Specifically, the objectives were to configure an unmanned entry research vehicle having a hypersonic L/D of 3.0 at 20,000 fps and 200,000 feet altitude; and to confirm vehicle aerodynamic and heat transfer performance through wind tunnel test. In addition to this requirement, the vehicle was to be designed for maximum volume with the relationship between volume and L/D to be identified. Horizontal landing was the primary recovery mode, but alternate recovery concepts were to be investigated. A structure concept and the vehicle subsystems were to be selected based on earlier work and the experience gained in other USAF programs including ASSET, ASCEP, and PRIME.

(U) The contract effort was divided into two phases: the first consisted of the development of the parameters affecting the selection of candidate configurations; the second included supersonic and hypersonic wind tunnel testing of one candidate configuration and selection of the structure and subsystems.

(U) In a parametric study, over 200 relationships among configuration geometry, volume, aerodynamic heating, and aerodynamic performance and stability were evolved. These data trends were based on hypersonic theories, results of ASSET flight data, and results of USAF AFFDL and Lockheed in-house wind tunnel tests of high performance lifting bodies. The sources for each of these data are documented in this final report. The purpose in developing these parameters was to provide the rationale for selecting the test geometry for the test and design phase.

(U) Two classes of configurations emerged from the configuration studies: (1) a dual finned geometry designated the HDL-35 series, and (2) a unique high volume geometry designated as the FDL-5 series.

(U) The FDL-5 was selected for wind tunnel testing and structure design in the test and design phase. Its size was varied during the study from 30 to 35 ft in length.

(U) The principal conclusions and results derived from the two study phases are:

1. (U) A new class of lifting entry vehicle designs (FDL-5 series) was defined and tested.
2. (U) The FDL-5 configuration has demonstrated through wind tunnel test that it is stable and controllable from supersonic to hypersonic speeds. Freedom exists to tailor the base geometry and control surfaces for subsonic and transonic control and performance. Variable geometry may be considered to improve landing performance.
3. (U) Heat transfer wind tunnel test data revealed no unusual or unpredictable heating phenomena.
4. (U) An insulated and cooled structure concept was selected for the vehicle design. The primary structure is made of aluminum and the heat shields are made of coated columbium on the lower surface and Inconel on the upper surface. Leading edges are made of coated tantalum.
5. (U) Candidate subsystems for conducting a three quarter orbit mission were selected.
6. (U) Launch weight of the 35-foot-long unmanned research vehicle is estimated to be 7700 pounds.

SECTION 2

(U) PARAMETRIC CONFIGURATION DEVELOPMENT AND EVALUATION

(U) Figure 1 depicts the status of high L/D configuration development at the initiation of this contract. The configurations designated by AF prefixes were conceptual designs developed by the USAF Flight Dynamics Laboratory and were provided as the starting point for an earlier study contract (Reference 1).

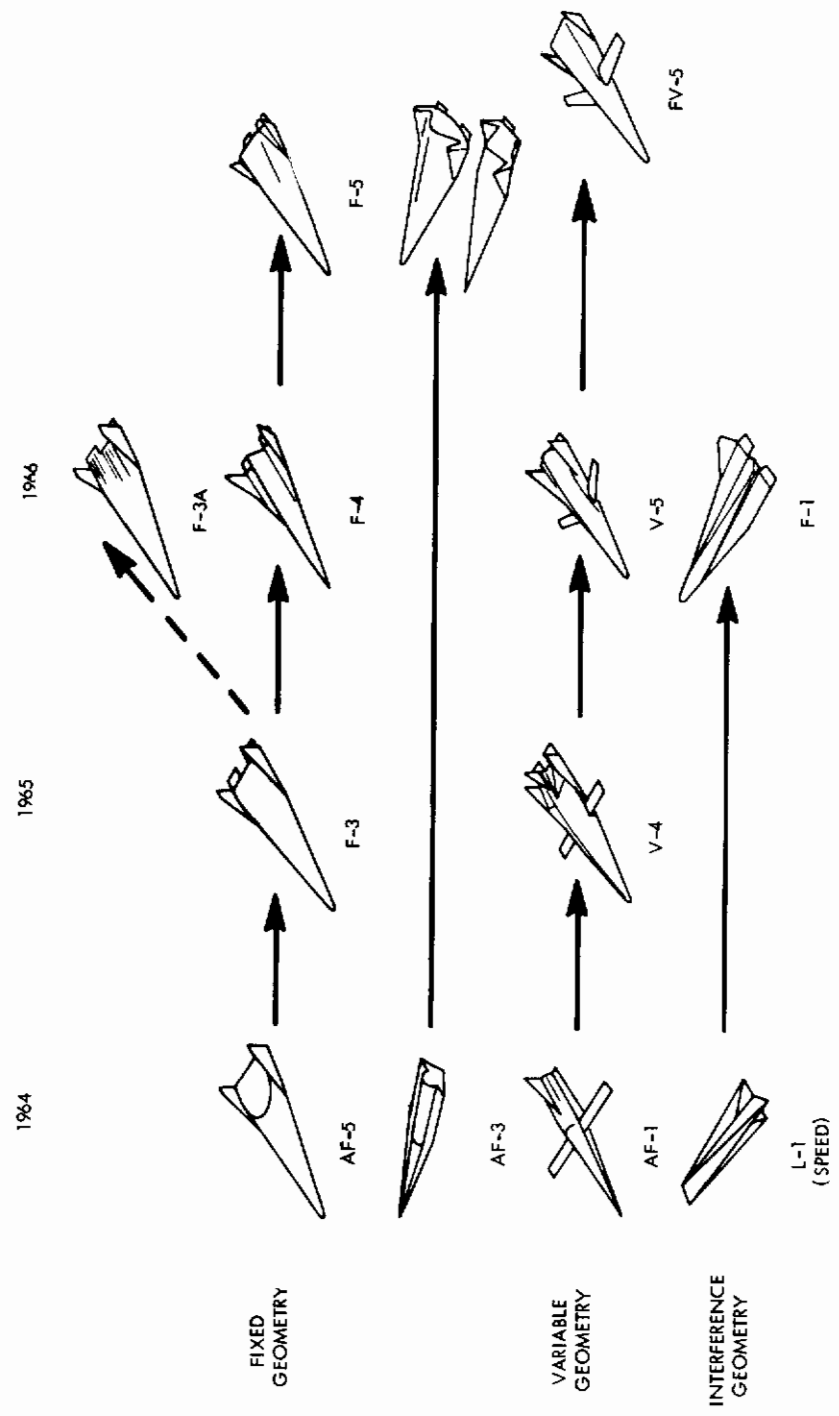
(U) Figure 2 shows the general arrangement of the F-5 configuration which served as the starting point and basic model about which the parametric configuration and structure trades were performed. The F-5 was chosen for this purpose, since it was in a more advanced state of definition than the other configurations.

(U) The first phase of this contract was concerned with development of the configuration geometry rationale. The interactions among geometry, aerodynamic performance, volume, stability and heating were achieved through an extensive series of parametric trades. Figure 3 illustrates the basic geometry elements that were systematically varied to accomplish the parametric trades.

(U) The following sections summarize the parametric trades that were conducted. The more significant trades are illustrated.

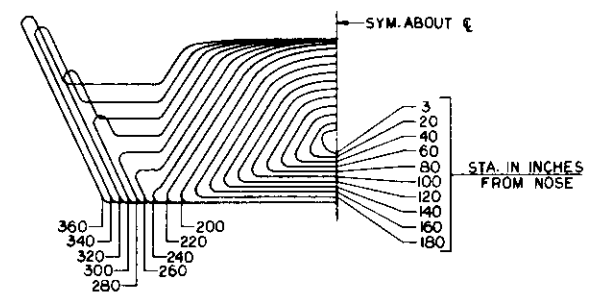
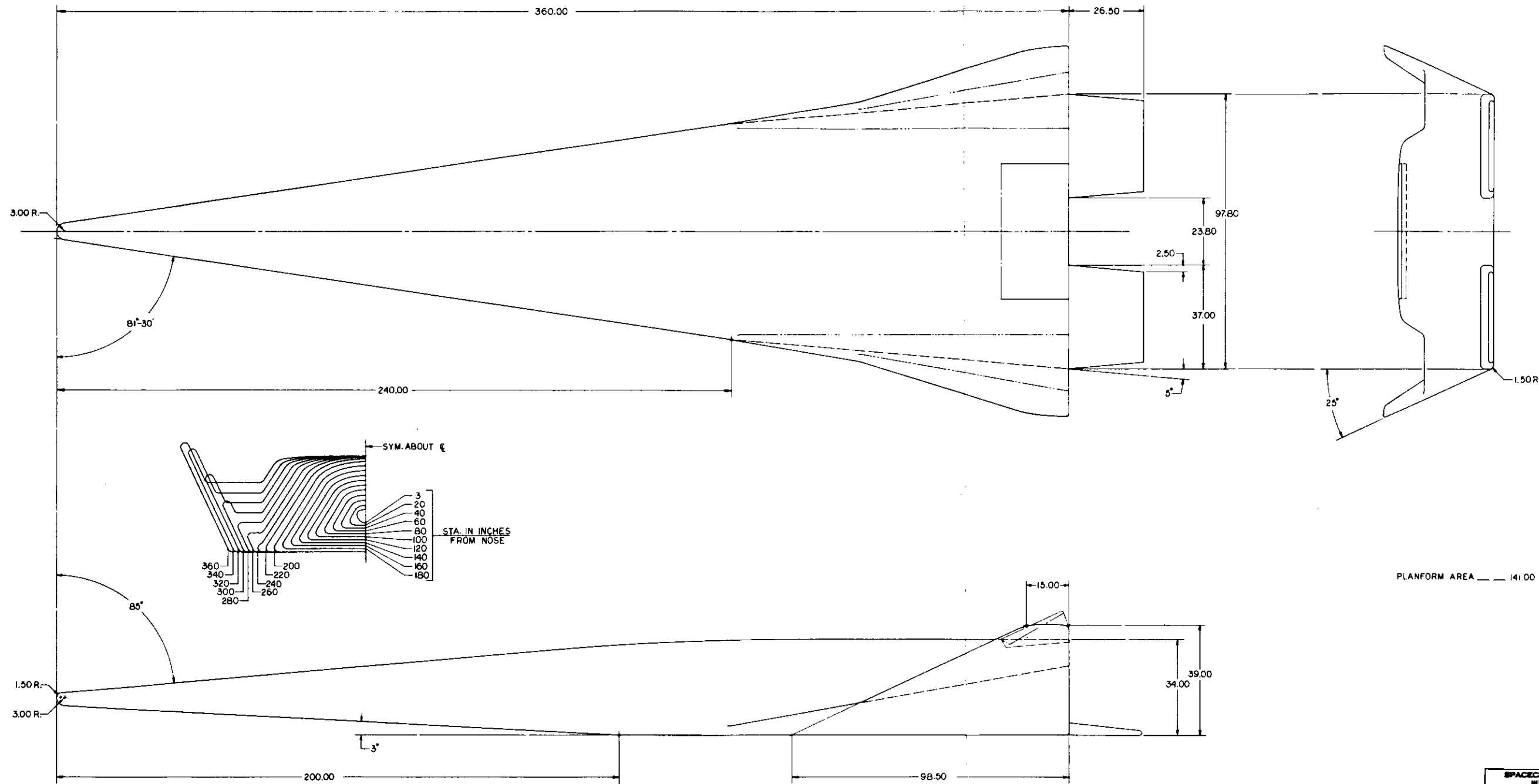
2.1 (U) AERODYNAMIC PARAMETRIC ANALYSES

(U) The scope of the aerodynamic trades which were developed for high L/D shapes is illustrated in Table 1. Variations in the geometry of each element of the vehicle have been analyzed, and the effects on the performance, stability and volume parameters shown across the top of the table have been determined. The designations within the table show the slopes of the trade about the nominal parameter values for a 30-foot F-5 vehicle, or they indicate the nature of the trade as coded by the table notes. For example, an increase of one degree in the body leading-edge sweep angle increases the hypersonic L/D_{max} by +0.007, and decreases vehicle volume by 19.7 cubic feet; effects on stability are negligible. Since most of the trades are nonlinear, the parametric trade slopes or derivatives in Table 1 are representative only at or near the F-5 parametric values. Large deviations from the F-5 values require consideration of the complete parametric trade.

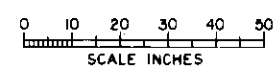


UNCLASSIFIED

FIGURE 1 (U) EVOLUTION OF HIGH L/D VEHICLE CONCEPTS



PLANFORM AREA 141.00 SQ. FT.

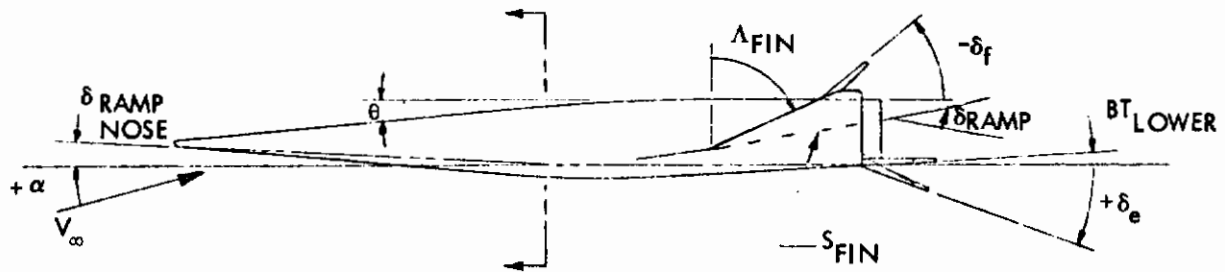
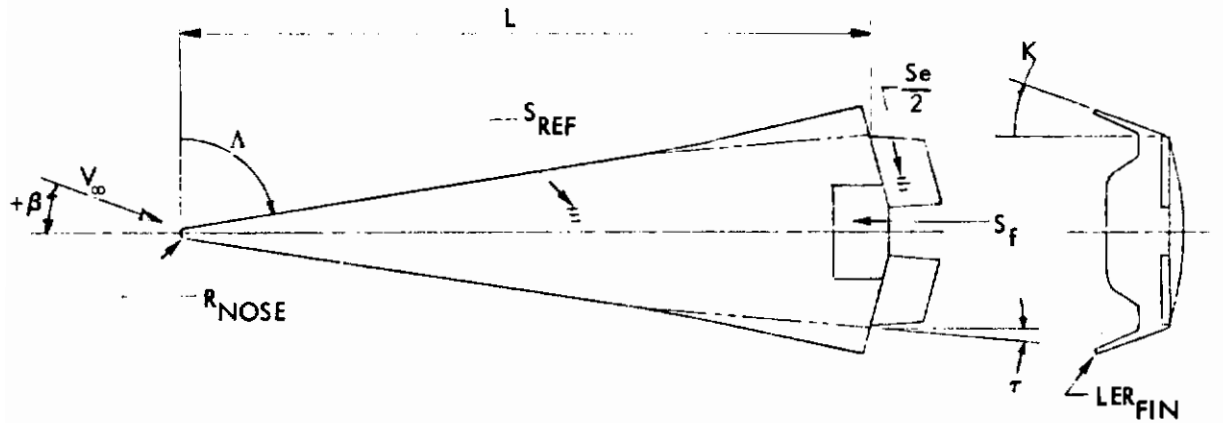


SPACECRAFT ENGINEERING	
NEW DESIGN DIVISION	
GENERAL ARRANGEMENT	
MAXIMUM VOLUME	
DATE	NO.
19-21-62	CL 639-1
SCALE	1/10
DATE	NO.
19-21-62	CL 639-1-74
LOCKHEED-CALIFORNIA COMPANY	
A DIVISION OF LOCKHEED CORP.	
BURBANK, CALIFORNIA	

UNCLASSIFIED

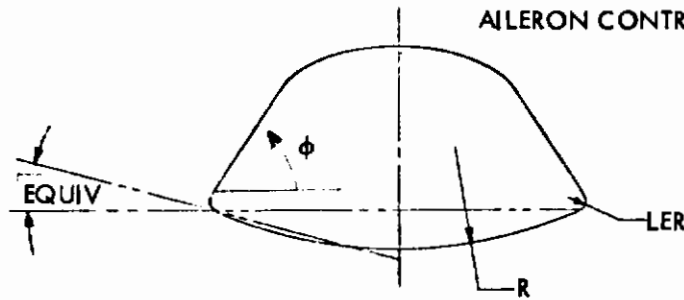
F-5

FIGURE 2 (U) F-5 GENERAL ARRANGEMENT



PITCH CONTROL: $\delta_p = \delta_{el} + \delta_{er}$

AILERON CONTROL: $\delta_A = \delta_{el} - \delta_{er}$



UNCLASSIFIED

FIGURE 3 (U) BASIC GEOMETRY

TABLE 1

(C) AERODYNAMIC TRADES

	L/D		C _m			C _{η_p}			C _{l_p}			VOL Ft ³
	Sub	Super	Sub	Super	Hyp	Sub	Super	Hyp	Sub	Super	Hyp	
FLNS:												
Tce-In, τ (Deg.)	+0.02	-0.018	*	*	*	-0.00006	+0.00019	+0.00019	-0.00016	-0.0001	-0.0001	2.64
Holl-out, K (Deg.)	+0.42	0	*	*	*	-0.00006	+0.00002	+0.00002	-0.00006	-0.00002	-0.00002	.333
Camber, (% chord)	+11	A	*	A	A	-0.00031	A	A	+0.00006	A	A	A
Area, S (% Planform)	C	C	*	*	*	+0.0006	C	D	-0.0008	C	D	A
LE Sweepback, A _{Fin} (Deg.)	A	C	A	A	*	A	A	A	A	A	A	A
LE Radius, LER _{Fin} (In.)	A	C	A	A	*	A	A	A	A	A	A	A
S _E Fin Area, S _E (% Planform)	A	A	A	A	A	+0.059	+0.004	+0.002	-0.043	-0.002	-0.001	A
UPPER BODY:												
Length, L (Feet)	A	C	B	B	B	B	B	B	B	B	B	25.38
LE Sweepback, A _{Body} (Deg.)	A	C	A	A	A	A	A	A	A	A	A	-19.7
Side Roll-over, θ (Deg.)	A	C	A	*	*	A	C	*	A	C	+0.00001	2.87
LE Radius, LER _{Body} (In.)	A	C	A	A	A	A	A	A	A	A	A	A
Trochle Angle, θ (Deg.)	C	C	A	*	*	A	O	O	A	O	O	17.15
Base Area, S _{Base} (% Planform)	-17	A	B	B	B	B	B	B	B	B	B	6.93
Flag Area, S _F (% Planform)	-19	-0.02	*	*	*	B	B	B	B	B	B	B
Flap Deflection, δ _F (Deg.)	-0.35	-0.06	*	*	*	B	B	B	B	B	B	B
Flevon Area, S _E (% Planform)	-0.36	C	X	C	*	B	B	B	B	B	B	B
Elevon Deflection, δ _E (Deg.)	+0.41	C	*	*	*	B	B	B	B	B	B	B
Fin Hems, δ _g (Deg.)	A	-0.45	D	*	*	A	A	A	A	A	A	2.11
Afterons, δ _A (Deg.)	B	B	B	B	B	B	B	B	*	*	*	B
Nose Cap Radius, R (In.)	A	-0.36	A	A	A	A	A	A	A	A	A	A
LOWER SURFACE:												
Nose Ramp Area, S _R (% Planform)	A	C	A	*	*	A	A	A	A	A	A	A
Nose Ramp Angle, δ _R (Deg.)	A	C	A	X	*	A	C	+0.00007	A	C	-0.00006	A
Dihedral Bottom, Γ (Deg.)	-0.16	C	A	*	*	A	C	-0.00036	A	C	-0.00003	3.33
Curved Bottom, Γ _{Vol.} Equiv. (Deg.)	-0.016	C	A	*	*	A	C	-0.00024	A	C	-0.00026	3.33
Boat Tail	-0.016	C	*	*	*	D	A	A	A	A	A	*

(*) Complex Trade
CONFIDENTIAL

NOTE
A. Not Applicable
B. Not Applicable
C. Hypersonic and Supersonic Trends Similar
D. Not Determined

(U) Figure 4 shows the impact of equivalent lower surface dihedral angle, Γ , side rollout angle, ϕ , body sweep angle, Λ , and vehicle length on hypersonic L/D_{\max} and volume. It is noted that all of these geometric parameters (excepting length) produce a loss in L/D with an increase in volume. Furthermore, for a fixed vehicle length, volume can be obtained with least penalty to L/D_{\max} by decreasing sweep angle. Increasing the side rollout angle is seen to be the least desirable approach to increasing volume. Variations in these parameters are ultimately limited by aerodynamic heating and stability considerations.

(U) Volume and L/D_{\max} are also shown in Figure 4 for the earlier F and V series configurations. The trend of reduced L/D_{\max} with increased volume is consistent with the observations made from the parametric analyses.

(U) A separate series of parametric trades was performed on various arrangements of finned and finless aft body geometry elements. These trades, which led to the evolution of the "compression-sharing" concept and the FDL-5 geometry, are described in Part II.

2.2 (U) AEROTHERMODYNAMIC PARAMETRIC ANALYSES

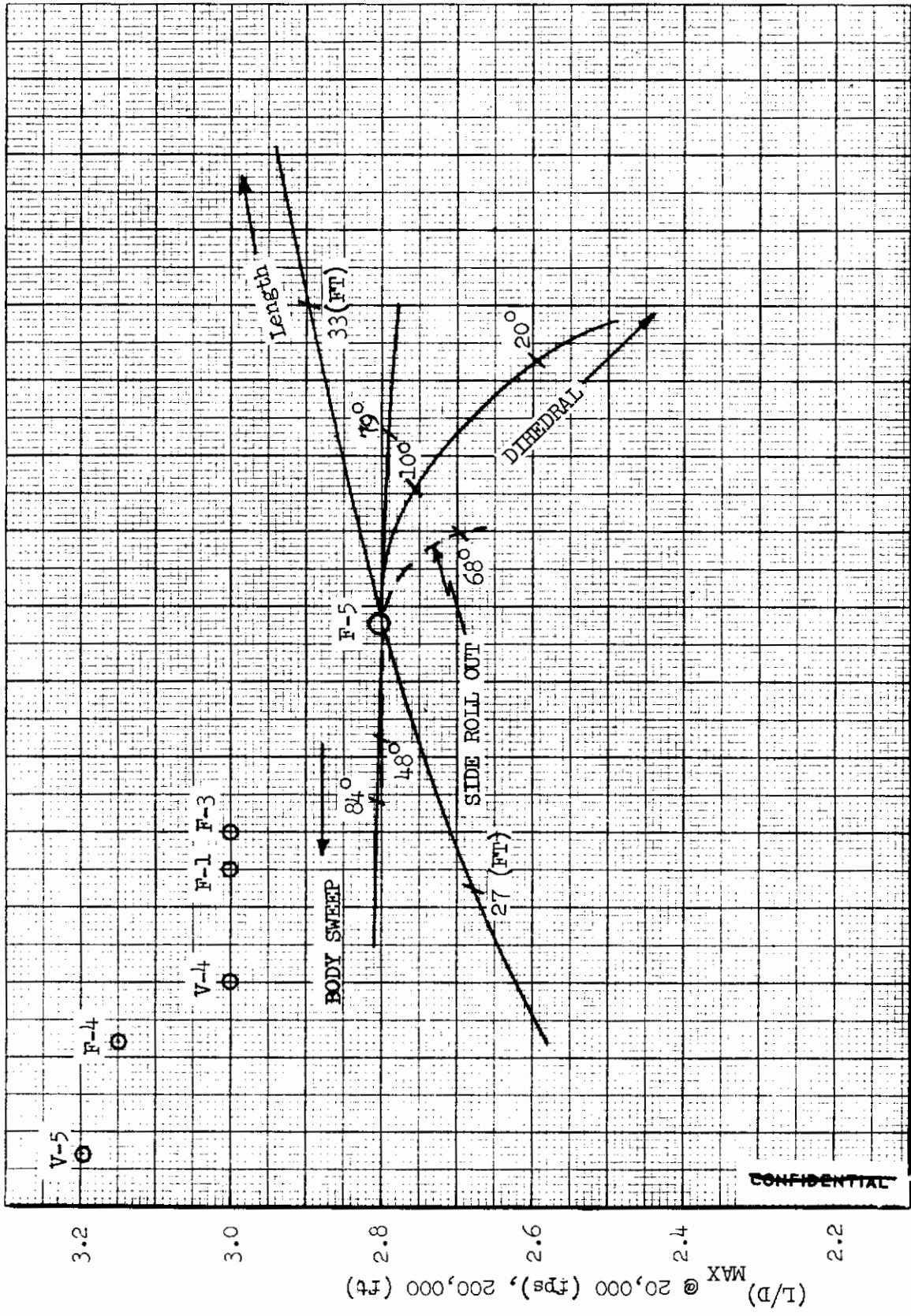
(U) The heat transfer parameter trades that were conducted during the study are indexed in Table 2. As in the aerodynamic analyses, variations of the F-5 geometry parameters were analyzed. The effect on the surface temperature of the various configuration elements were then determined. In addition to the basic geometry parameters, two attitude parameters, α and β were investigated. Two of the more significant heat transfer trades are illustrated in Figures 5 and 6.

(U) Figure 5 combines the aerodynamic and heat transfer trades at the stagnation point to illustrate the change in hypersonic L/D with stagnation temperature for various nose radii. The selection of an equivalent nose radius of three inches is based on a maximum temperature of 4500°F and a low penalty in hypersonic L/D . Table 2 indicates the rate of change of nose stagnation temperature with change in nose radius to be -200°F per inch increase in radius.

(U) Figure 6 shows that increasing the body side rollout angle, ϕ , results in a significant increase in upper surface temperatures. Furthermore, the effects of yaw are such that, for a fixed temperature limit, body side angle must be reduced by 2-1/2 degrees for every degree of yaw that will be tolerated during peak heating.

2.3 (U) DESIGN CONSIDERATIONS

(U) The alternate recovery modes shown in Figure 7 were considered during the study to estimate their effects on weight and vehicle geometry. Recovery weight (in fraction of unassisted landing weight) determined for each of the alternates is tabulated in Table 3. All the modes considered can be



Volume (ft³)

FIGURE 4 (U) VARIATION OF L/D_{MAX} WITH VOLUME

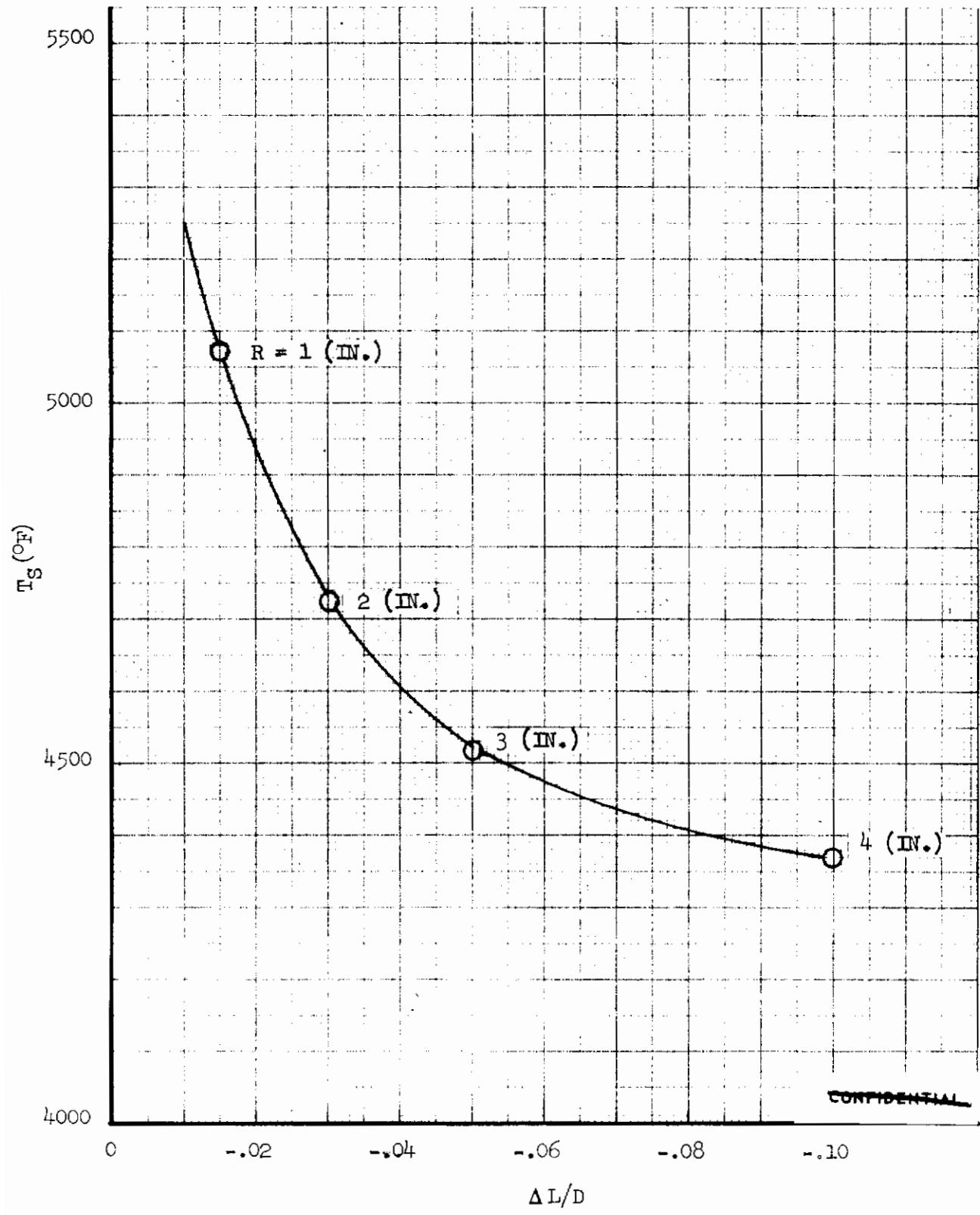
CONFIDENTIAL

TABLE 2
(U) AEROTHERMODYNAMIC SENSITIVITY SUMMARY

Parameter	F-5 Design Value	Predicted F-5 Temperatures (°F)						Nose Stagnation Point 4300	
		Fin Stagnation Line 3230	Fin Outboard Panel (X=3 ft) 1830	Wing Stagnation Line 2870	Body Upper Surface 1300(a) 780(b) 1400(c)	Lower Surface Centerline (X=10 ft) 1780	Elevons 2200		
		$\Delta T/\Delta$ Parameter (°F/degree or °F/in.)							
Toe-in Angle	5 deg	25	41						
Roll-out	25 deg	80	5						
Leading-edge Sweepback Angle	63 deg	-35	0						
Leading-edge Radius	1.5 in.	-300	0	-37	0	0			
Leading-edge Sweepback Angle	81.5 deg								
Leading-edge Radius	1.5 in.								
Body Side Angle	57 deg				38(a)				
Profile Angle	6 deg				0				
Fin Ramp Angle	10 deg				100(c)				
Elevon Deflection Angle	5 deg								
Nose Radius	1.5 in.								-200
Forward Ramp Angle	3 deg			55				50	
Lower Surface Curvature								0	
Dihedral Angle								0	
Boattail Angle	0 deg							0	
Angle of Attack	10 deg	-32	22	52	38(a)			42(e)	
Yaw Angle	0	40	35	40	170(a)			30	

(a) Side Panel, X = 1 ft
 (b) Upper Forebody Centerline, X = 5 ft
 (c) Fin Ramp, X = 1 ft
 (d) Assuming Separated Flow
 (e) Laminar Flow

UNCLASSIFIED



~~CONFIDENTIAL~~

FIGURE 5 (U) NOSE RADIUS TRADE

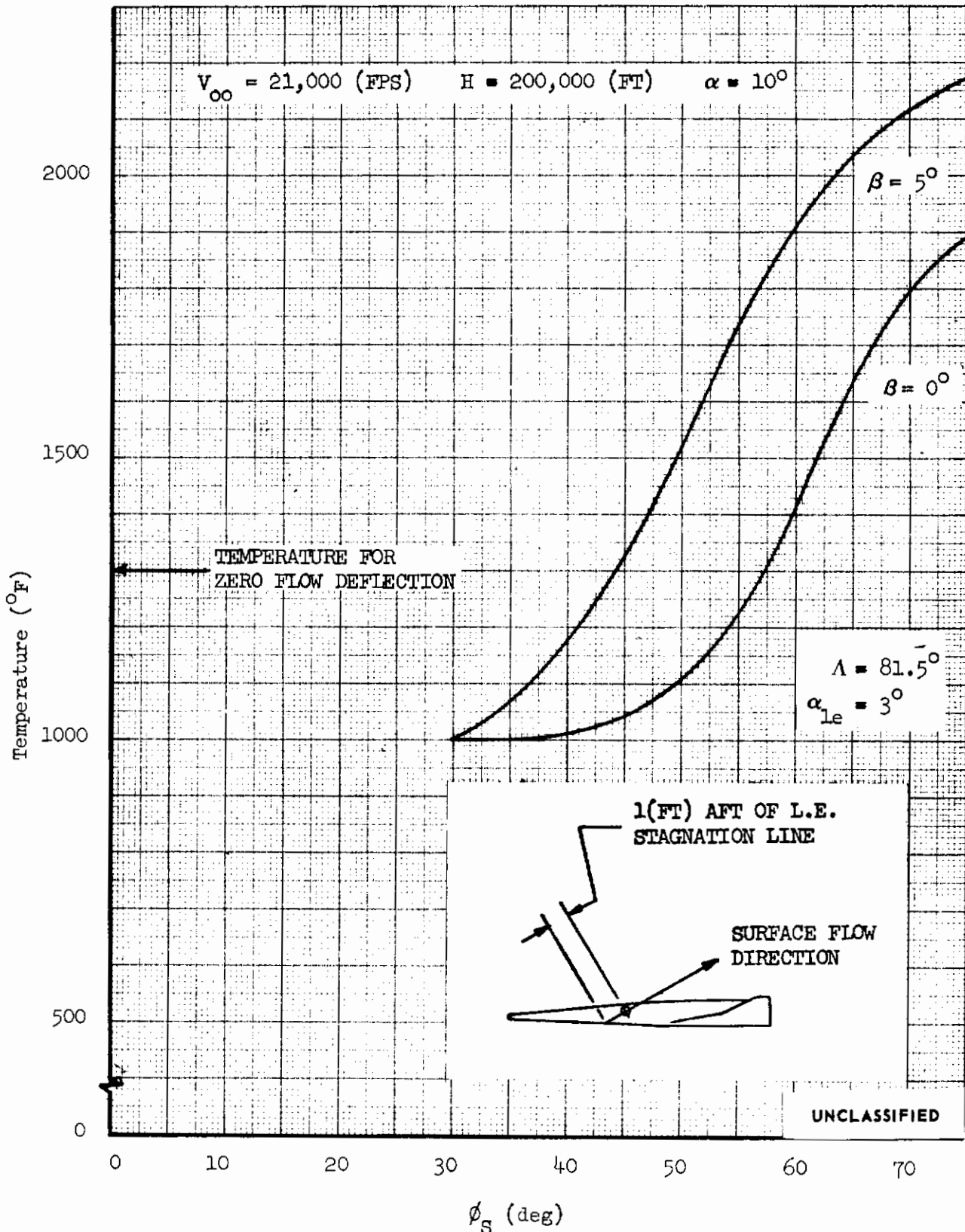









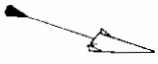
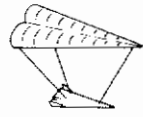


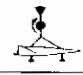



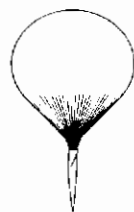



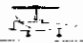



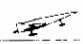


FIGURE 6 (U) EFFECT OF BODY SIDE ANGLE AND YAW ANGLE ON SIDE PANEL SURFACE TEMPERATURES

	HORIZONTAL LANDING			
	HORIZONTAL LANDING WITH THRUST			
PARACHUTE AND DERIVATIVES	LANDING SHOCK ATTENUATION			
	WATER RECOVERY			
	AIRSNATCH			 
	PARACHUTE REEL			
	RETRO-ROCKET			
	PARAVULCOON			
	ROTOR SYSTEM			 
	VARIABLE GEOMETRY			 

UNCLASSIFIED

FIGURE 7 (U) ALTERNATE RECOVERY TECHNIQUES

TABLE 3
(U) ALTERNATE LANDING SYSTEMS

System	Weight/Horizontal Landing Weight*	Comments
Horizontal Landing	1.00	Lowest weight. However, with no thrust available to offset the high base drag, the sink speed may be too high for reasonable landing gear design.
Horizontal Landing W/Thrust	1.05	This system is based on ground contact at $V_y = 10$ ft/sec and thrust time of approximately 20 sec.
Vertical Descent Recovery (All)	1.09	Landing thrust and horizontal-type landing gear not required.
Parachute + honeycomb shock strut	1.05	The lightest weight of this combination occurs when parachute decelerates vehicle to 25 fps. Honeycomb shock strut then accelerates vehicle to zero fps.
Parachute (water recovery)	1.01	This system may operate with high vertical descent, 30 fps, if vehicle is allowed to enter water nose first.
Parachute (air snatch)	1.04	This system is sized with a parachute system to decelerate vehicle to 25 fps.
Parachute (reel)	1.07	Keel system to wind parachute lines rapidly just before touchdown can be rocket-powered.
Parachute + retrorockets	1.11	The lowest weight of this combination occurs when parachute decelerates vehicle to 26 fps. Retrorockets are fired just before touchdown.
Paravulcoon	1.13	This system was sized to hover at an assumed altitude of 5000 ft.
Rotor	1.17	System sized for vehicle simulating horizontal landing at an altitude, then deploying rotors to obtain an average descent of 25 fps and adding collective pitch just before impact to reduce descent rate to 8 fps.
Paraglider	1.20	Paraglider system weight for this vehicle was scaled from other data.
Horizontal Landing (Variable Geometry)		Weight based on $1-g$ load factor and use of wing flaps, ailerons, and slots.

*Based on 5000-lb vehicle

configured and packaged in a manner which will not significantly change the hypersonic configuration.

(U) A trade study was made between the weight of the vehicle-booster adapter and the weight of a solid rocket motor used to overcome base drag during landing. This trade arises from the fact that a reduction in vehicle base area to improve landing L/D leads to the requirement for a larger, heavier adapter. The use of a rocket engine precludes the need for base area reduction and the associated larger adapter section. The trade is summarized in Figure 8, and includes consideration of adapter weight, rocket weight, and subsonic base drag.

2.4 (U) GEOMETRY SELECTION

(U) Tables 4 and 5 summarize the geometry parameters that resulted from the parametric trades. The columns headed "Effect of Decrease" and "Effect of Increase" define the competing considerations that result in the recommended geometry elements. Table 4 is concerned with the geometry, performance and volume trades; and Table 5 is concerned with stability requirements.

(U) The resulting geometry is similar to that for the original F-5 configuration except for the contoured lower surface. The general arrangement is shown in Figure 9 and incorporates the recommended geometry elements of Table 4 and 5. This system was designated the HLD-35-1.

2.5 (U) CONFIGURATION EVOLUTION

(U) The HLD-35-1 has two unattractive features. These are (1) the large base area which requires thrust-augmented landing or some other landing mode and (2) the use of heavy, high temperature fins for stabilization. Several alternate aft vehicle geometries were considered in attempting to overcome these deficiencies.

(U) The first aft vehicle geometry variation is described in Figure 10 and was given the designation HLD-35-2. Its geometry elements are similar to those of the HLD-35-1 except that the base area has been reduced by boat-tailing and elimination of the fin/body ramps. This geometry has satisfactory performance, stability and control and satisfies the requirement for minimizing base area; but it retains the discrete high temperature fins.

(U) A second excursion was identified as HLD-35-3 and is shown in Figure 11. This geometry was the first attempt to remove the outboard fins by substituting slab body sides. It was found to have adequate directional stability at high angle of attack but only marginal stability at low angle of attack. A center fin is provided for low-speed directional stability. The base area is greater than that of the HLD-35-2.

(U) Figure 12 illustrates the approach suggested by AFFDL to minimize the fin and accomplish base fairing simultaneously. This initial geometry

Contrails
~~CONFIDENTIAL~~

(THIS PAGE IS UNCLASSIFIED)

results in large reductions of the hypersonic L/D due to the aft upper surface contours that produce large down and drag loads. It achieves more than adequate directional stability, however, and suggested that hypersonic directional stability could be obtained without fins.

(U) The geometry that was ultimately selected for the test phase is shown in Figure 13. It is designated FDL-5. This configuration resulted from parametric analyses of the effects on stability and performance of the aft contouring suggested by the geometries of Figures 5 and 6. The large increase in directional stability with increase in angle of attack observed on the HLD-35-3 and the large value of directional stability observed on the AFFDL configuration suggested a compromise geometry might accomplish a nearly uniform value of directional stability with various angles of attack while minimizing the penalties in hypersonic L/D. This compromise contouring philosophy was found to provide the desired stability and is the basis for the "Compression-sharing" concept defined in detail in Part II.

~~CONFIDENTIAL~~

(THIS PAGE IS UNCLASSIFIED)
Approved for Public Release

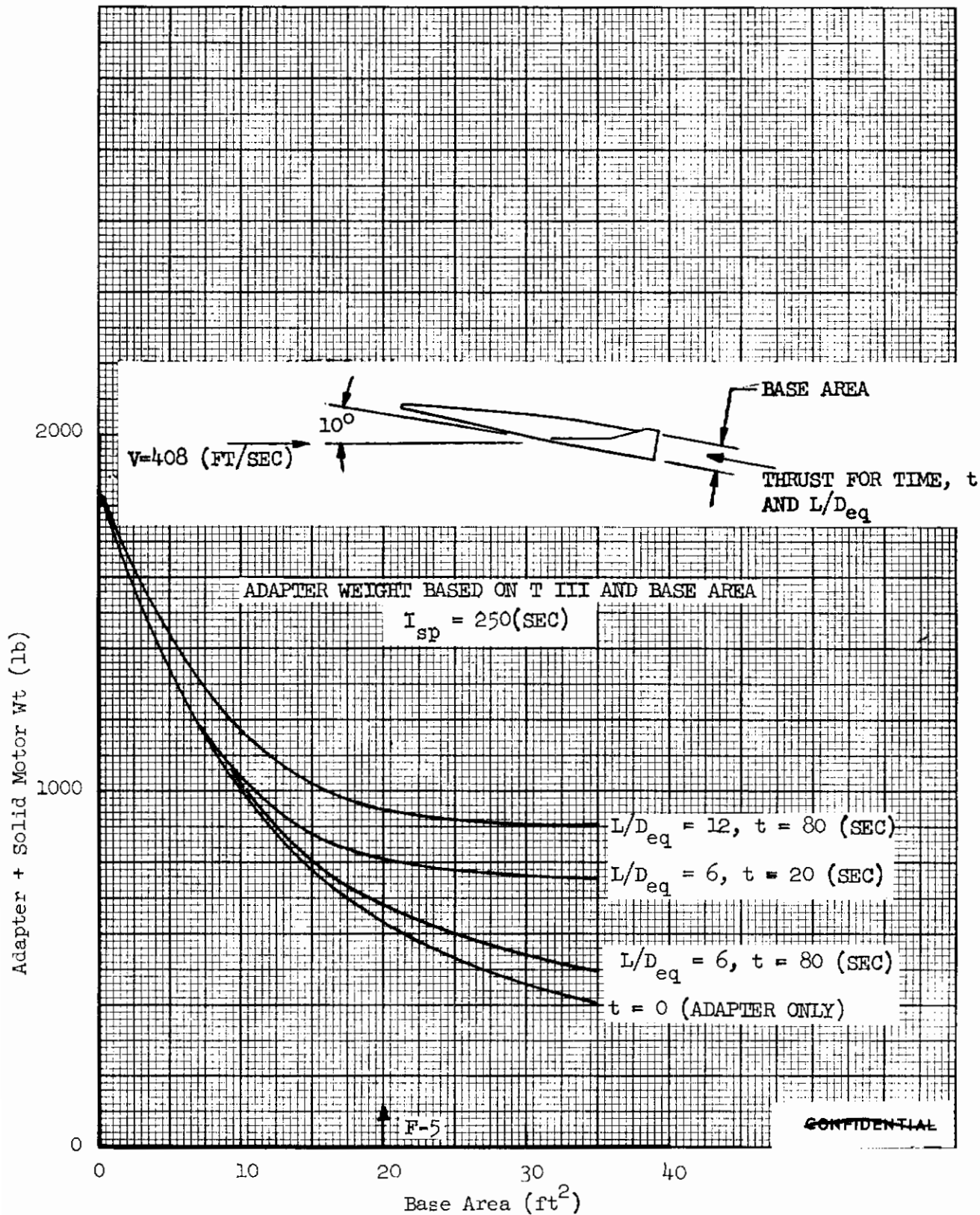


FIGURE 8 (U) LANDING WEIGHT PENALTY

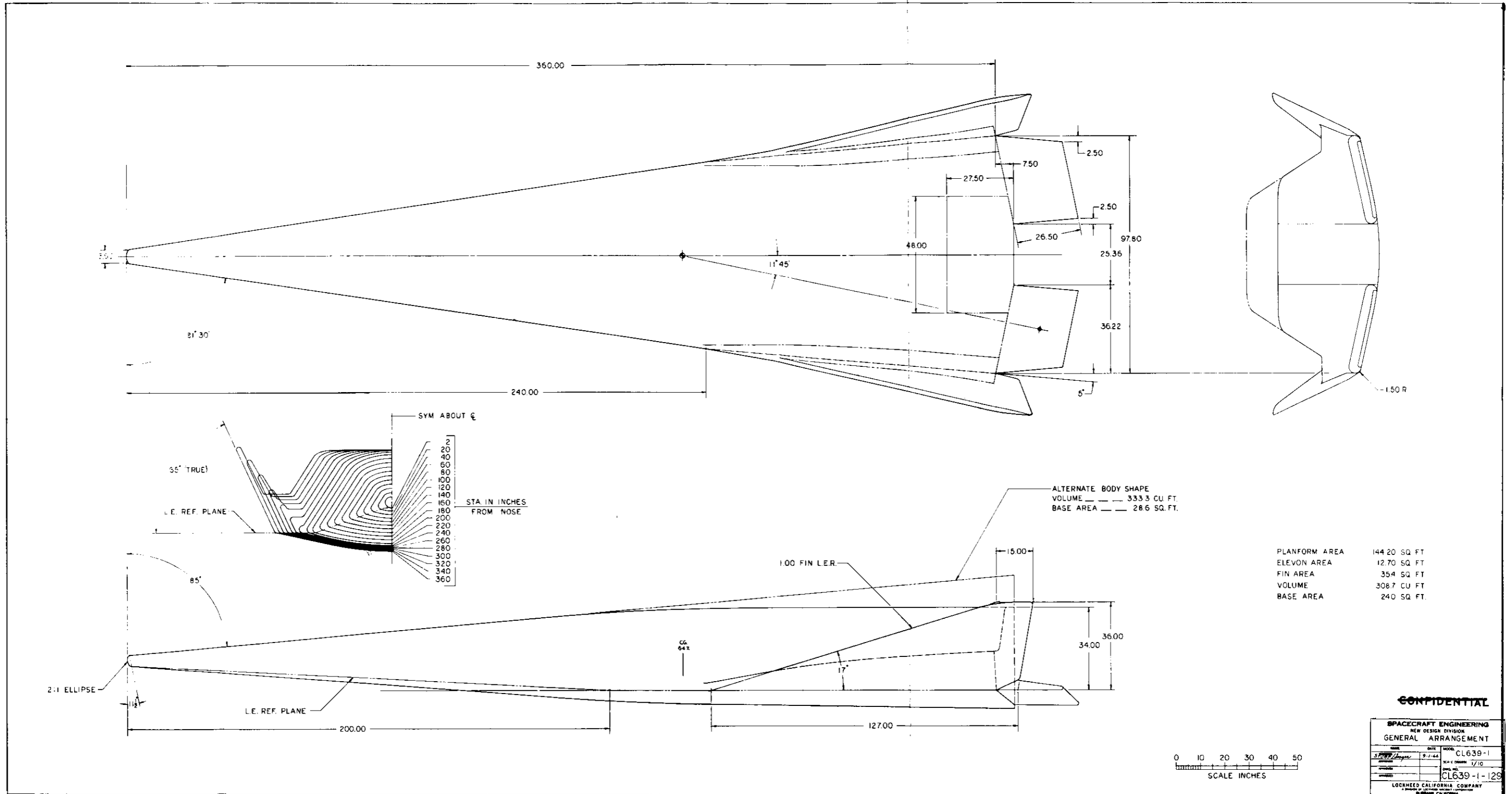
TABLE 4
(U) GEOMETRY TRADES

Geometry	Effect of Increase	Recommended Values	Effect of Decrease
Equivalent Nose Radius	Decreased Heating	3 in.	Increased Hypersonic L/D
Leading Edge Radius	Decreased Heating	1.5 in.	--
Leading Edge Sweep	Decreased Fin Toe-in/CP Movement Side Surface Heating	81-1/2°	Increased Volume Decreased Side Surface Heating & Volume Sensitivity to Yaw
Side Angle	Increased Volume	58°	Increased Yaw Stability Increased Hypersonic L/D Decreased Heating
Profile Angle	Increased Volume	5°	Increased Hypersonic L/D Increased Yaw Stability
Equivalent Dihedral Angle	Increased Volume Increased Depth	10°	Increased Hypersonic L/D Increased Yaw Stability
Base Area	Increased Hypersonic L/D (Lwr. Surf.) Decreased Adapter Weight	24 ft ²	Increased Subsonic L/D
Length	Increased Volume Increased Hypersonic L/D	30 ft	Decreased Weight

UNCLASSIFIED

TABLE 5
(U) STABILITY TRADES

Geometry	Effect of Decrease	Recommended Value	Effect of Increase
Fins:			
Toe-in	$\left\{ \begin{array}{l} \ell_0 \alpha \text{ pitch-up (sub)} \\ \text{pos } \Delta C_m \text{ (hyp)} \end{array} \right\}$	$\left\{ \begin{array}{l} 5 \text{ deg.} \\ 25 \text{ deg.} \end{array} \right.$	excessive heating (hyp)
Roll-out			
LE Sweep	Neg Δ L/D, incr. temp (hyp)	73 deg.	effectiveness loss (sub)
LE Radius	excessive heating (hyp)	1 in.	neg. Δ L/D (hyp)
Camber	Neg ΔC_m , Δ L/D (sub)	2%	neg. $\Delta C_{n\beta}$ (sub)
Area	Pos ΔC_m , loss $C_{n\beta}$, $C_{\ell\beta}$	12.5%	excessive static margin (all speeds)
Height	N/A	low	$C_{n\beta}$, $C_{\ell\beta}$ loss (hyp)
Elevons:			
Area	destabilizing (hyp)	9%	neg ΔC_m (sub)
Nose Ramp:			
Deflection	Neg ΔC_{m_0} (sub)	3 deg.	destabilizing (hyp)
Area	Neg ΔC_m (hyp)	40%	neg ΔC_m (hyp)
Lower Surface:			UNCLASSIFIED
Eq. Dihedral	small vol increase	10 deg.	excessive hyp L/D loss



PLANFORM AREA	144.20 SQ. FT.
ELEVON AREA	12.70 SQ. FT.
FIN AREA	35.4 SQ. FT.
VOLUME	308.7 CU. FT.
BASE AREA	240 SQ. FT.

CONFIDENTIAL

SPACECRAFT ENGINEERING
NEW DESIGN DIVISION
GENERAL ARRANGEMENT

DATE	9-1-44	MODEL	CL639-1
SCALE	17/10	DWG. NO.	CL639-1-129

LOCKHEED CALIFORNIA COMPANY
A DIVISION OF LOCKHEED CORP.
BURBANK, CALIFORNIA

FIGURE 9 (U) HLD-35-1 GENERAL ARRANGEMENT

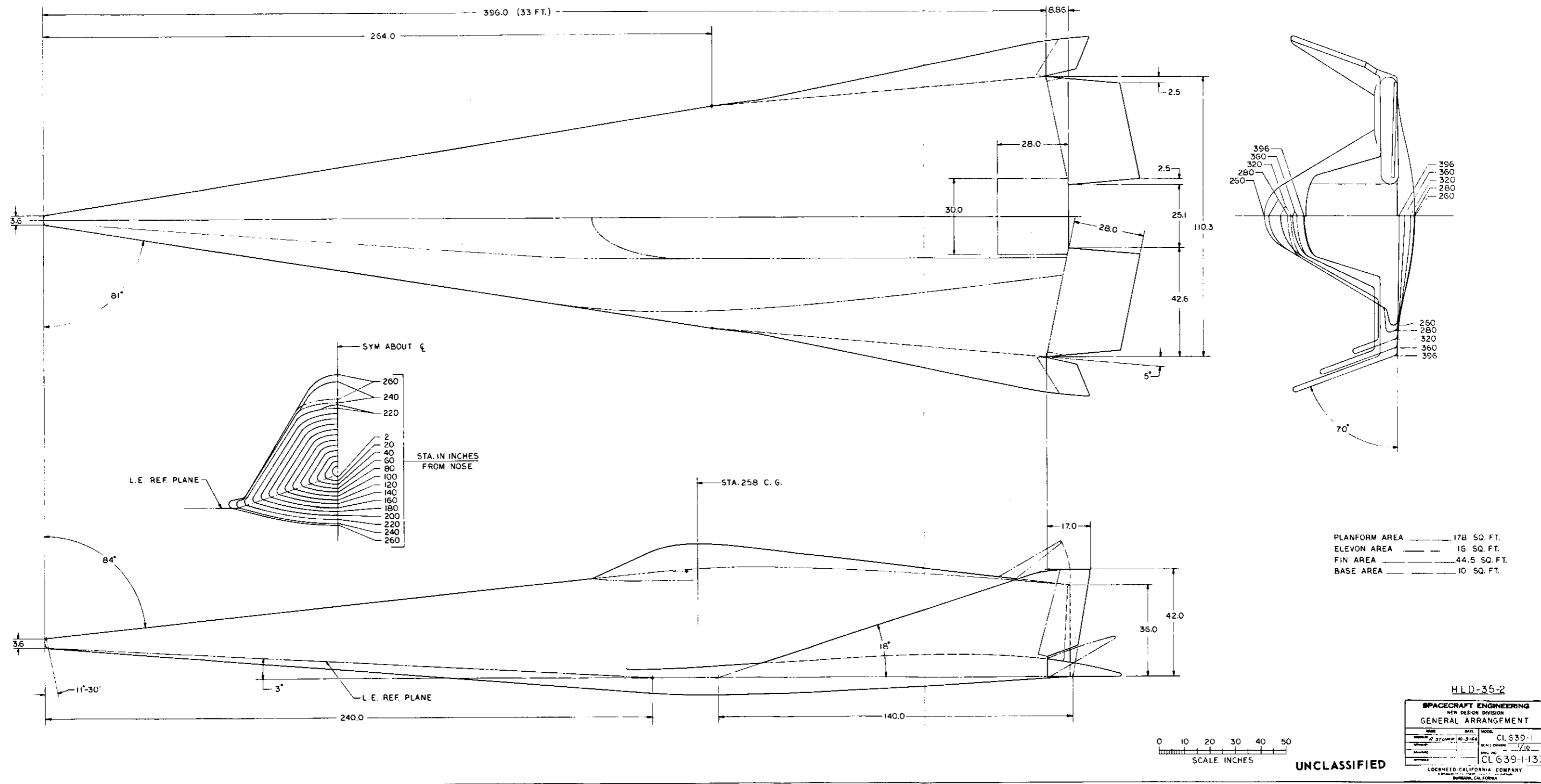


FIGURE 10 (U) HLD-35-2 GENERAL ARRANGEMENT

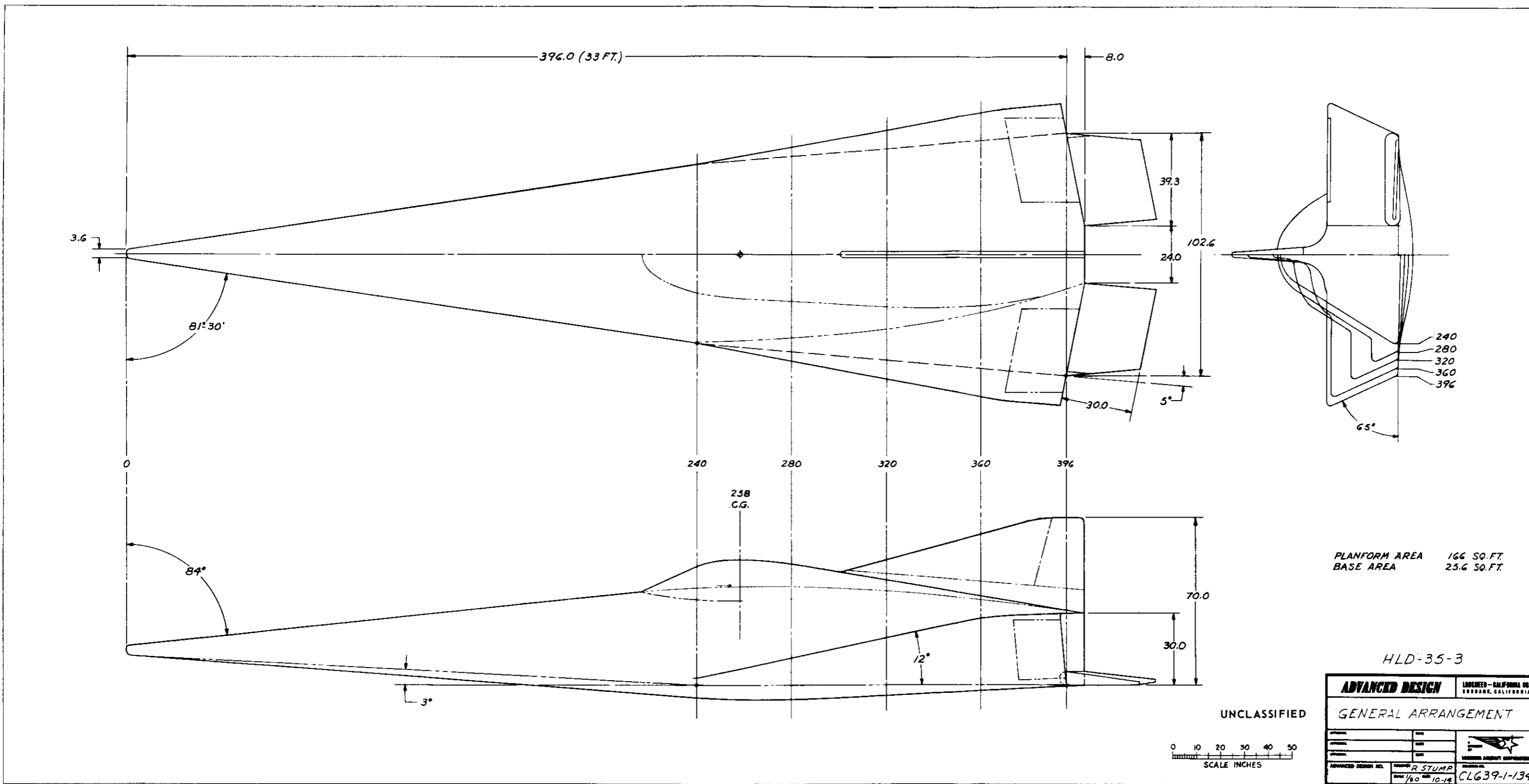


FIGURE 11 (U) HLD-35-3 GENERAL ARRANGEMENT

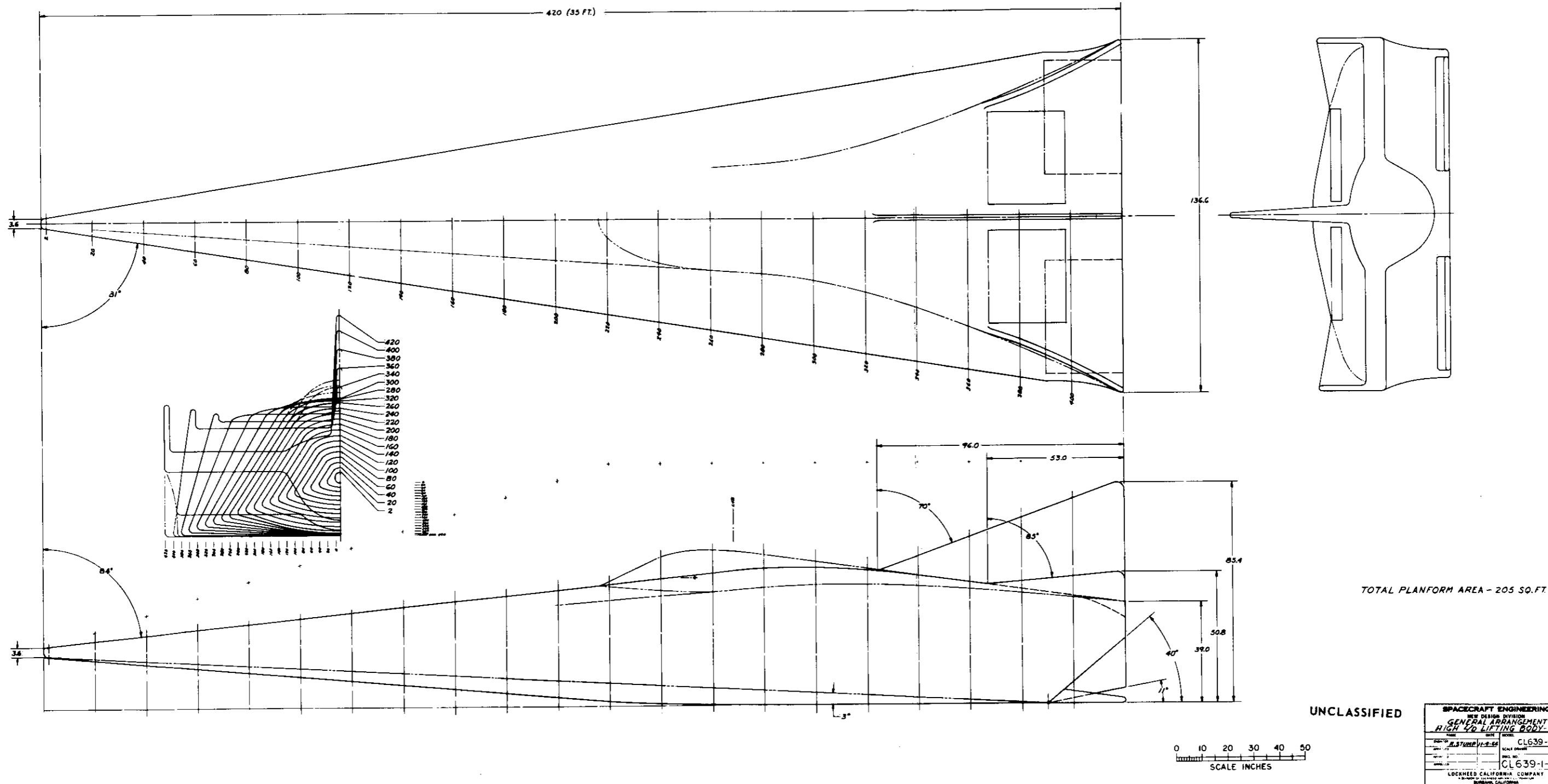


FIGURE 12 (U) GENERAL ARRANGEMENT - HIGH L/D LIFTING BODY - 35 FT

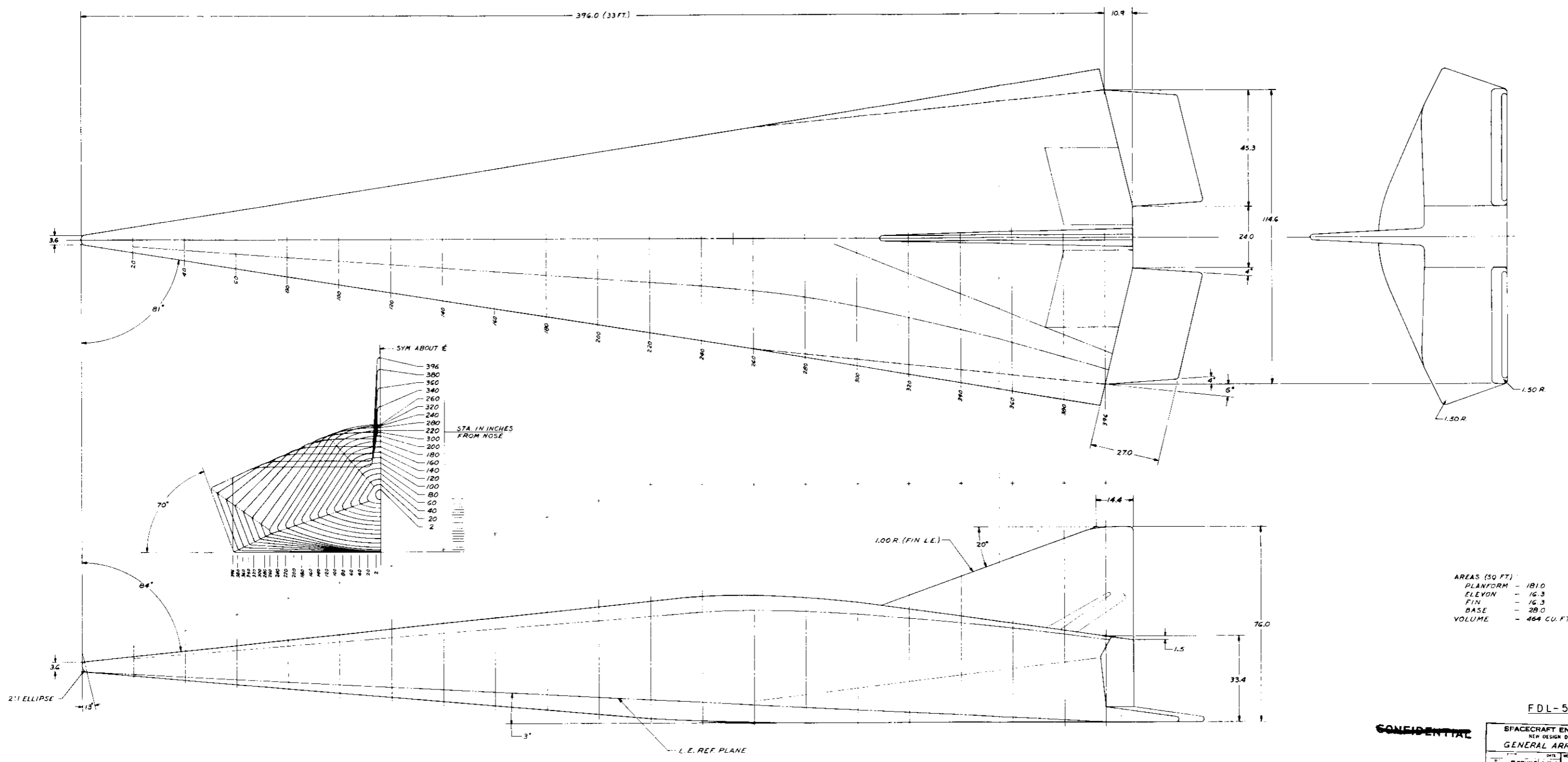


FIGURE 13 (U) FDL-5 GENERAL ARRANGEMENT

(REVERSE SIDE IS BLANK)

SECTION 3

TEST PROGRAM

(U) The wind tunnel test program was conducted in the AEDC wind tunnels A, B, C and F. Table 6 summarizes the test runs and test conditions. Approximately 25,000 separate data points were obtained during this test series. The FDL-5 configuration was exercised through the complete range of test attitudes and test conditions that could be expected of the test vehicle. The wind tunnel models used in the test series are described in Table 7 and shown in Figures 14, 15, 16, 17, and 18.

TABLE 7

(U) MODEL SUMMARY

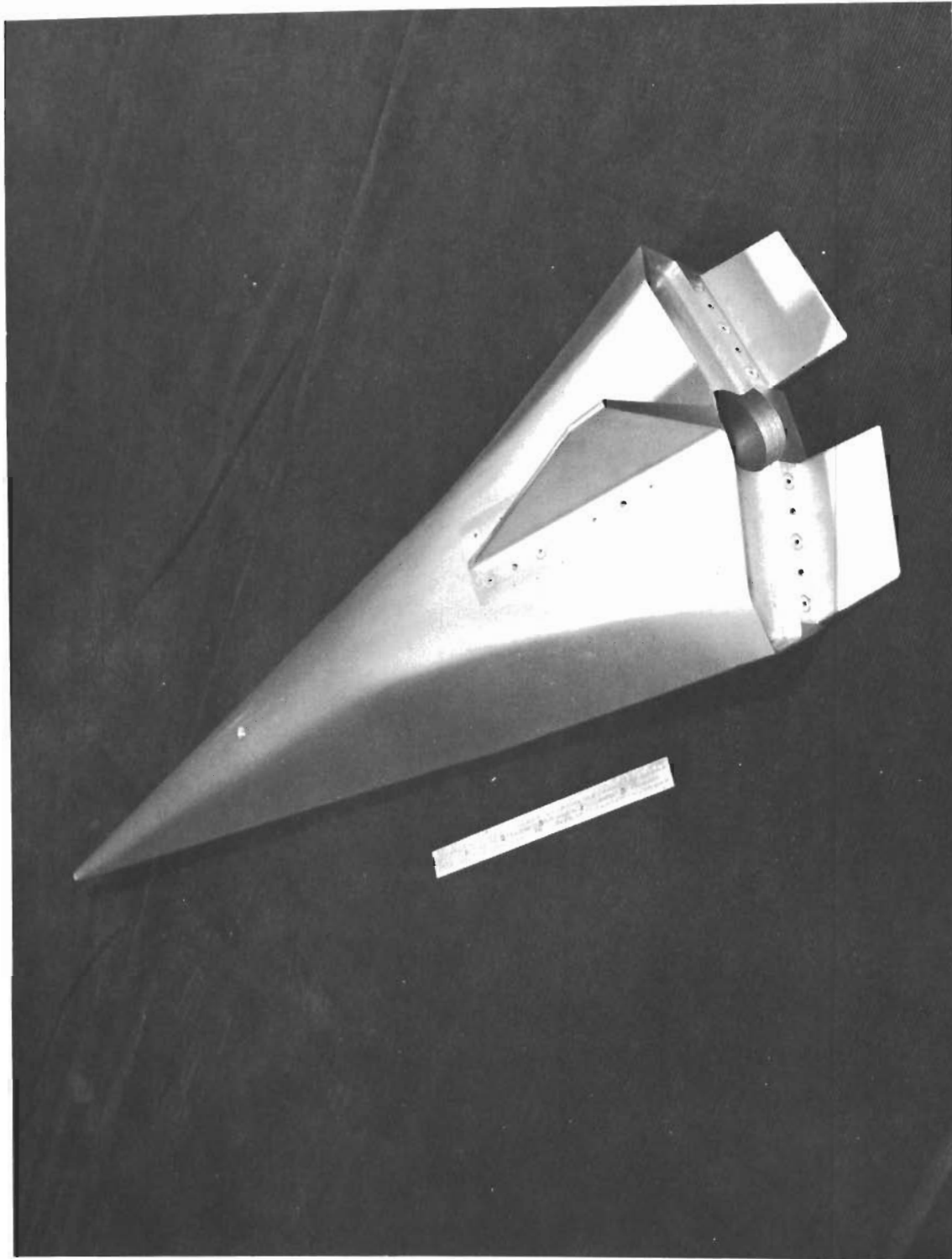
Model Size	Construction	AEDC Facility
20-inch	Steel force	A, B, C
15-inch	Fiber glass force	F
20-inch	Aluminum pressure/ht transfer	F
20-inch	Steel pressure	C
20-inch	Steel thin skin ht transfer	C

(U) Details of the aerodynamic force, pressure, and heat transfer test program are contained in Parts III and IV of this report.

TABLE 6
(U) TFST SUMMARY

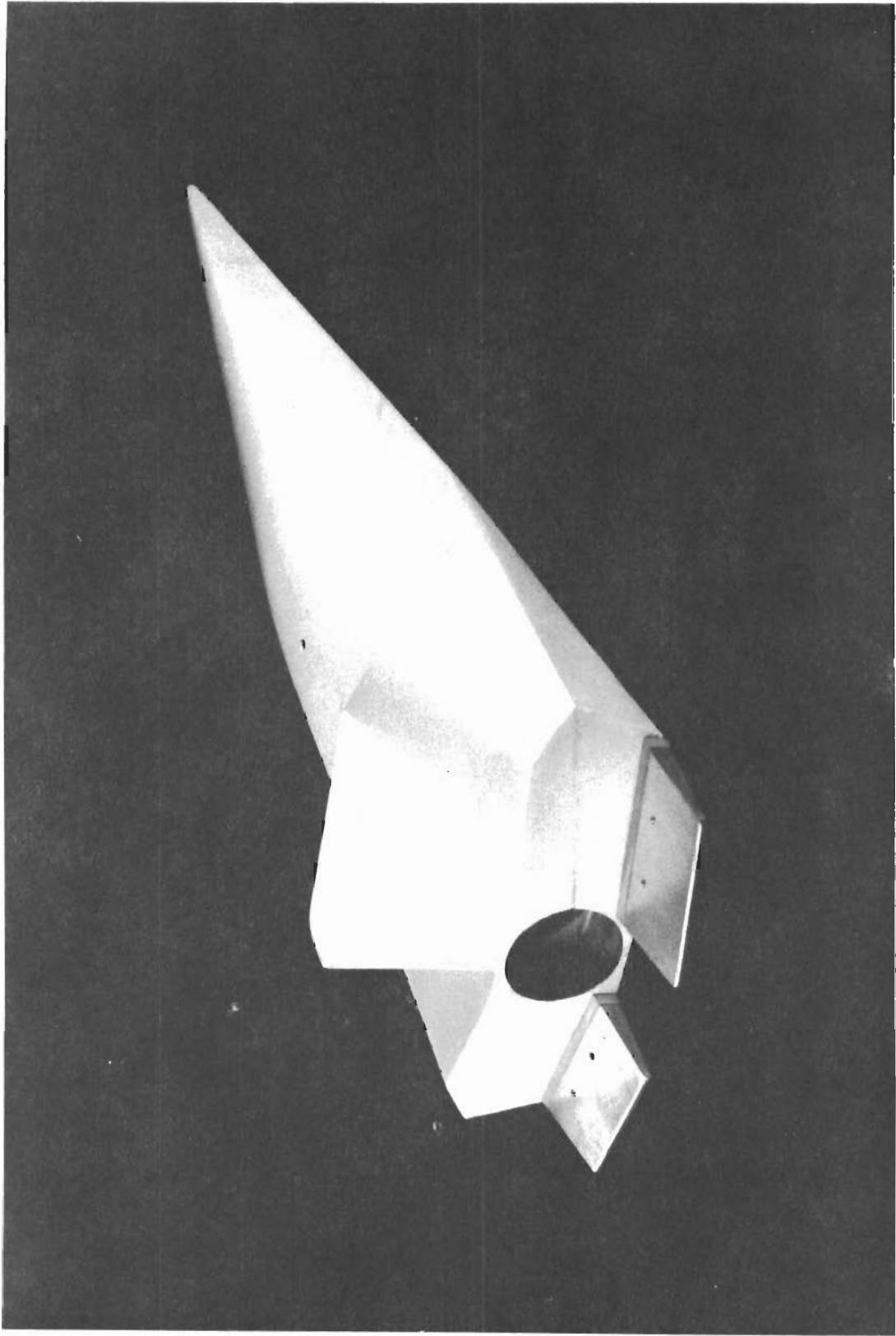
AEDC Facility	Test Data	Number of Groups of Runs	Angle of Attack - Deg	Yaw - Deg	Mach Number	Reynold Number Per Foot
A	Force and moment	135	-5 to 22	-2 to 8	1.5, 2.0, 2.5, 3.5, 5.0	1.2 to 6.4 x 10 ⁶
B	Force and moment	19	-4.5 to 25	-2 to 8	8	2.35 x 10 ⁶
C	Force and moment	45	-4 to 47	-2 to 8	10	0.4 to 2.1 x 10 ⁶
F	Force	64	0 to 21	0 to 8	14 to 19	0.11 to 2.1 x 10 ⁶
A	Pressure	122	0 to 20	0 to 8	1.5, 2.0, 2.5, 3.5, 5.0	2.4 to 6.3 x 10 ⁶
C	Pressure	49	0 to 35	-2 to 6	10	0.5 to 2.1 x 10 ⁶
F	Pressure	25	0 to 30	-2 to 6	19	5.6 to 6.2 x 10 ⁵
C	Heat transfer	75	0 to 35	-2 to 6	10	0.4 to 2.1 x 10 ⁶
F	Heat transfer	22	0 to 25	-2 to 6	19	5.0 to 5.8 x 10 ⁵

UNCLASSIFIED



UNCLASSIFIED

FIGURE 14 (U) 20-INCH STEEL FORCE MODEL FOR TUNNELS A, B, C



UNCLASSIFIED

FIGURE 15 (U) 15-INCH FIBER GLASS FORCE MODEL FOR TUNNEL F

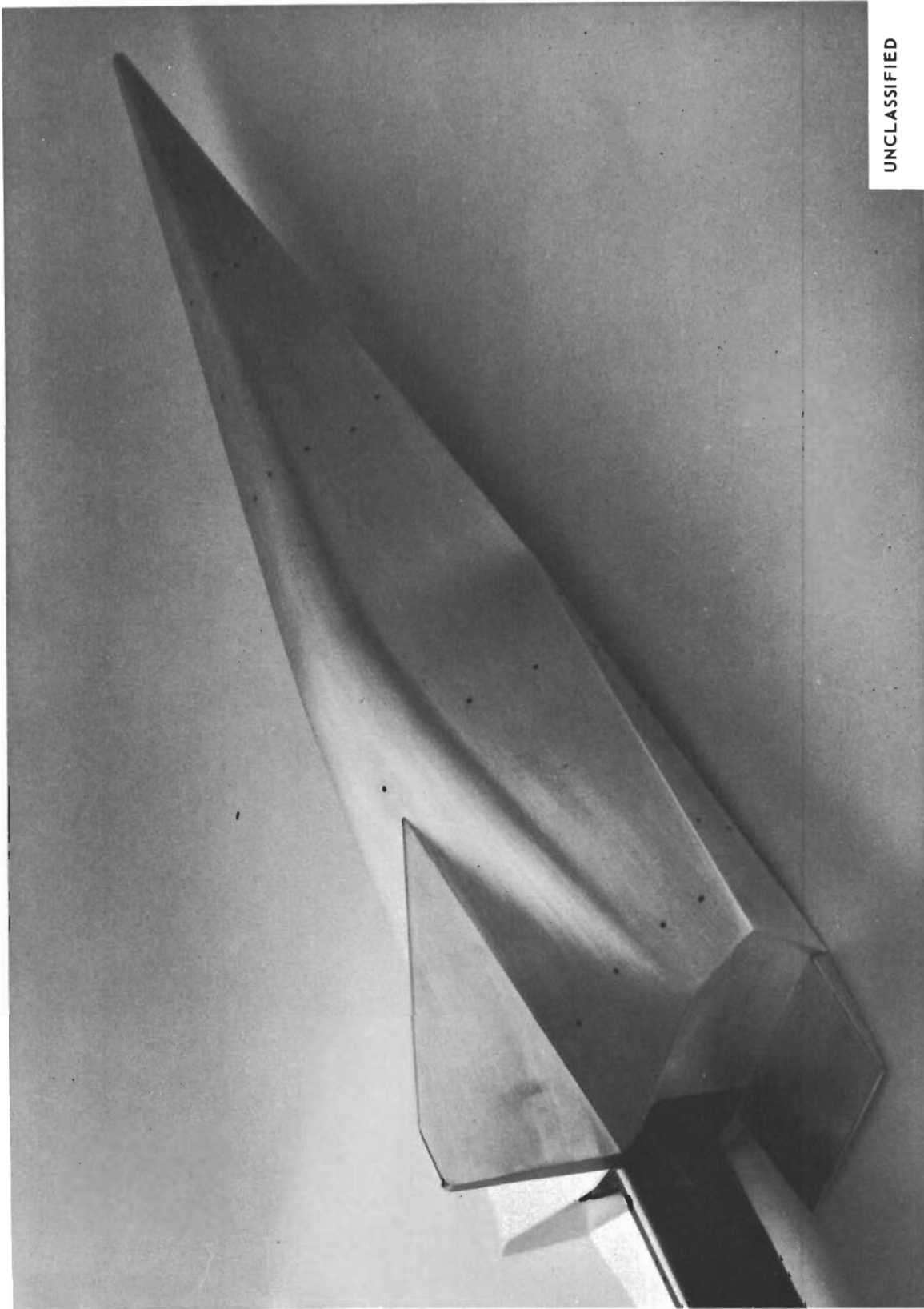
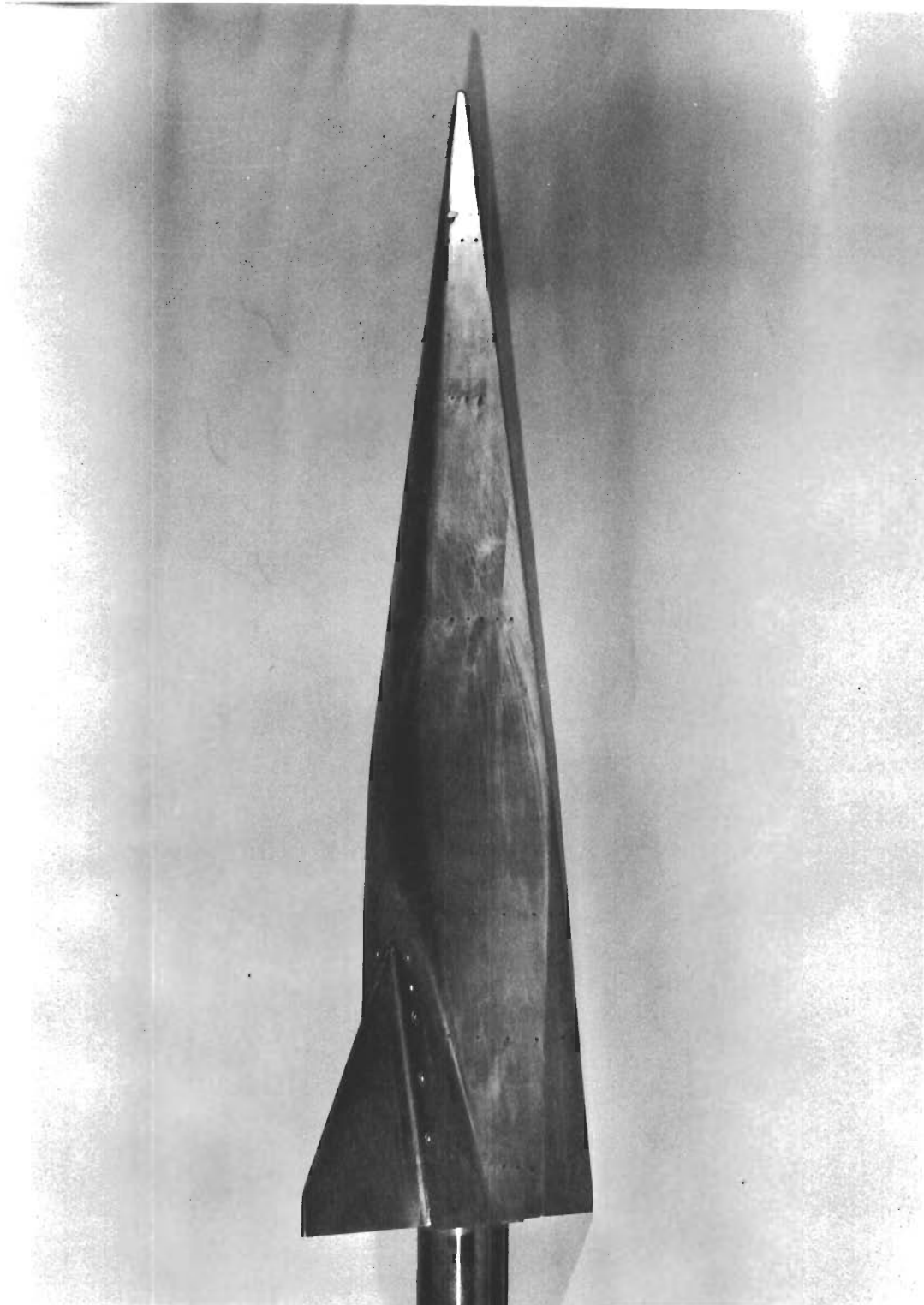


FIGURE 16 (U) 20-INCH ALUMINUM PRESSURE/HEAT TRANSFER MODEL FOR TUNNEL F
(PRESSURE PLUGS INSTALLED)



UNCLASSIFIED

FIGURE 17 (U) 20-INCH STEEL PRESSURE MODEL FOR TUNNELS A AND C

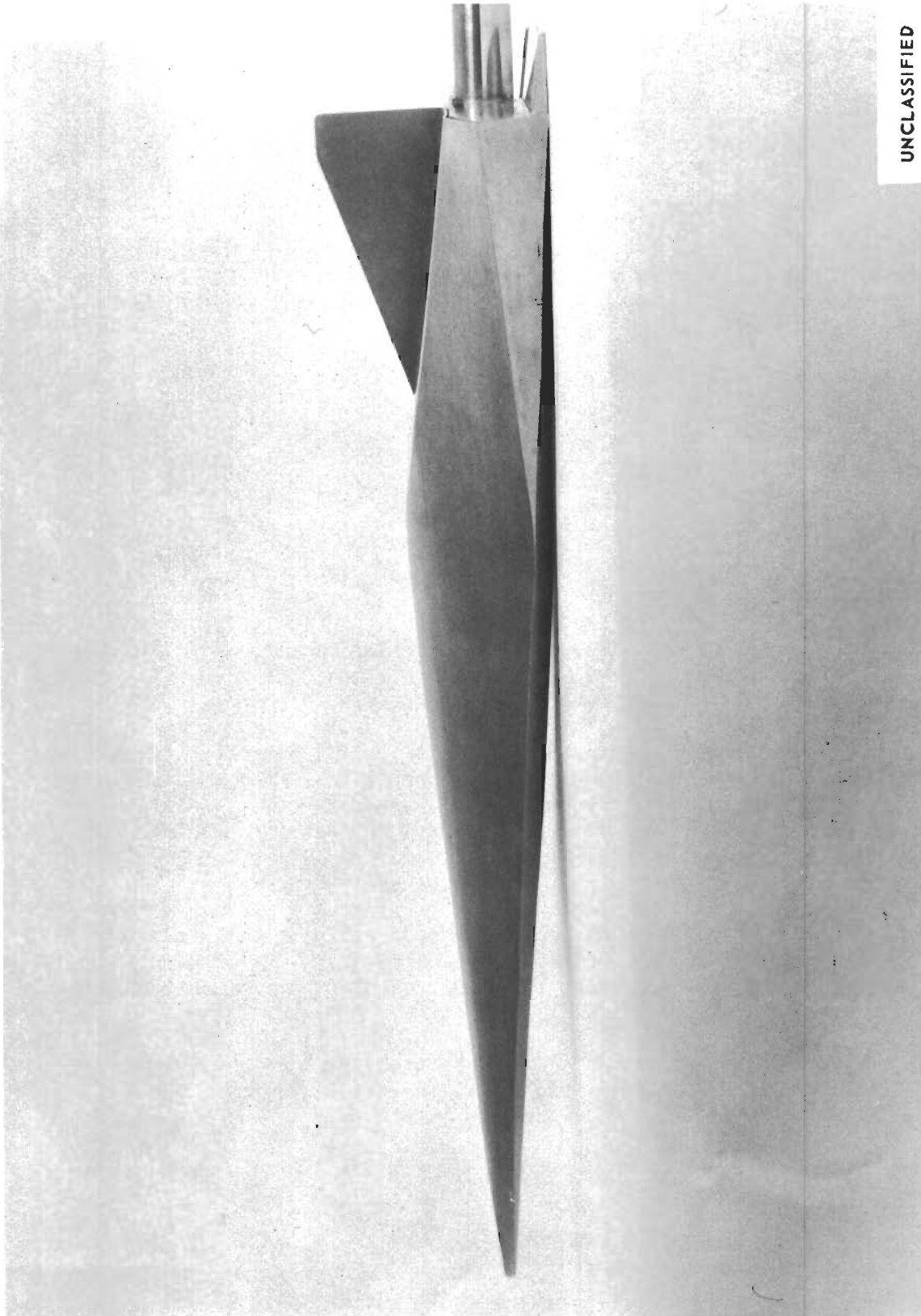


FIGURE 18 (U) 20-INCH THIN SKIN HEAT TRANSFER MODEL FOR TUNNEL C

SECTION 14

(U) FDL-5 AERODYNAMIC PERFORMANCE SUMMARY

(U) Predicted and measured aerodynamic performance of the FDL-5 is summarized in Figures 19 through 32. The basic geometry achieves high aerodynamic performance and is stable and controllable in pitch, roll and yaw at all Mach numbers at a center of gravity location of 62%.

(C) Figure 19 correlates measured L/D_{\max} obtained from force tests in AEDC tunnels B, C and F with the rarefaction parameter

$$\frac{M_{\infty} \sqrt{C^*}}{\sqrt{Re_{L_{\infty}}}}$$

A line faired through the data intersects the design condition of 20,000 fps and 200,000 feet altitude at L/D_{\max} (trimmed) of 2.84. The design condition shown on the figure is based on a vehicle length of 35 feet.

(C) Figure 20 summarizes the trimmed L/D_{\max} of the FDL-5 from $M = 0$ to $M = 20$. The curve is compiled from the wind tunnel test data. The maximum value of L/D_{\max} is 3.3 and occurs near $M = 12$. Measured L/D_{\max} values at supersonic speeds are sensitive to base geometry and area. With additional modification of aft body contours, it is expected that the potential L/D values shown by the upper faired curve could be achieved.

(U) Figures 21 and 22 are typical comparisons of analytical and experimental values of axial and normal force coefficients at $M = 19$. Predictions are based on wind tunnel test conditions and show excellent agreement with the data.

(C) Figure 23 shows the experimental variation of L/D with angle of attack and elevon deflection at $M = 19$. Maximum measured L/D (trimmed) at $M = 19$, $Re = 0.800 \times 10^6$ is 2.4.

(U) Typical experimental pitching moment data at $M = 19$ are compared with analytical values in Figure 24.

(C) Longitudinal stability and control characteristics at $M = 19$ are shown in Figure 25. Satisfactory trim at L/D_{\max} ($C_N = 0.12$) occurs with approximately 10 degrees of up elevon and with a center of gravity of 62%.

(C) Figure 26 shows the typical longitudinal trim and stability variations with maximum elevator and flap deflection for $M = 1.5$ to 5.0 . Maximum elevator and flap deflection provide positive values of C_{M0} and stable trim throughout the Mach number range tested. Center-of-gravity positions of 62, 64 and 66 percent of the body reference length are shown. Trim through the angle of attack range of 5 to 30 degrees can be accomplished throughout the supersonic regime with a suitable combination of center of gravity and control surface geometry.

(C) Yaw and roll stability of the FDL-5 are summarized in Figures 27, 28, 29 and 30. The configuration has satisfactory directional stability and dihedral effect over the entire speed range tested as shown in Figures 29 and 30. It is particularly noteworthy that the compression-sharing concept provided stability over the entire range of Mach number and angle of attack tested.

(C) Typical pressure data at two positions on the vehicle lower surface (Figures 31 and 32) show that maximum pressure coefficients occur at low supersonic speeds. These data, considered with the typical launch trajectory, lead to the conclusion that maximum design loads occur during boost, at low supersonic speeds in the peak wind shear environment. Detail pressure distributions are contained in Parts III and IV.

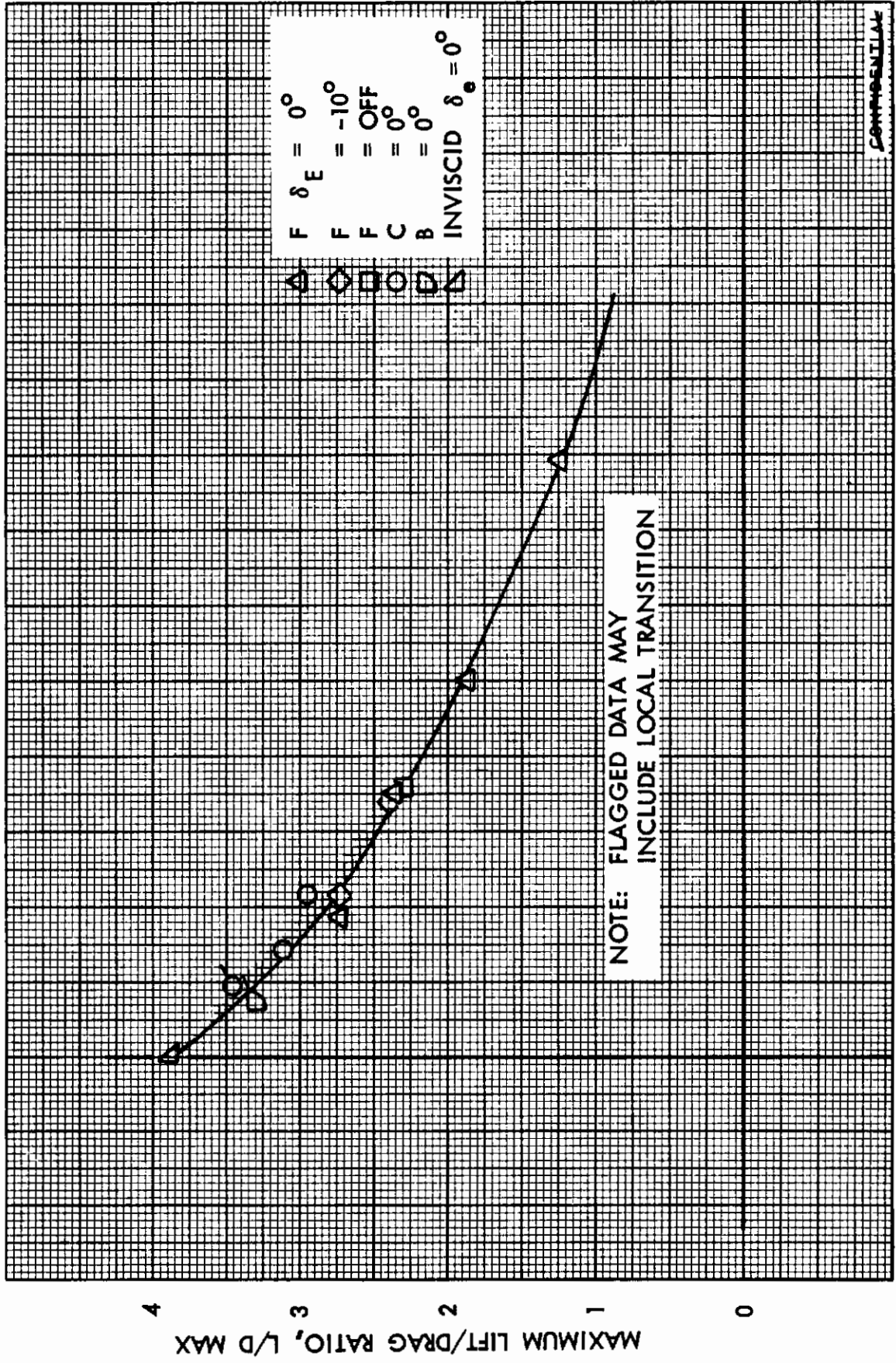


FIGURE 19 (U) FDL-5 VARIATION OF MAXIMUM L/D WITH \bar{v}^*

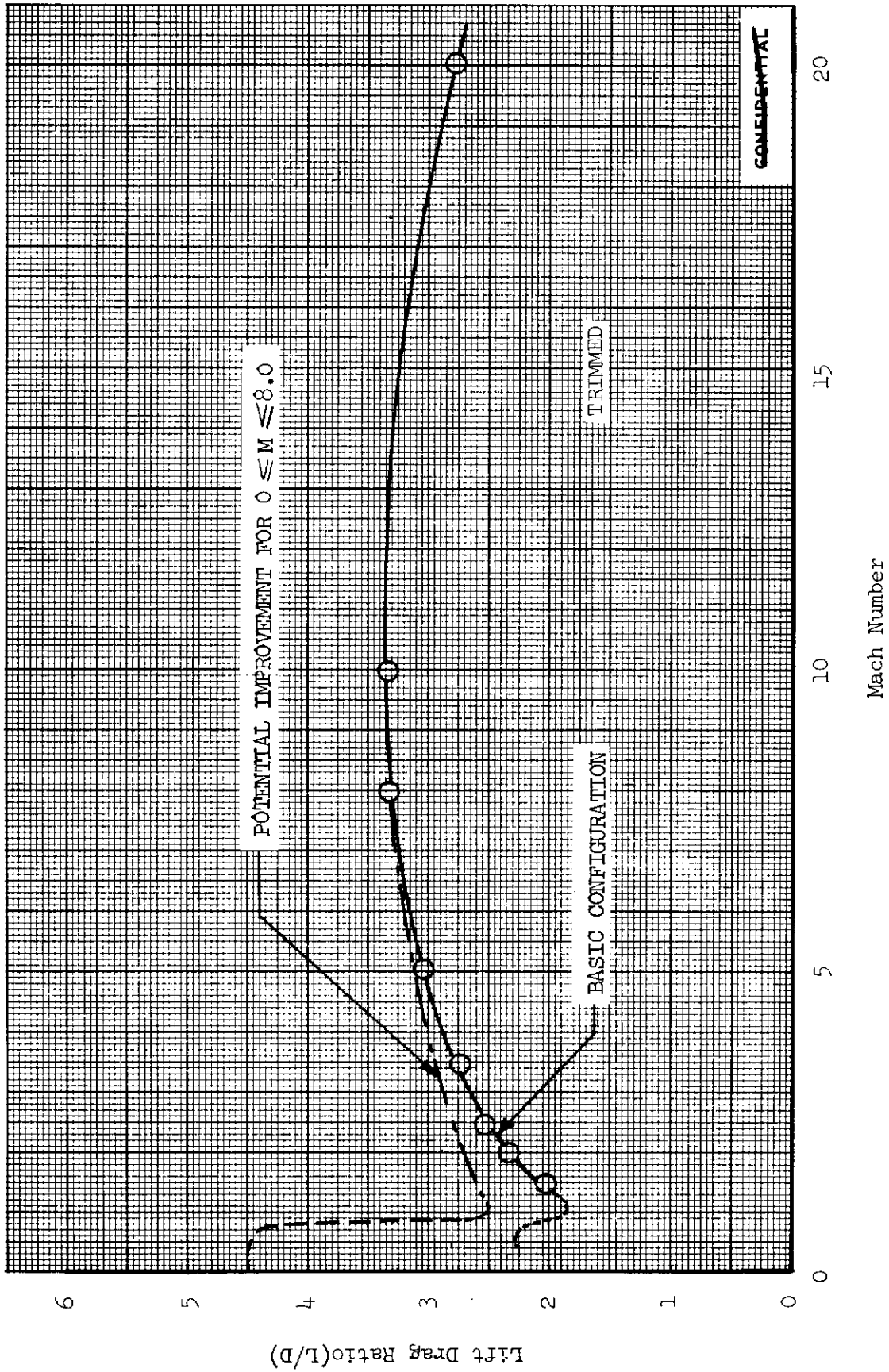


FIGURE 20 (U) FDL-5 VARIATION OF MAXIMUM L/D

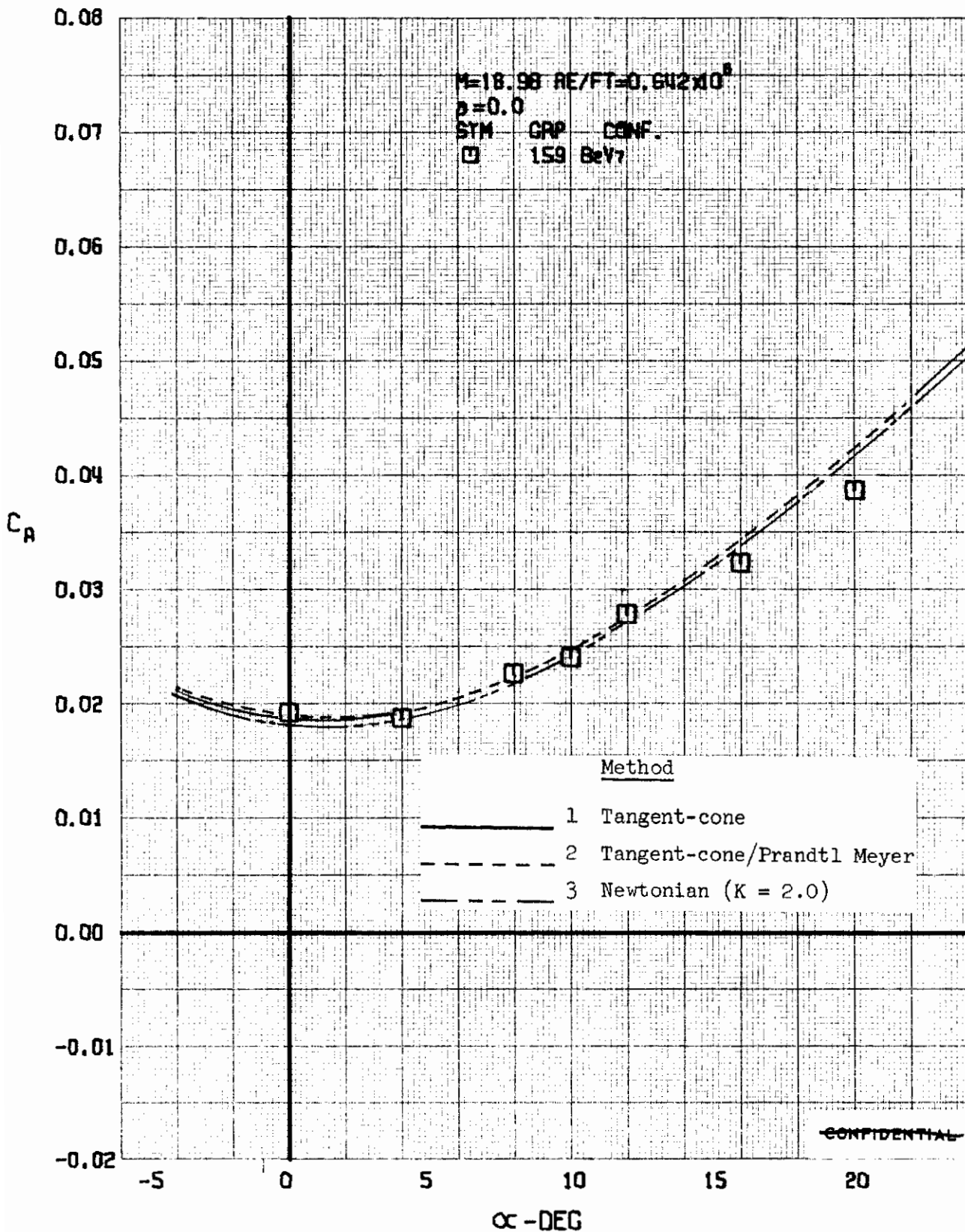


FIGURE 21 (U) COMPARISON OF ESTIMATED AND EXPERIMENTAL COEFFICIENTS - AXIAL FORCE COEFFICIENT VARIATION WITH ANGLE OF ATTACK (M = 18.98)

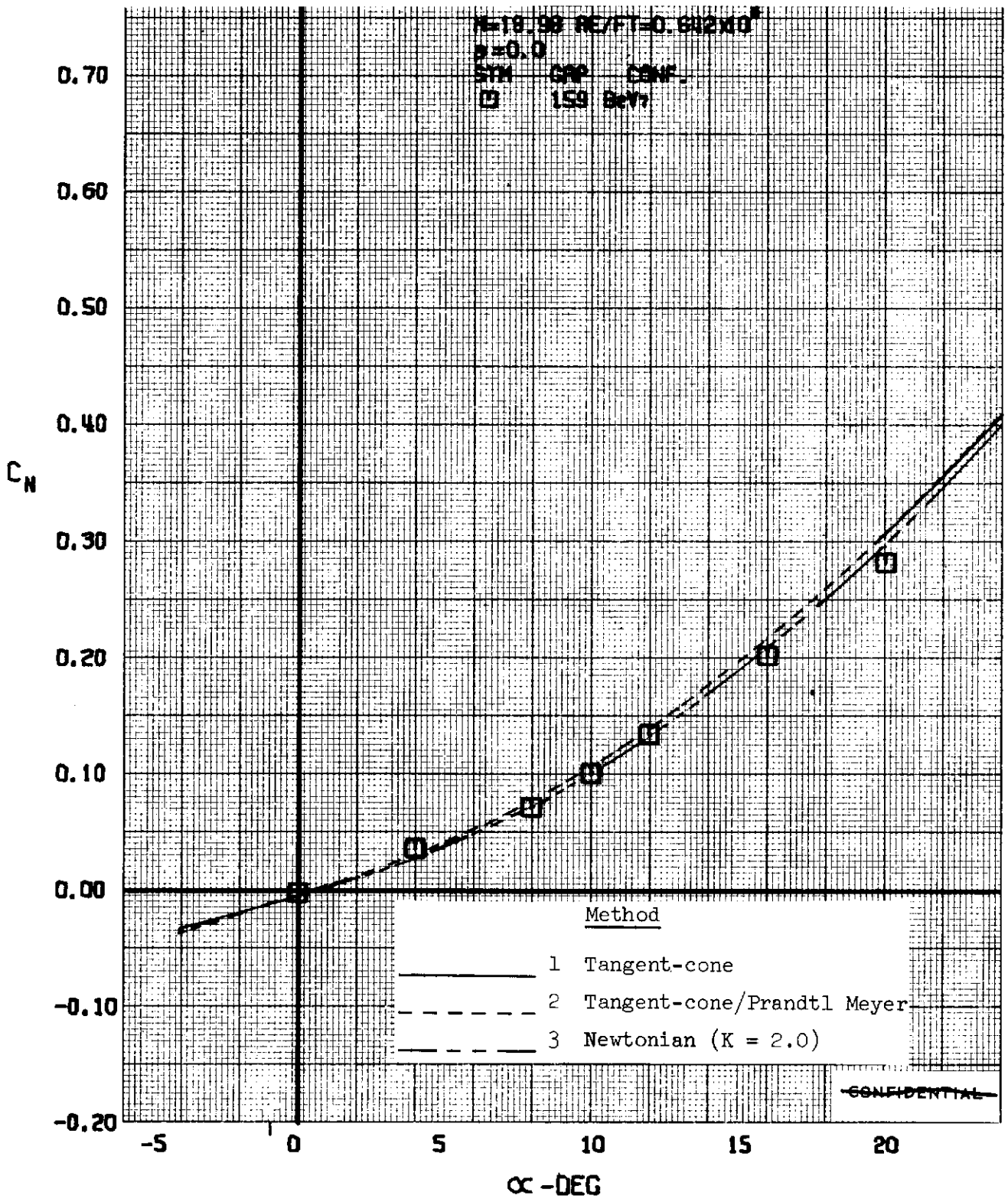


FIGURE 22 (U) COMPARISON OF ESTIMATED AND EXPERIMENTAL COEFFICIENTS - NORMAL FORCE COEFFICIENT VARIATION WITH ANGLE OF ATTACK (M = 18.98)

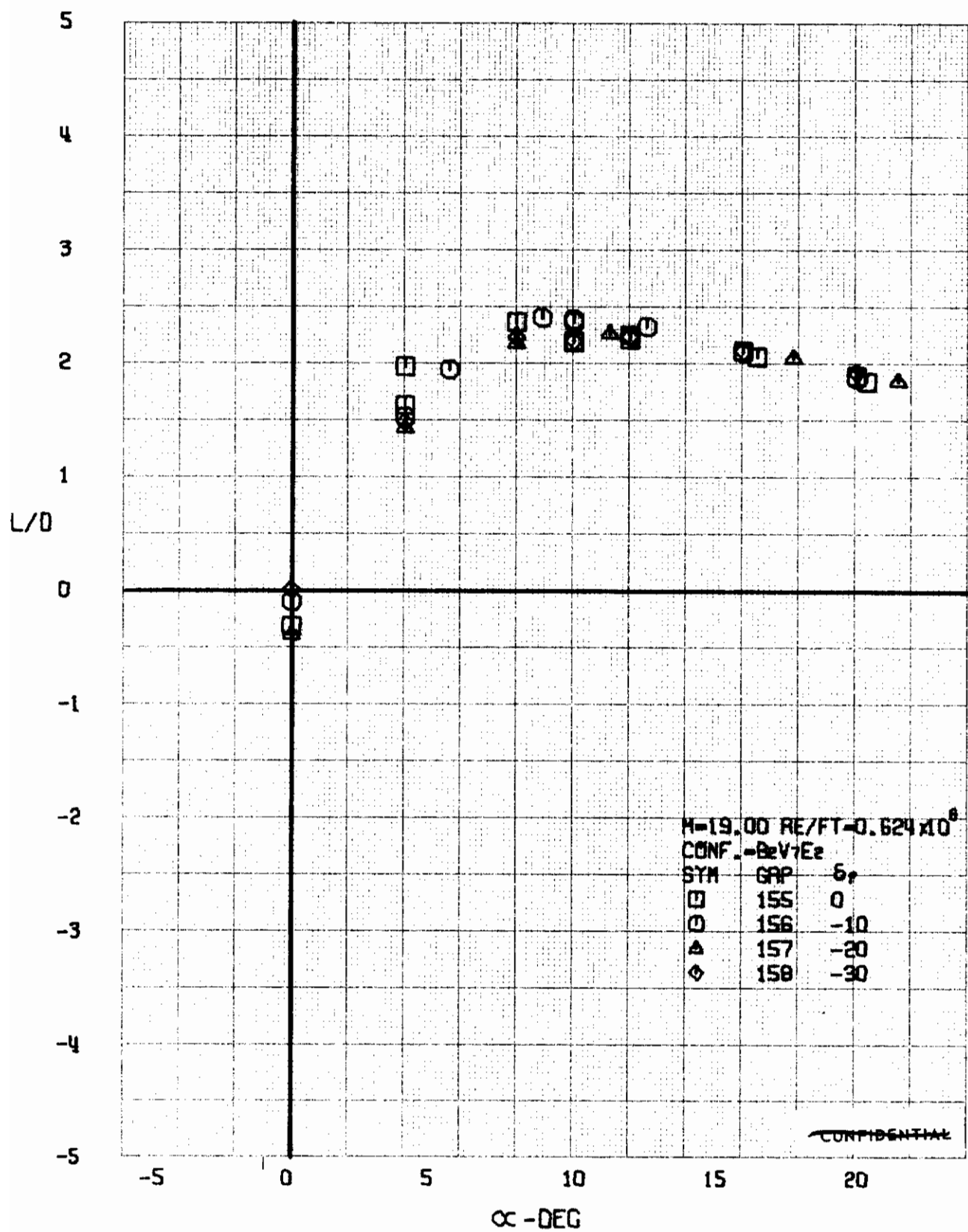


FIGURE 23 (U) ELEVON EFFECTS - LIFT/DRAG RATIO VARIATION WITH ANGLE OF ATTACK ($M = 19.00$)

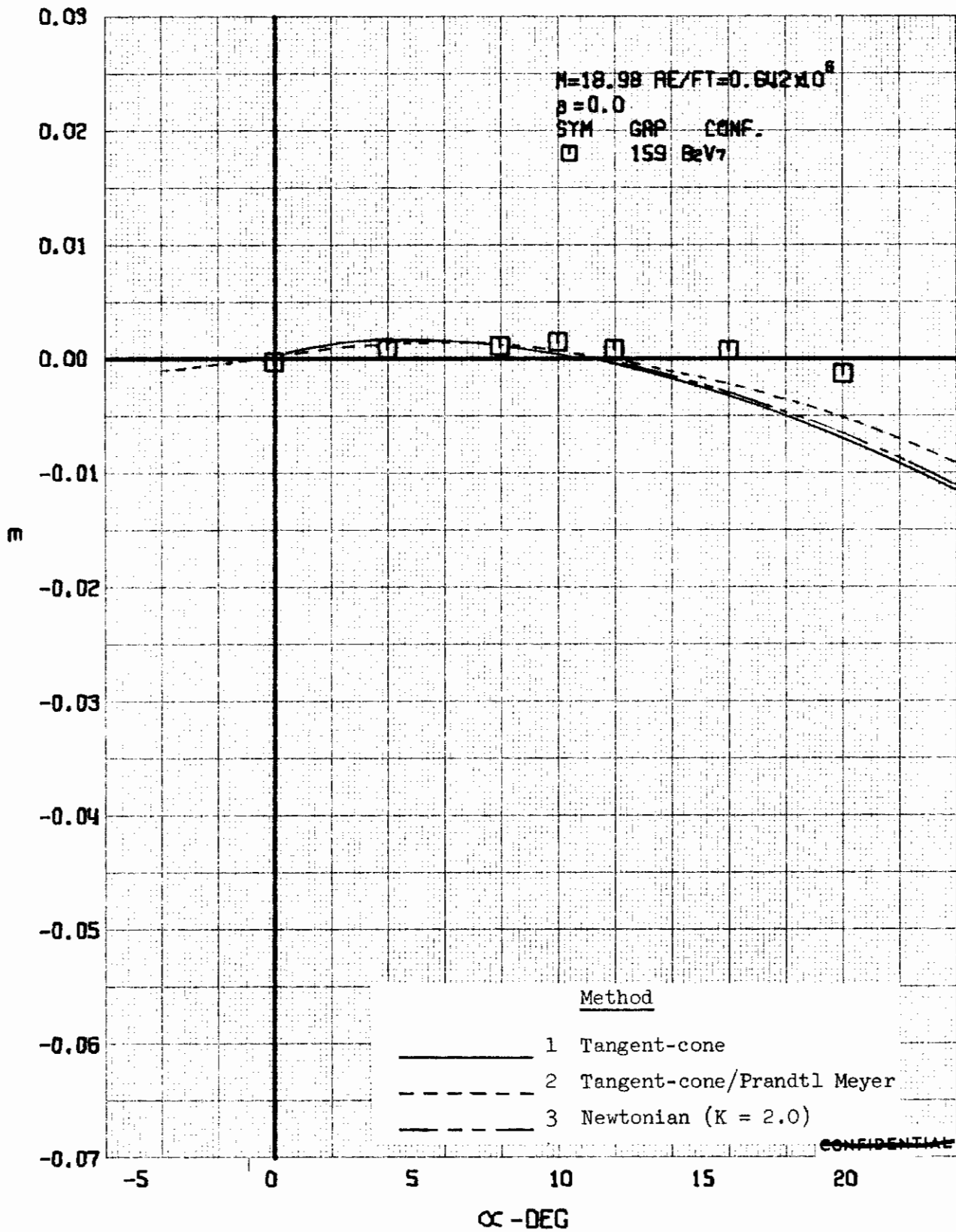


FIGURE 24 (U) COMPARISON OF ESTIMATED AND EXPERIMENTAL COEFFICIENTS - PITCHING MOMENT COEFFICIENT VARIATION WITH ANGLE OF ATTACK ($M = 18.98$)

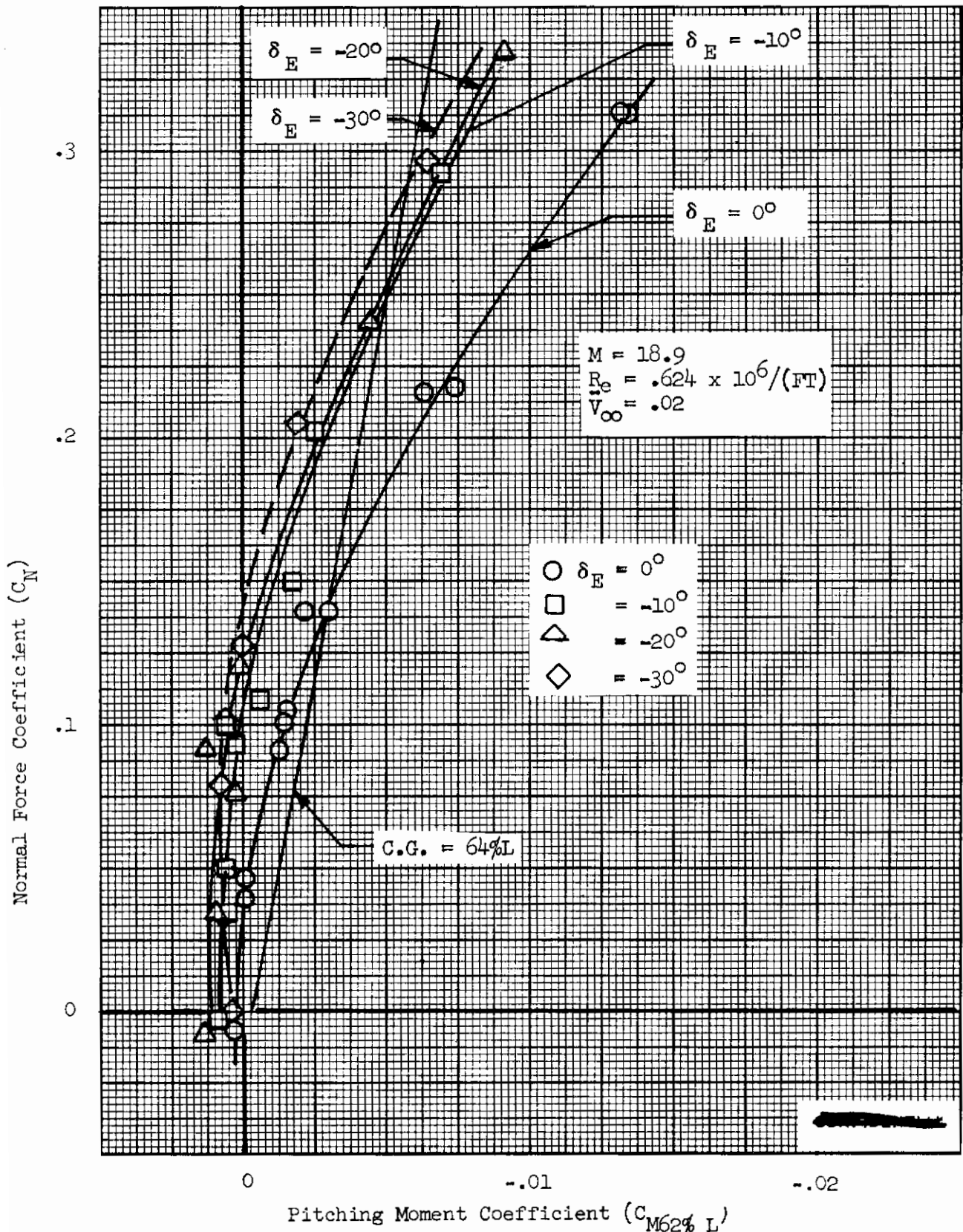


FIGURE 25 (U) FDL-5 LONGITUDINAL STABILITY ($M = 18.9$)

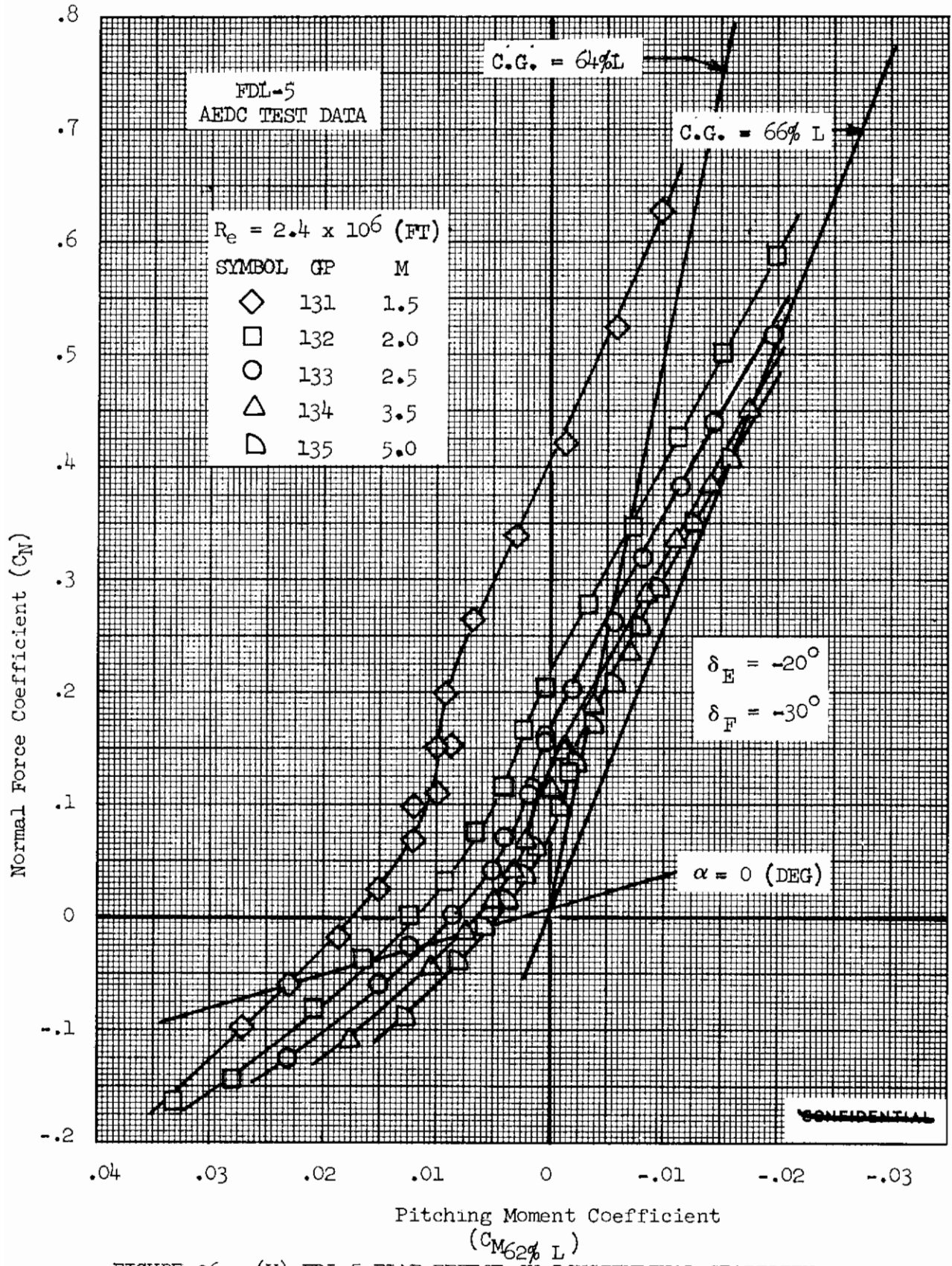


FIGURE 26 (U) FDL-5 FLAP EFFECT ON LONGITUDINAL STABILITY AT VARIOUS MACH NUMBERS

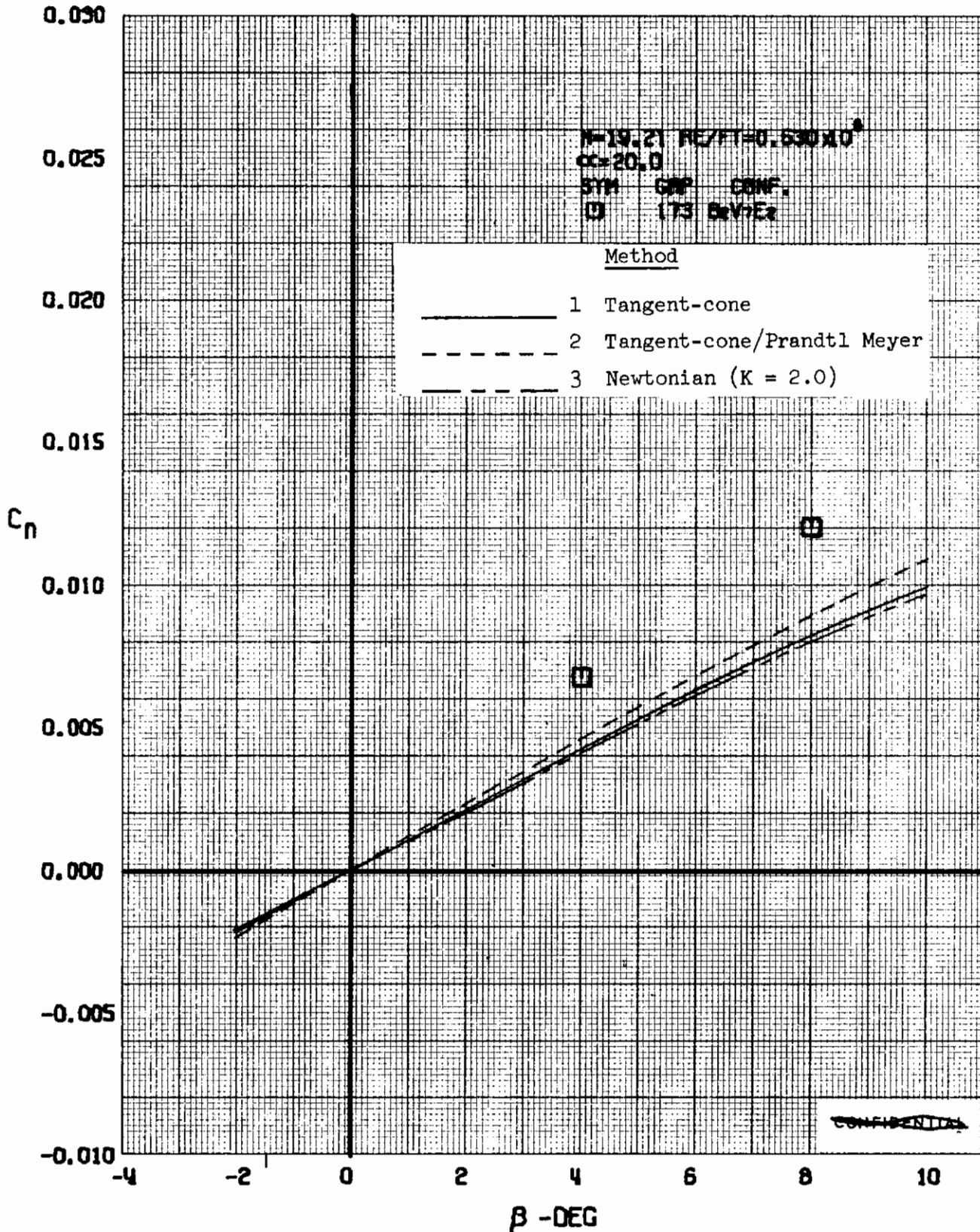


FIGURE 27 (U) COMPARISON OF ESTIMATED AND EXPERIMENTAL COEFFICIENTS - YAWING MOMENT COEFFICIENT VARIATION WITH ANGLE OF YAW ($M = 19.21$)

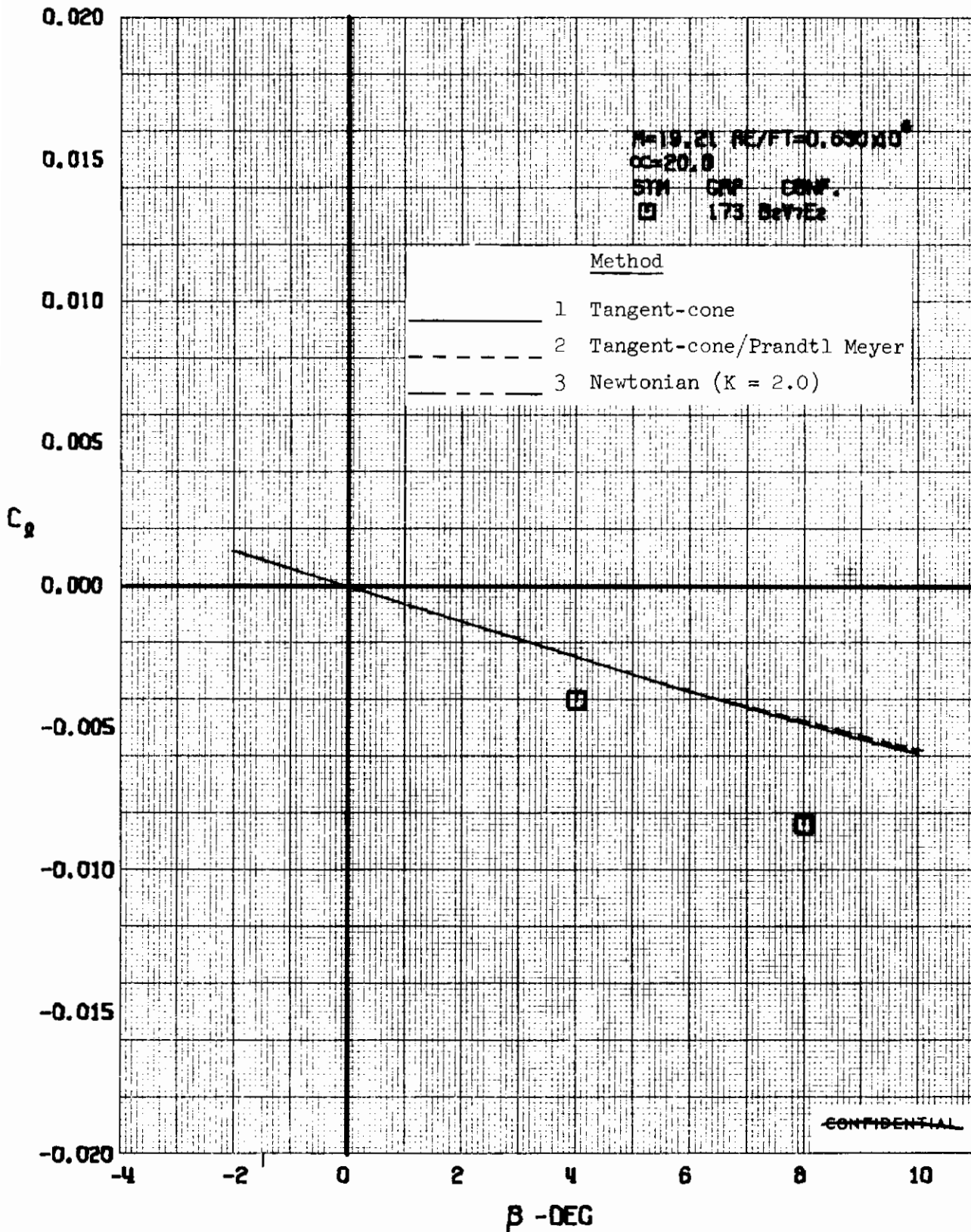


FIGURE 28 (U) COMPARISON OF ESTIMATED AND EXPERIMENTAL COEFFICIENTS - ROLLING MOMENT COEFFICIENT VARIATION WITH ANGLE OF YAW (M = 19.21)

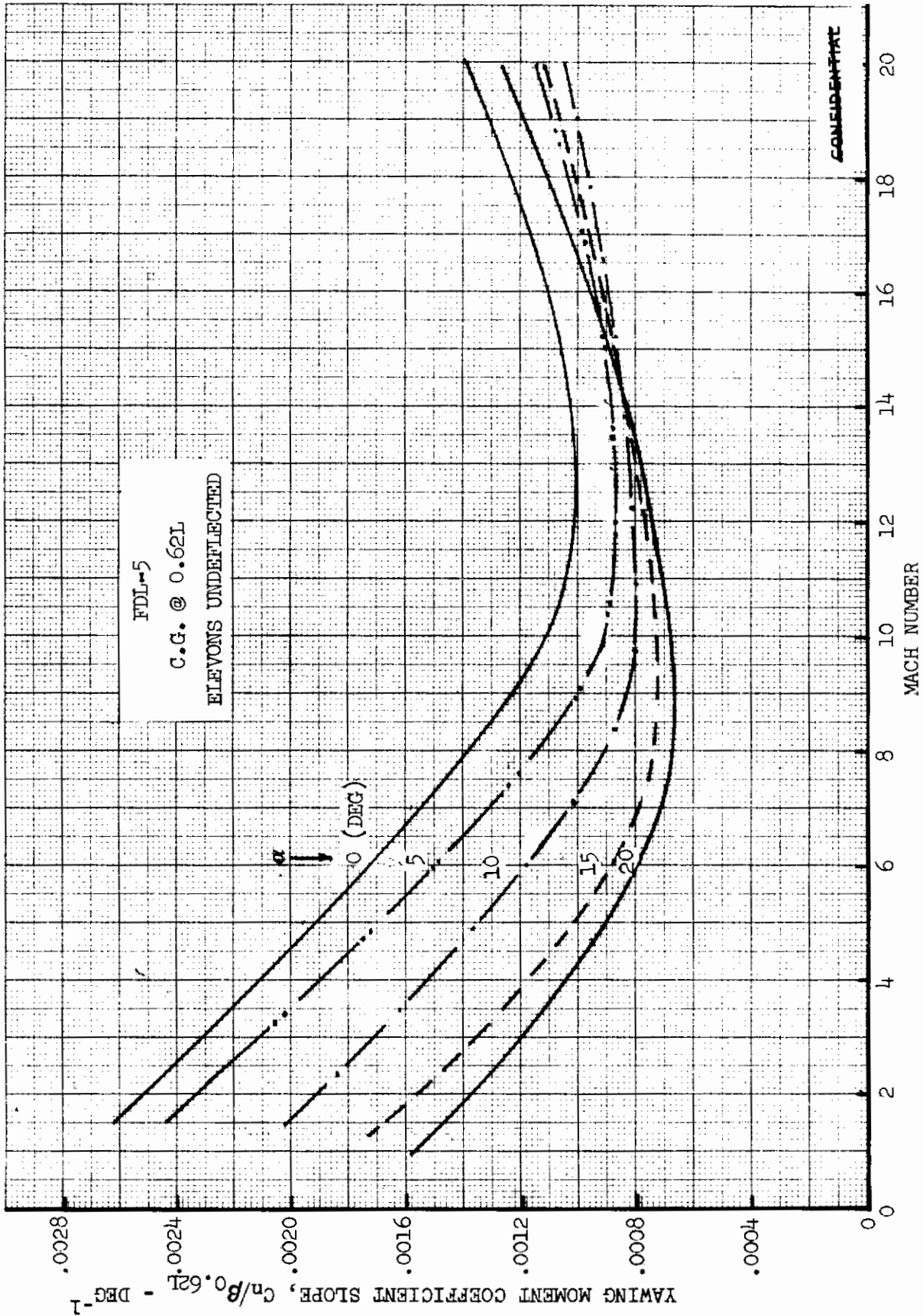


FIGURE 29 (U) FDL-5 YAWING MOMENT COEFFICIENT SLOPE VARIATION WITH MACH NUMBER

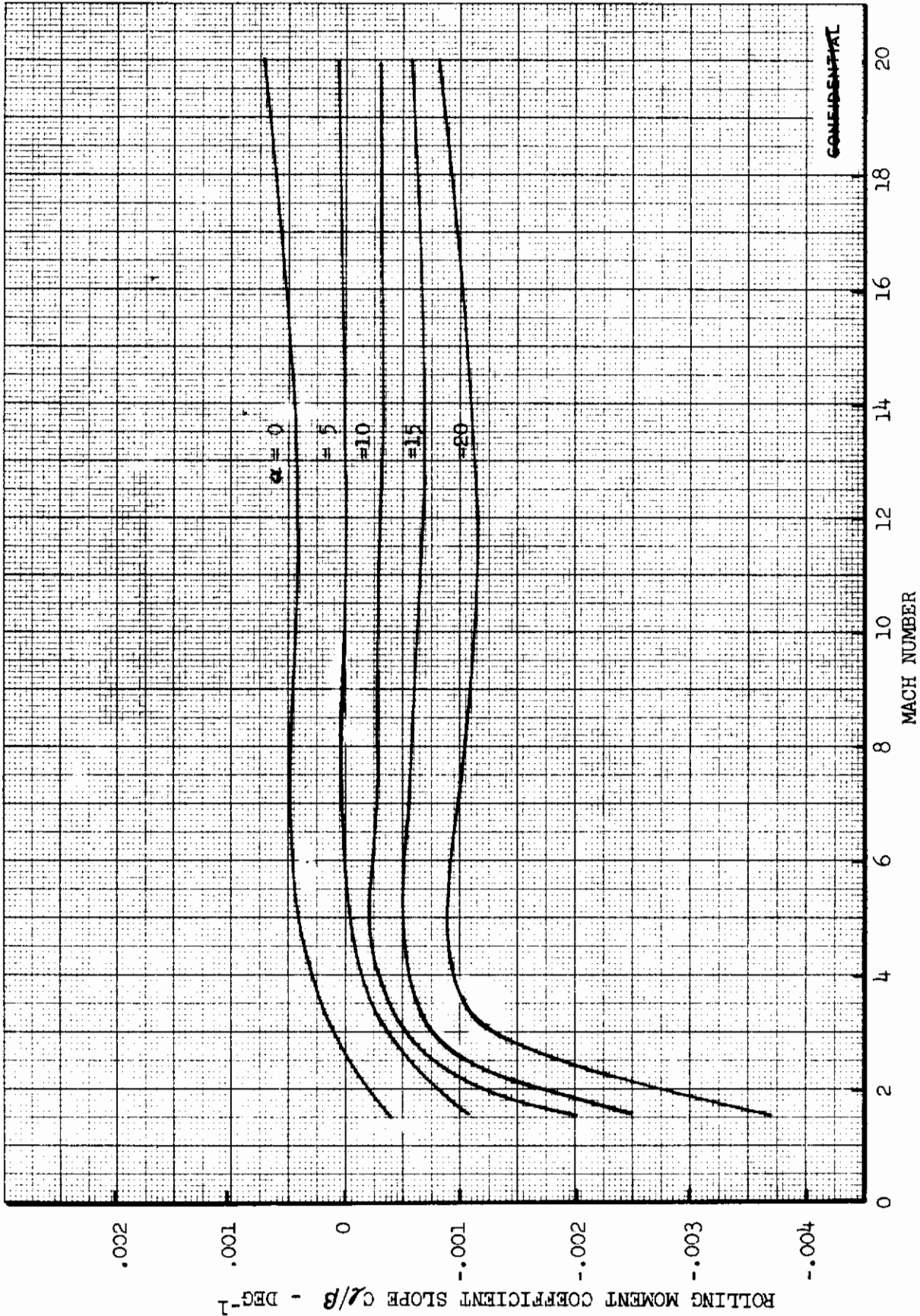


FIGURE 30 (U) FDL-5 ROLLING MOMENT COEFFICIENT SLOPE VARIATION WITH MACH NUMBER

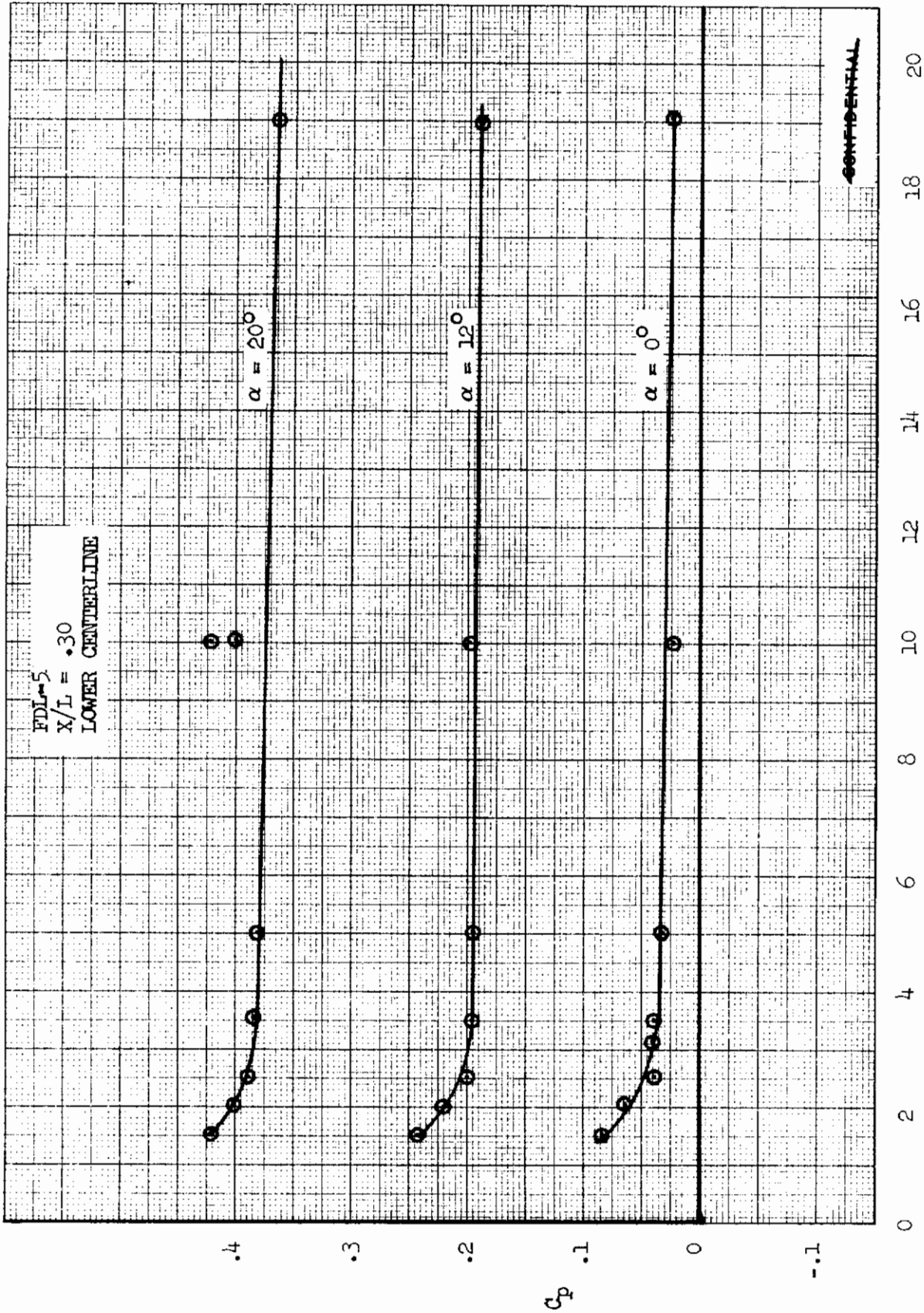


FIGURE 31 (U) VARIATION OF A LOWER SURFACE CENTERLINE PRESSURE COEFFICIENT WITH MACH NUMBER ($X/L = .30$)

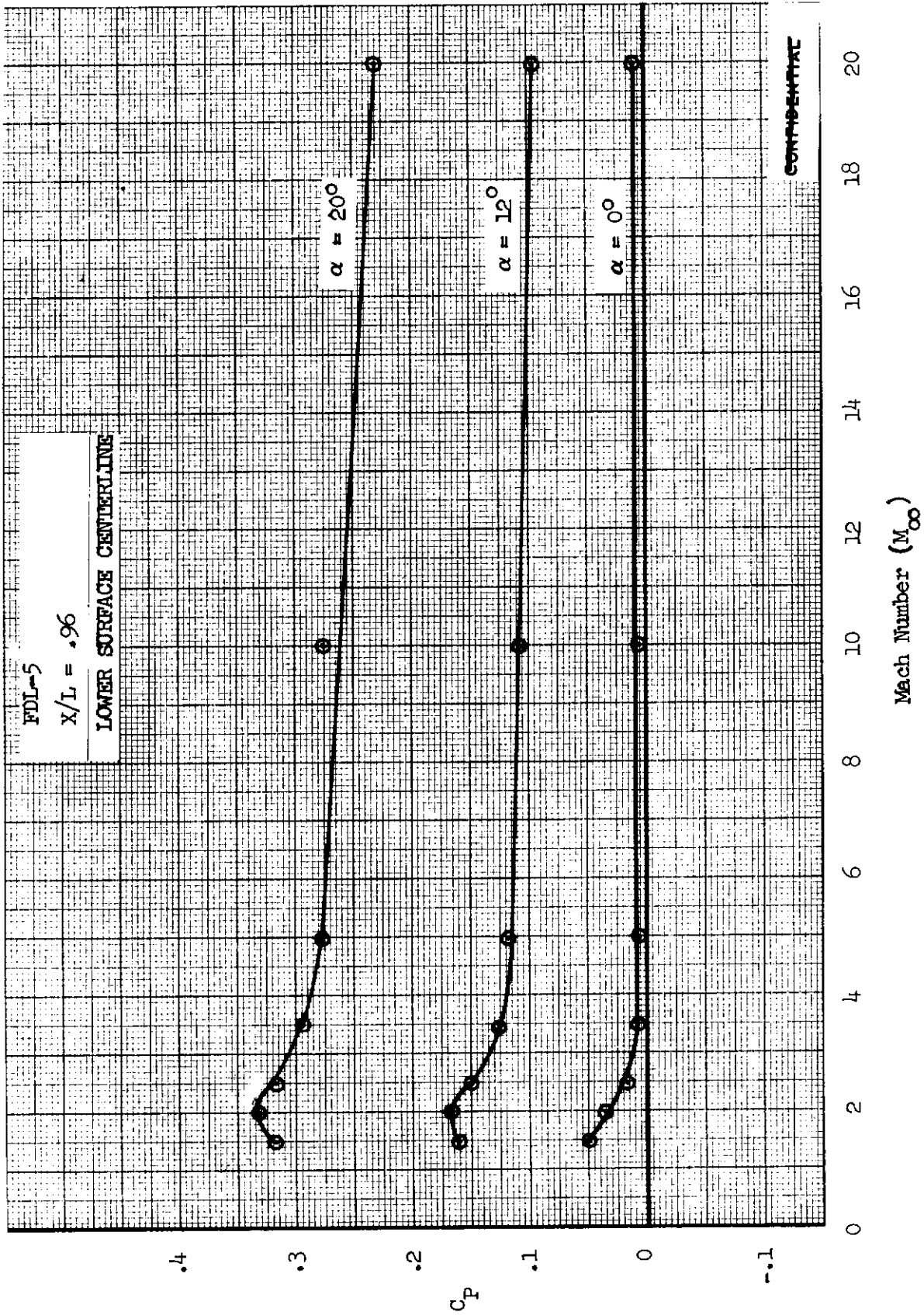


FIGURE 32 (U) VARIATION OF A LOWER SURFACE CENTERLINE PRESSURE COEFFICIENT WITH MACH NUMBER ($X/L = .96$)

SECTION 5

(U) FDL-5 HEAT TRANSFER SUMMARY

(U) Heat transfer and structure design data are based on the reference trajectory shown in Figure 33 and the reference design condition of 11 degrees angle of attack, 20,000 fps and 200,000 feet altitude. The trajectory and the reference design point are based on the work reported in Reference 1 for a typical high angle of attack history and a typical banked history. The banked low-altitude trajectory results in higher surface temperatures and is based on an angle of attack of 11 degrees and bank angle of 34 degrees. Launch injection conditions are conservatively based on accomplishing the ETR to EAFB glide with these flight attitudes.

(U) Predicted temperature histories on the FDL-5 vehicle are shown in Figure 34 for the stagnation point, leading edge and lower surface. Surface emittance is assumed to be 0.7 on all surfaces. Boundary-layer transition is accounted for in the figure and causes the step increase in temperature late in the flight. Maximum temperatures are 4400 and 2900°F at the stagnation point and leading edge, respectively.

(C) Composite peak temperatures (occurring at different times during the low reference trajectory flight) are shown in Figure 35 for the lower surface centerline. Maximum temperature is 2450°F at station 140 and is the result of turbulent heating.

(C) The effect of transition criterion on peak lower surface temperature is shown in Figure 36. The recommended criterion of $Re_{\theta}/M_e = 150$ is seen to result in highest design temperature aft of station 180. It is believed that this criterion is conservative and flight temperatures may be lower.

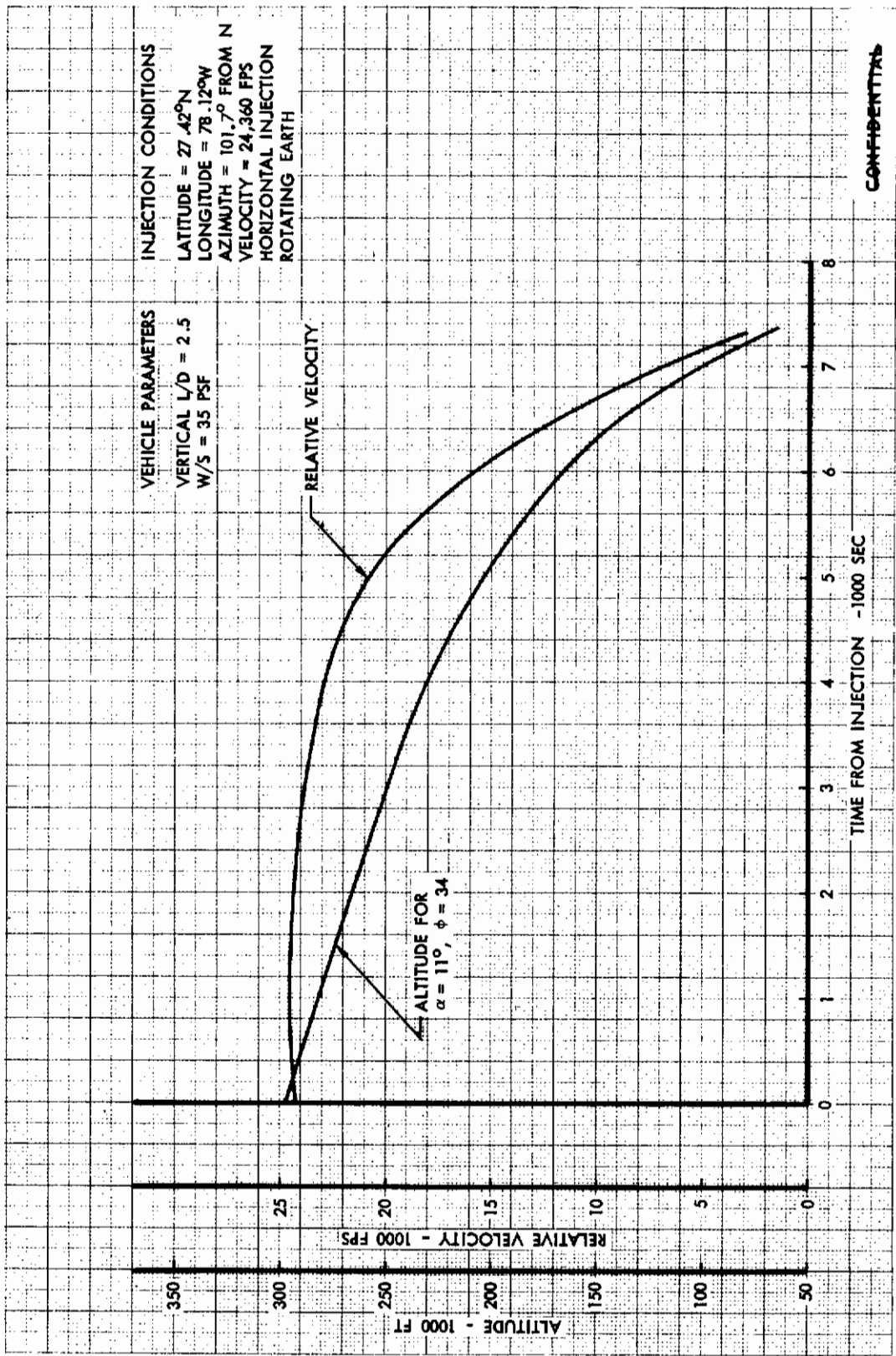
(C) The effect of wing loading on peak temperature is depicted in Figure 37. Increasing the wing loading from 30 to 40 psf would increase the maximum lower surface temperature to 2500°F based on the 34-degree, banked, low-altitude trajectory.

(C) Typical correlation of experimental and theoretical heat transfer data is shown in Figure 38. Lower surface heating is seen to correlate most satisfactorily with swept cylinder theory. Strip (flat plate) theory underpredicts the heating at high angles of attack while cone theory overpredicts the heating at low angle of attack.

(C) A typical comparison of predicted and measured temperatures at vehicle stations 210 and 403 ($X/L = 0.50$ and 0.96) is shown in Figure 39. The inside temperatures are based on predicted heating at 200,000 feet altitude.

20,000 ft/sec and 11 degrees angle of attack. The outer temperatures are based on extrapolation of measured heat transfer rates to the same conditions. Comparison of the data shows good agreement (within 200°F) between predicted and measured temperatures. Detail heat transfer and pressure correlations are contained in Part IV.

(U) Figures 40 and 41 summarize the laminar peak temperature distributions occurring at the design point of 20,000 fps, 200,000 feet altitude and angle of attack of 11 degrees. The data are based on the tunnels C and F heat transfer tests and were computed based on a surface emittance of 0.7.



~~CONFIDENTIAL~~

FIGURE 33 (U) REFERENCE TRAJECTORY

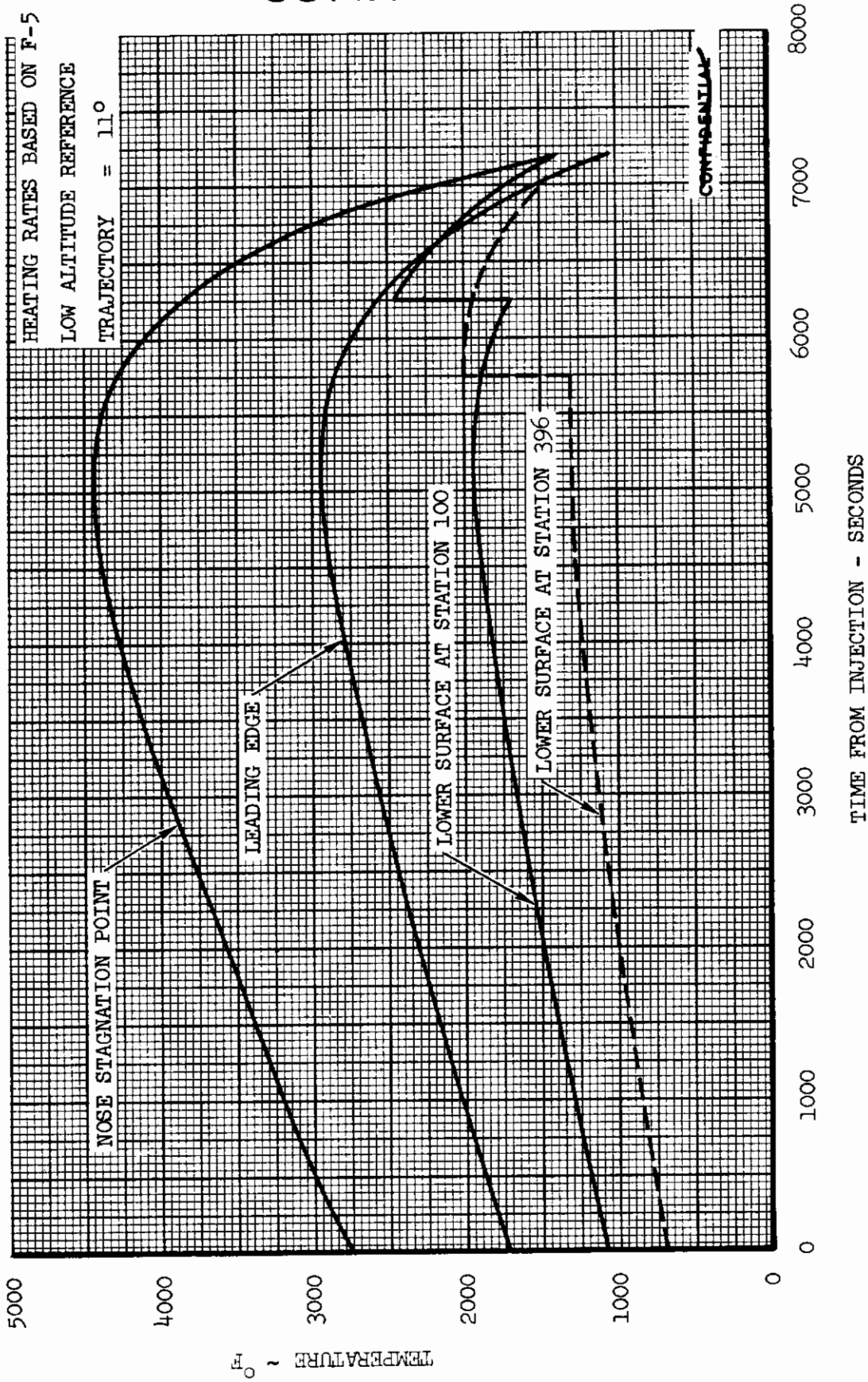


FIGURE 34 (U) TEMPERATURE HISTORIES AT VARIOUS VEHICLE LOCATIONS

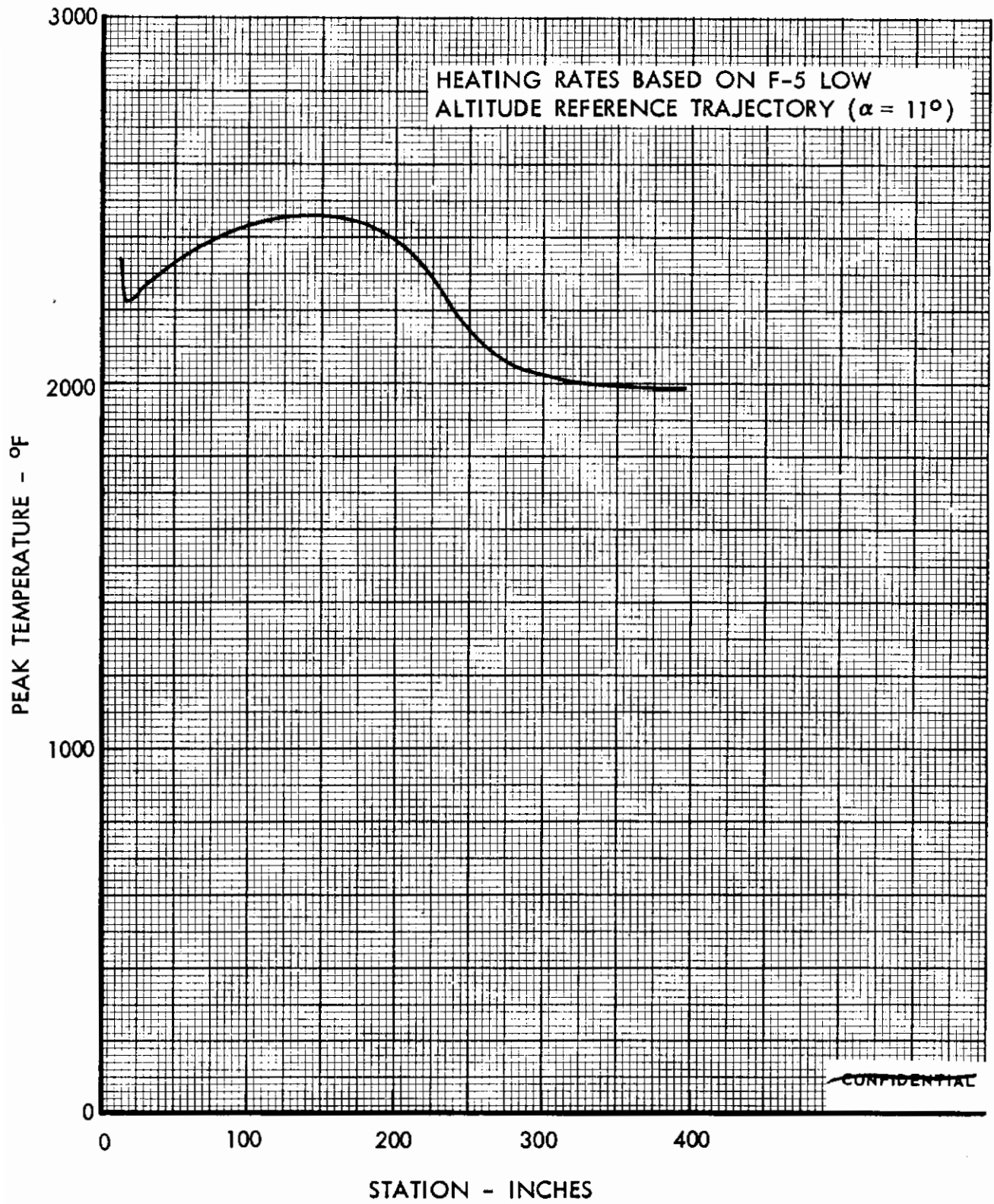


FIGURE 35 (U) PEAK LOWER SURFACE CENTERLINE TEMPERATURES

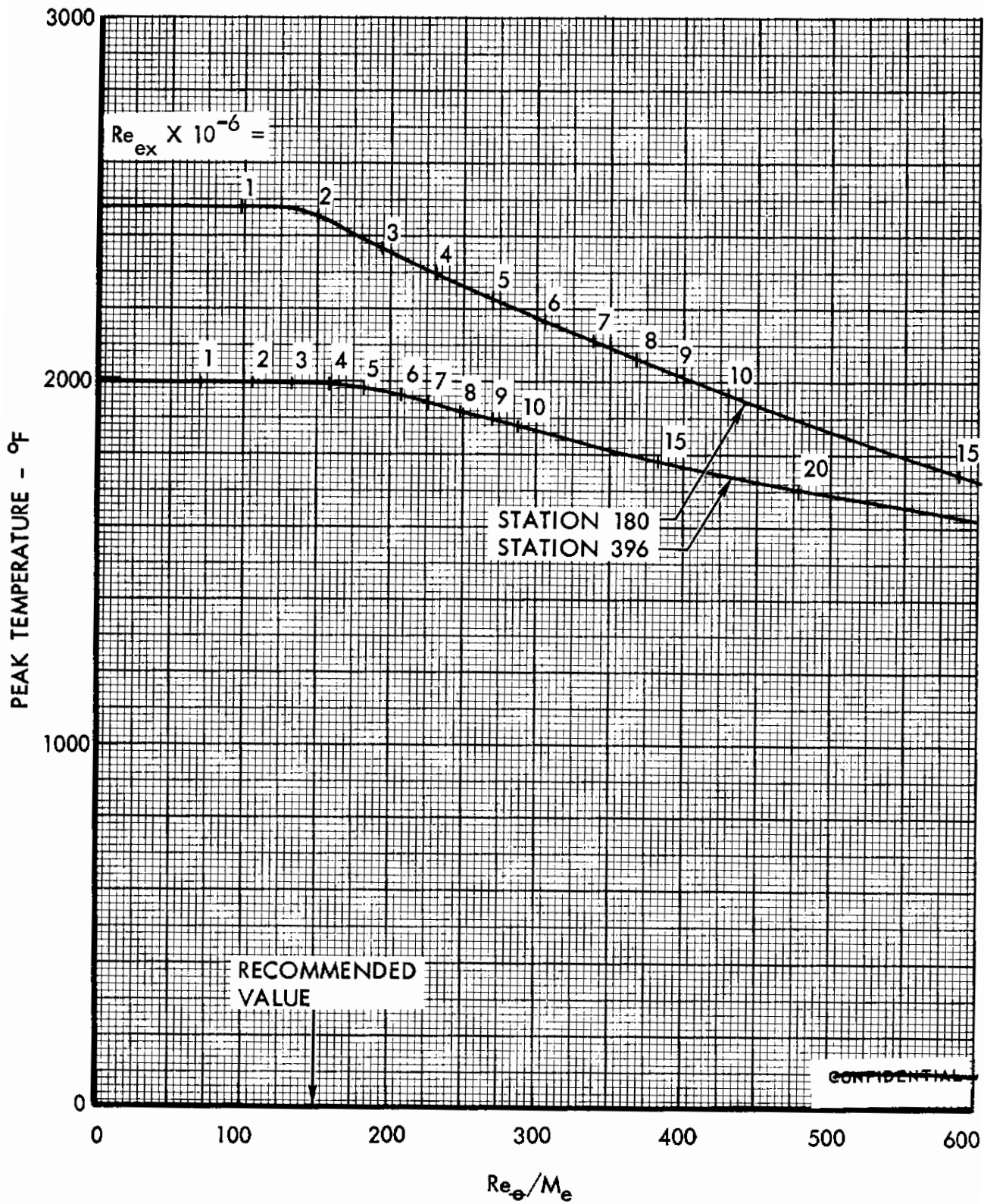


FIGURE 36 (U) EFFECT OF TRANSITION CRITERION ON PEAK LOWER SURFACE CENTERLINE TEMPERATURES

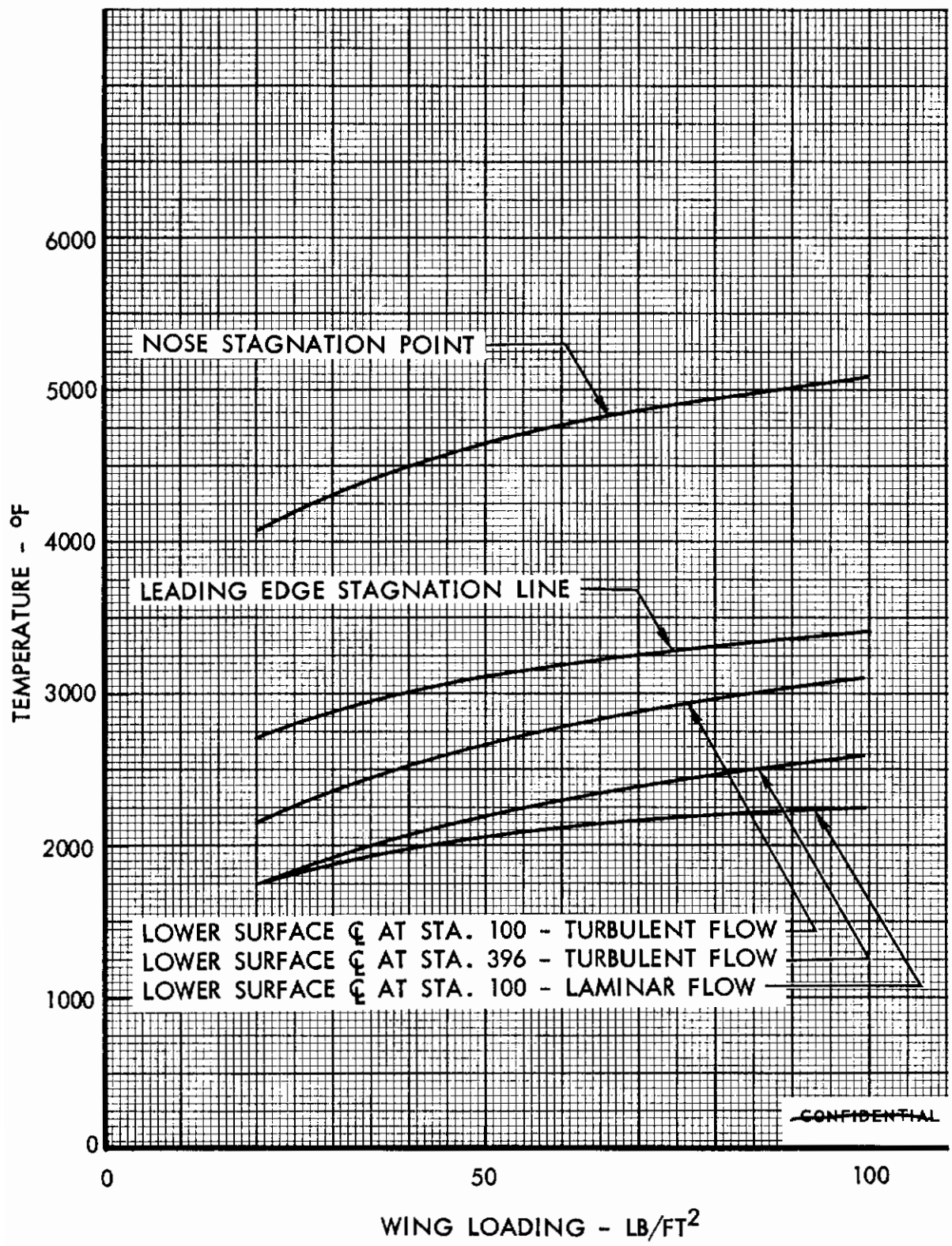


FIGURE 37 (U) EFFECT OF WING LOADING ON PEAK TEMPERATURES

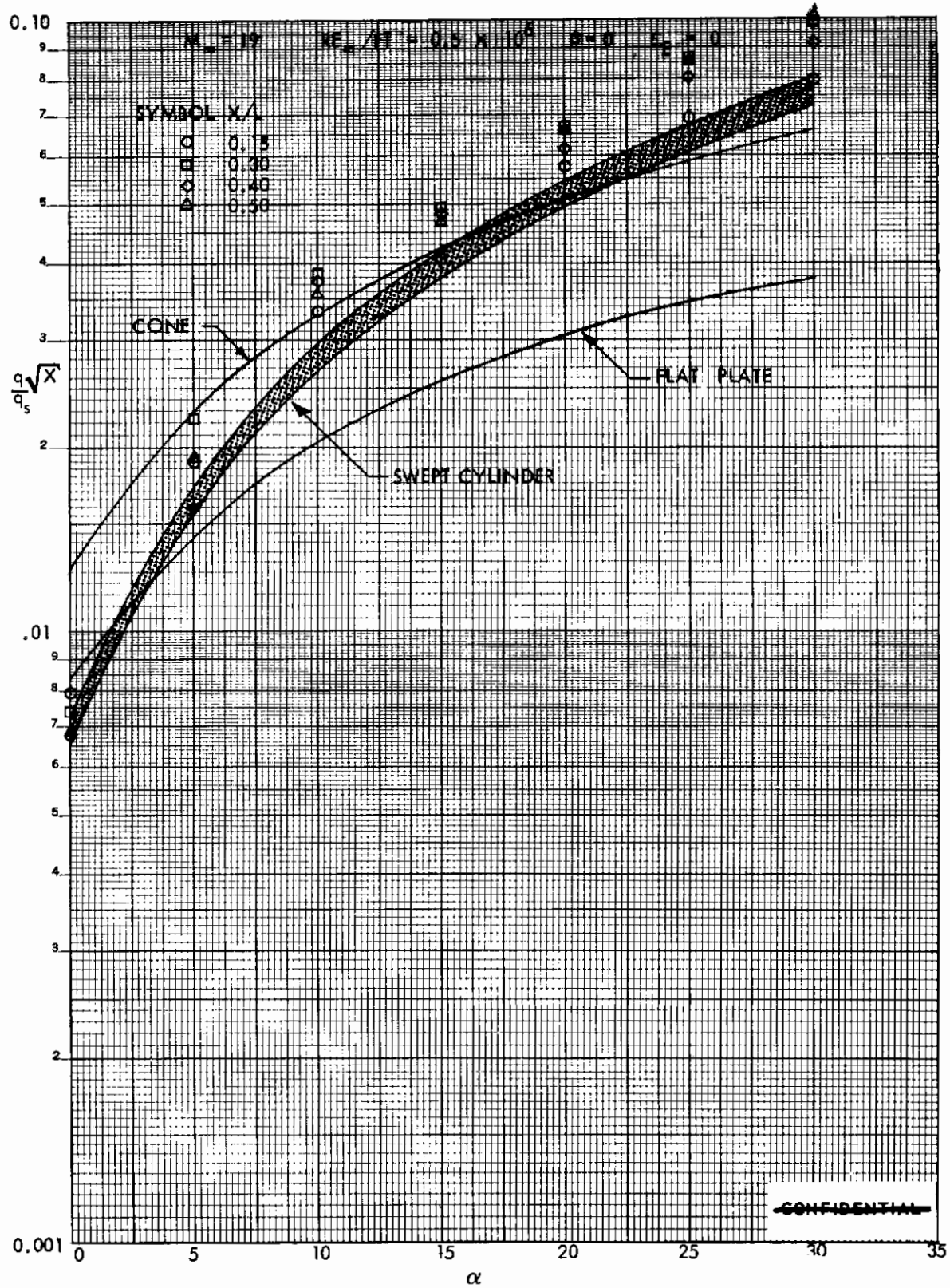
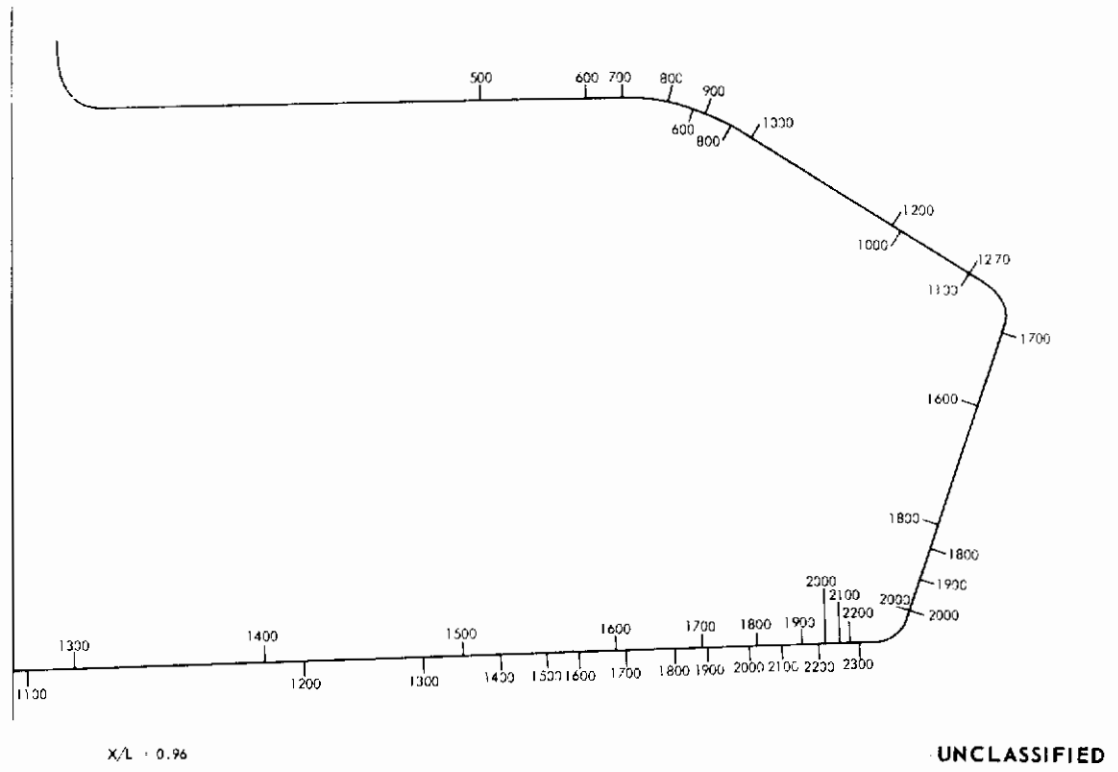
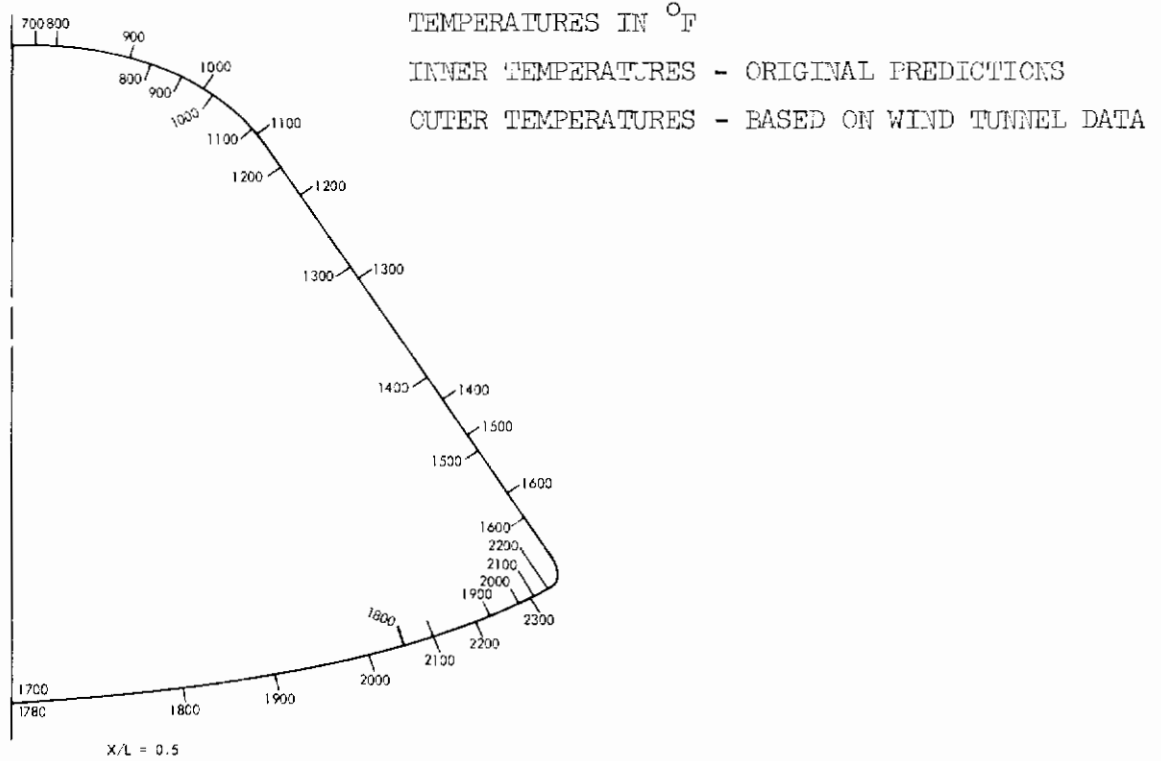


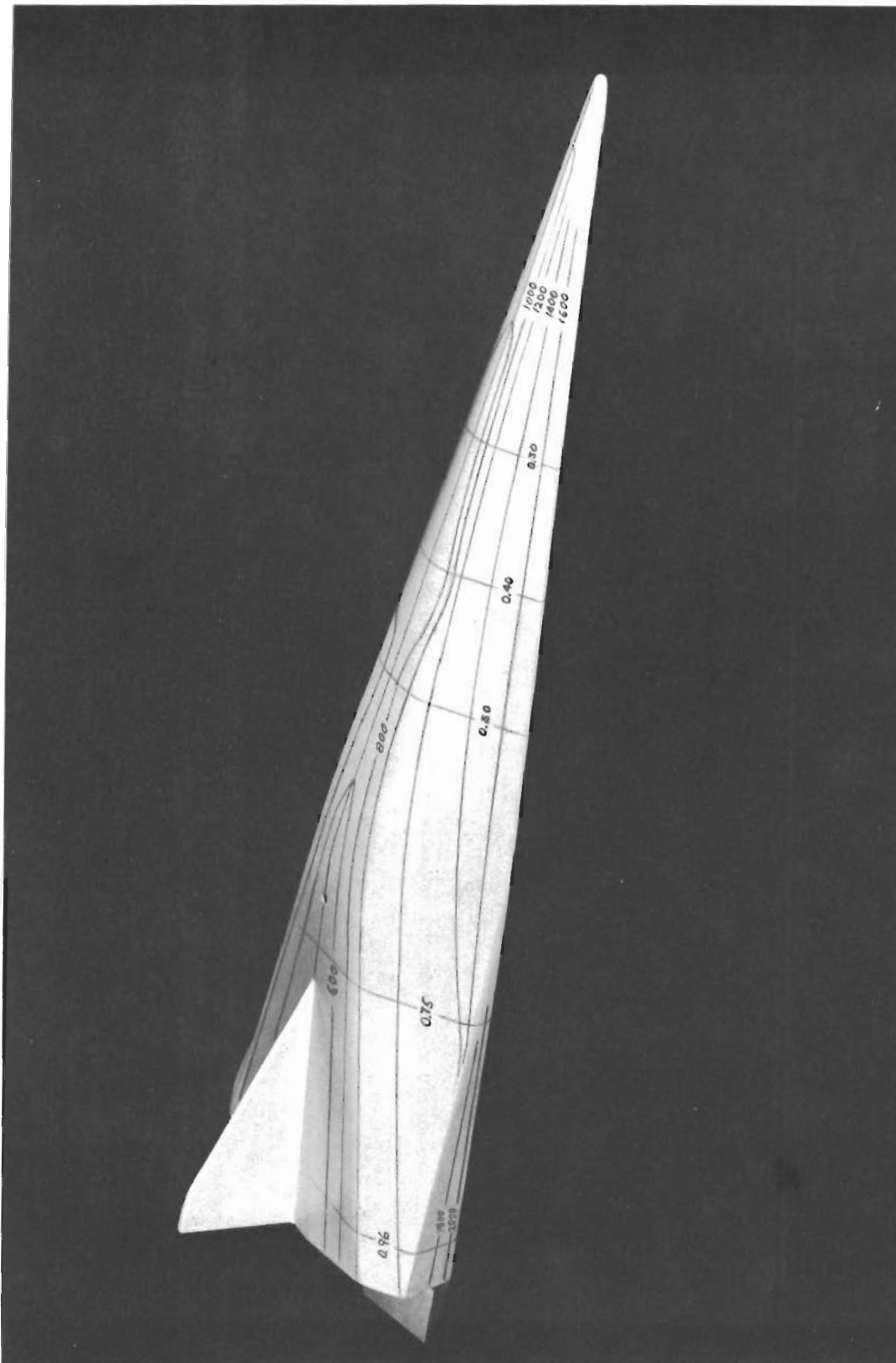
FIGURE 38 (U) CORRELATION OF TUNNEL F FORWARD RAMP CENTERLINE HEATING DATA

(THIS PAGE IS UNCLASSIFIED)



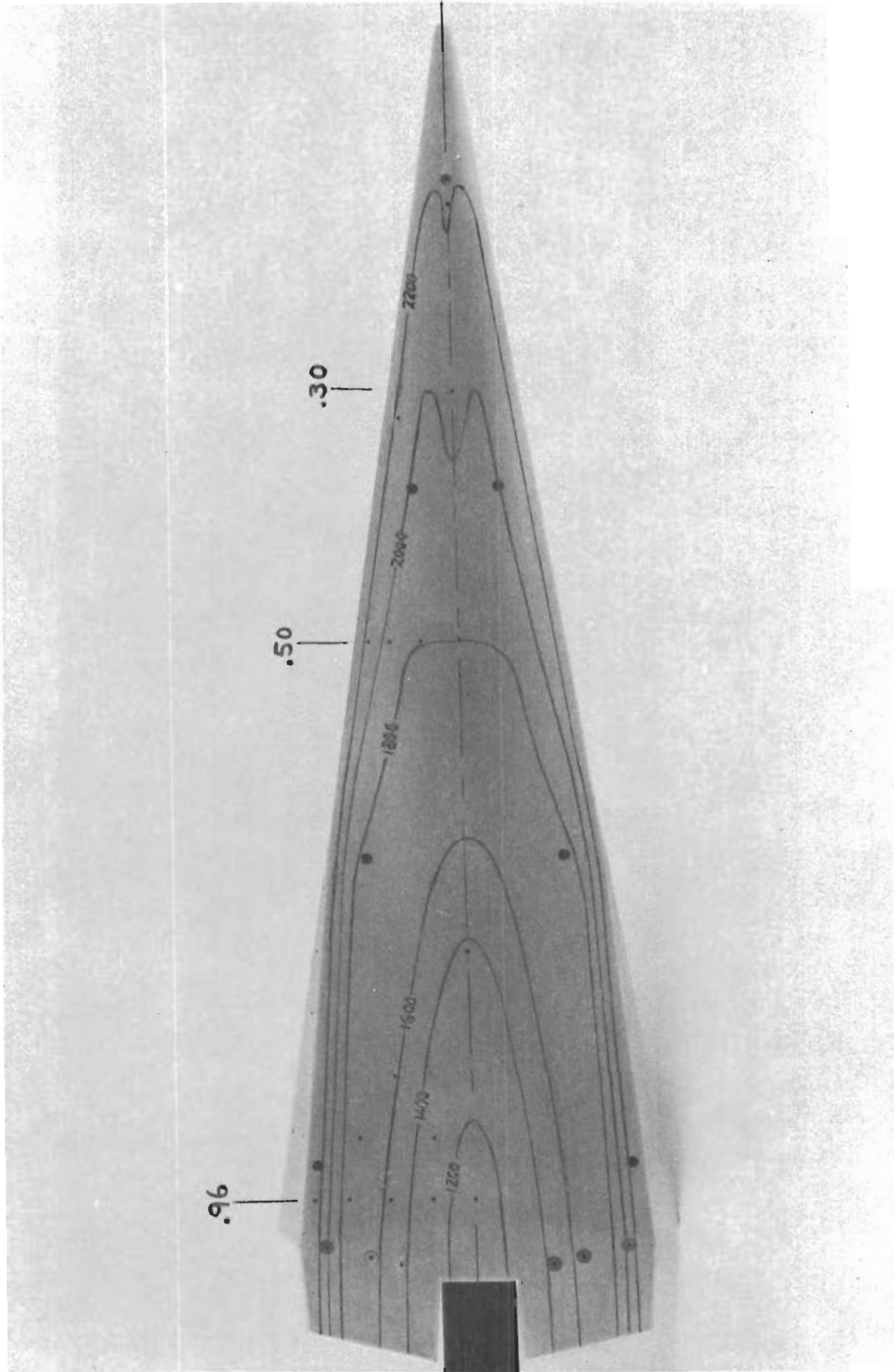
UNCLASSIFIED

FIGURE 39 (U) COMPARISON OF PREDICTED AND REVISED DESIGN POINT RADIATION EQUILIBRIUM TEMPERATURE - AT 50 AND 96 PERCENT CHORD



UNCLASSIFIED

FIGURE 40 (U) UPPER SURFACE ISOTHERMS



UNCLASSIFIED

FIGURE 41 (U) LOWER SURFACE ISOHERMS

SECTION 6

(U) FDL-5 DESIGN

(U) Structure parametric trades, systems selections and vehicle weight estimates of the unmanned free flight research vehicle were accomplished during the study. Initially, these selections were based upon the early 30-foot-long F-5 configuration derived from Reference 1.

6.1 (U) STRUCTURES

(U) A Lockheed-sponsored structure parametric analysis provides the basic data for selection and design of a candidate vehicle structure concept. The parametric analysis is based on the 30-foot F-5 configuration with the general structure arrangement shown in Figure 42.

(U) Design loads are based on estimated pressures occurring during the Titan IIIB launch (Figure 43).

(C) Payload capability of the T-II or T-III core for the ETR flight is from 8000 to 9000 pounds and is marginally adequate to launch the 35-foot FDL-5 vehicle (7,391 pounds) and adapter (approximately 800 pounds). Strength of the T-IIIB is compared to the loads induced by the 30- and 35-foot F-5 configurations in Figure 44. The data are based on a dynamic response factor of 1.33 and a factor of safety of 1.5. It can be seen that the loads for the 30-foot vehicle do not exceed the booster strength, while the loads for the 35-foot vehicle do exceed the booster strength. With a dynamic response factor of approximately 1.27, the 35-foot vehicle is compatible with the booster capability. Reduction of the dynamic response factor would require limiting the test launches to days with low wind shears.

(U) Table 8 shows the materials and design minimum gages considered during the parametric analysis. Minimum gage is based on practical manufacturing and application problems. The importance of minimum gage to the vehicle design and weight is shown in Figure 45, which compares the equivalent panel and skin thickness required to support loads with the minimum gage. Minimum gage is seen to prevail in the design requirements for the front 30 feet of the vehicle length.

(U) Figures 46 and 47 summarize the effects on weight of many variations of material, panel design, and insulated, insulated-and-cooled, and hot-structure concepts for upper and lower surfaces of the vehicle. Lowest vehicle weight is realized if no internal thermal conditioning is required, as shown by the high back-face temperature part of the curves. If the inside of the vehicle is to be maintained at room temperature, the hot-load-carrying concept with internal insulation and cooling, or the insulated-and-cooled structure

concept is required. The insulated-and-cooled structure then is somewhat lighter than the hot-load-carrying concept with internal vehicle cooling. The unit weights shown in the figures include panel, longeron, and frame weights, but do not include weight provisions for fins, control surfaces, landing gear, or structure cutouts.

(U) Figure 48 shows the structural arrangement created for the 35-foot vehicle. The drawing illustrates typical panel concepts, and the location of primary load bearing longerons and frames. Materials are identified on the drawing, as are access panels, attachment details and landing gear support structure.

(U) A complete description of the structure concept is contained in Part V.

6.2 (U) SYSTEMS

(U) Figure 49 is a candidate systems general arrangement drawing which describes the location and preliminary selection of the vehicle systems. The systems have been positioned with consideration for geometry requirements, balance, and ease of access and servicing.

(U) The landing gear is a tricycle system using dual metal nose wheels and main gear metal brush skids. Shock attenuation is accomplished with crushable honeycomb cylinder inserts.

(U) Antenna placements assure satisfactory command and telemetry contact.

(U) The guidance and navigation system consists of an inertial platform and a general-purpose digital computer. Both are available as modified off-the-shelf or easily developed hardware. The inertial navigator was selected on the basis that an autonomous continuous means of determining the vehicle state vectors is necessary. An altitude-sensing system may be required to suppress the accumulation of altitude errors during the flight. A modified off-the-shelf radar altimeter could be used for this purpose, if further analysis indicates that this is warranted.

(U) The flight control system is comprised of an autopilot, a reaction control system, an aerodynamic control system and a landing propulsion system. Signals from the guidance and navigation systems are fed to the autopilot. Output from the autopilot controls the reaction control system and the aerodynamic control system.

(U) Aerodynamic controls are driven by hydraulic actuators in a cooled hydraulic power system; and the reaction control and landing rocket systems use monopropellant hydrogen peroxide fuel. The fuel for the reaction motors and landing motors is contained in common tanks located at the vehicle center of gravity.

(U) Eight reaction control motors are required to provide complete three-axis pure moment vehicle control. Pitch and roll motors are used during low dynamic pressure flight only while yaw motors are used throughout the flight to augment aerodynamic stability and control during maneuvering flight.

(U) Four 500-pound-thrust, off-the-shelf hydrogen peroxide landing motors are provided to augment landing. The maximum equivalent L/D of the basic vehicle with all engines thrusting is approximately 6. The use of thrust from zero to 4 of the engines allows the equivalent L/D to be varied from 2 to 6. The fuel provided for landing is adequate for 20 seconds of thrust from all four engines.

(U) The data management system includes all aspects of data acquisition, transmission, and post-flight data handling and processing. The functions of the system are to obtain basic research information and provide diagnostic performance data for the vehicle and supporting systems.

(U) Sensor data are fed into the PCM multiplexer encoder and RF transmitters. The PCM serial wavetrain is fed simultaneously to the VHF transmitter, microwave transmitter, and on-board tape recorders. VHF transmission is the main data link with microwave transmission providing data during the blackout period. Compressed time transmission of recorded data is provided over both VHF and microwave link during vehicle flight over ground stations.

(U) A total of 315 sensor measurements will be made during a typical research mission. All of the data management system equipments are available off the shelf or with minimum development.

(U) Vehicle tracking is accomplished with a C band transponder and skin track. The approach and landing is accomplished using the ground control system developed for the X-20 program. This system provides for eight channels of data on X band and uses a small onboard transponder. An X band tracking antenna is provided in the nose of the vehicle for the automatic landing system.

(U) The destruct system is an autonomous and ground-controlled system designed to induce ballistic flight of the test vehicle upon actuation. The ground control is provided on the standard 400 MHz frequency, while the autonomous control is based on use of a bank angle/time allowance similar to that employed on ASSET. Ballistic flight is achieved by pyrotechnic separation of the left elevon to obtain roll to the left. Separation of part of the vehicle structure cannot be achieved without larger weight for the destruct explosive and a more complex design of the destruct system installation.

(U) The environmental control system maintains room temperature conditions in the entire vehicle for the benefit of both structure and systems. Heat is rejected with a water/ammonia boiler/heat-exchanger system pressurized to maintain initial coolant temperature at 40°F. Water-glycol circulating in a

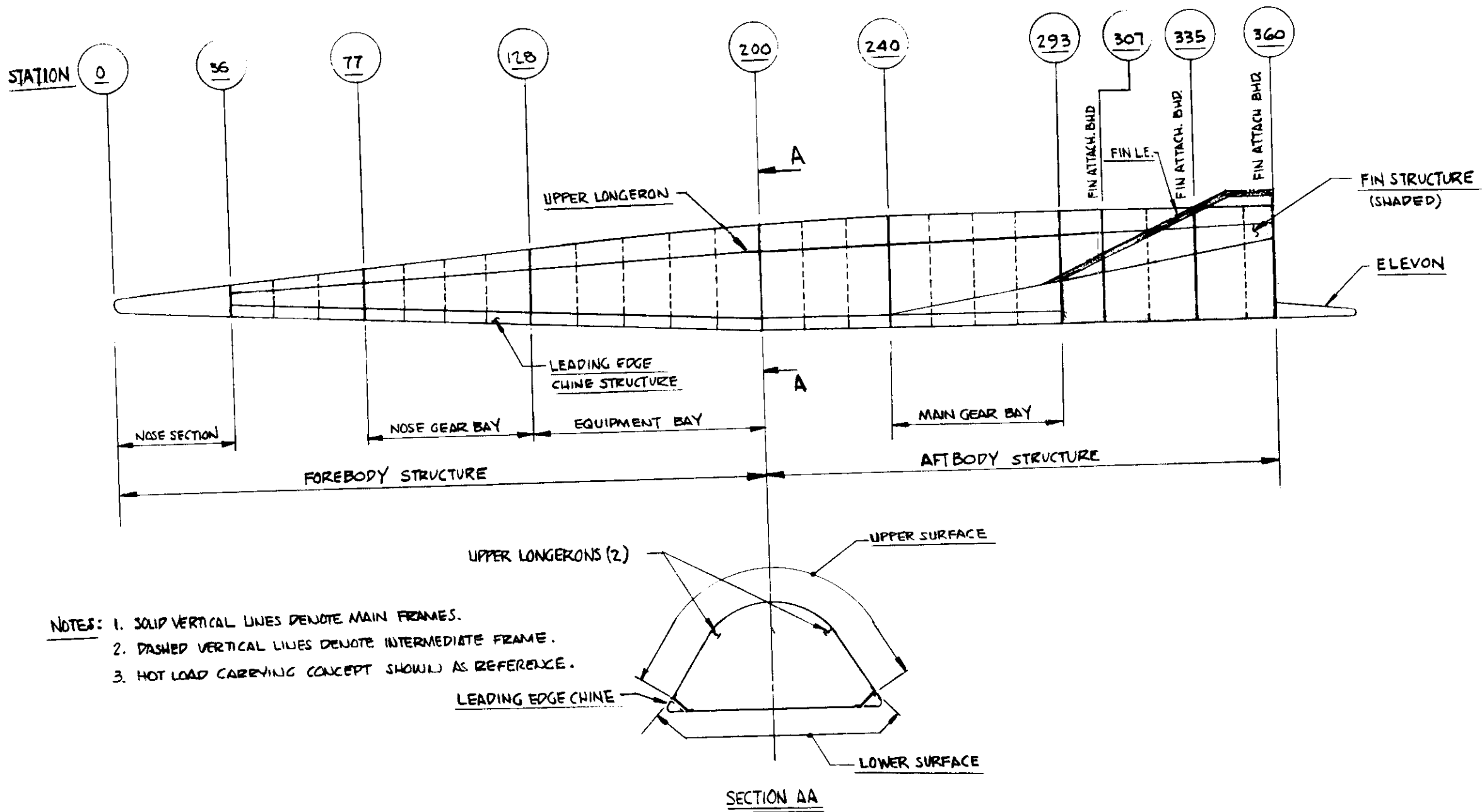
closed loop carries heat from the cooled structure and internal equipment to the water/ammonia boiler/heat-exchanger system. Water and ammonia tanks are located near the vehicle center of gravity.

(U) The electrical power system provides all onboard power from silver-zinc batteries. The system includes the batteries, inverters, regulators and distribution system. Total power capacity is 200 ampere-hours with a 250-ampere peak load.

6.3 (U) WEIGHT

(U) Vehicle and systems summary weight statements are shown in Tables 9 and 10. Total launch weight is 7666 pounds, including contingency and ballast. The structure is 59 percent, systems (including expendables) are 38 percent of the launch weight and the contingency is approximately 3 percent. Landing weight is 6790 pounds and landing wing loading is 33.5 psf. The expendable items weigh 876 pounds and include water, ammonia, and hydrogen peroxide.

(U) The largest subsystem weights are the expendable items associated with the environmental control system and reaction control system. Other equipment items weight 1829 pounds.

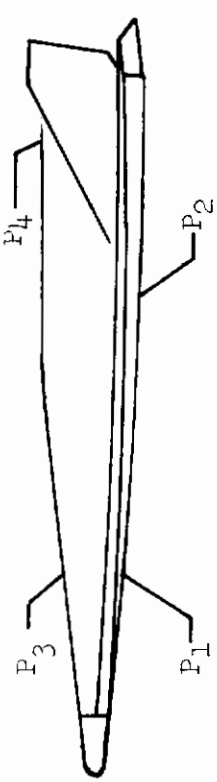


- NOTES: 1. SOLID VERTICAL LINES DENOTE MAIN FRAMES.
 2. DASHED VERTICAL LINES DENOTE INTERMEDIATE FRAME.
 3. HOT LOAD CARRYING CONCEPT SHOULD AS REFERENCE.

UNCLASSIFIED

FIGURE 42 (U) STUDY VEHICLE (F-5) STRUCTURAL ARRANGEMENT FOR DESIGN CONCEPT EVALUATION

F-5/TITAN IIIB DESIGN PRESSURES - EXIT PHASE

	LOCATION	LIMIT PRESSURE (PSI)
<div style="display: flex; justify-content: space-around; align-items: center;"> <div style="text-align: center;"> <p><u>F-5</u></p>  </div> </div>	NOSE	12.7
	LEADING EDGE	2.6
	P ₁	1.73;- 0.31
	P ₂	1.21;- 0.81
	P ₃	1.64
P ₄	0.81;- 1.21	

NOTE: + COMPRESSION;- SUCTION

UNCLASSIFIED

FIGURE 43 (U) DESIGN PRESSURES FLIGHT TEST VEHICLE

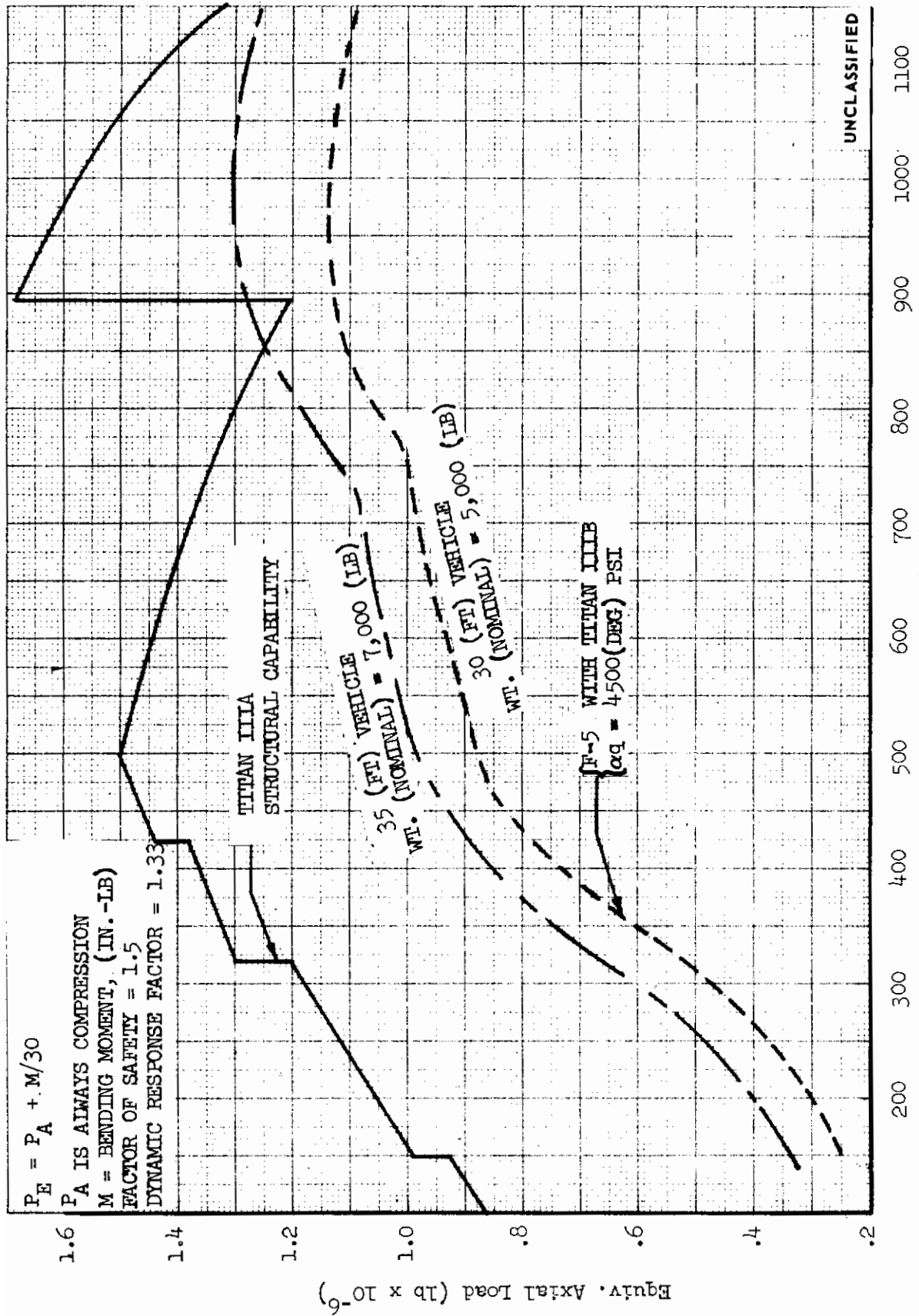


FIGURE 44 (U) COMPARISON OF MAXIMUM FLIGHT STRUCTURAL LOAD CAPABILITIES

TABLE 8
(U) MINIMUM GAGE FOR METALLIC MATERIALS (INCHES)

MATERIAL ALLOY DESIGNATION	STRUCTURAL CONFIGURATION							FRAME BULKHEAD APPLICATION
	SINGLE CORRUGATION	CORRUGATION-STIFFENED		INTEGRALLY STIFFENED	HONEYCOMB SANDWICH		CORE	
		SKIN	CORRUG.		SKIN			
Aluminum 2219T81	.016	.016	.012	.016 ⁽¹⁾	-	-	-	.020
Beryllium Be-38A1	.016	-	-	.016	-	-	-	.020
Beryllium AMS7902	.016	-	-	.016	-	-	-	.020
Titanium Ti 8Al-1Mo-1V	.016	.016	.012	.016	-	-	-	.020
Nickel base Inconel 718	.016 ⁽³⁾	.016 ⁽³⁾	.012 ⁽³⁾	(2)	.012 ⁽³⁾	.002	.002	.020
Nickel base Inconel 625	.010	.010	.010	(2)	.008	.002	.002	.012
Cobalt base Haynes 25	.010	.010	.010	(2)	.008	.002	.002	.012
Columbium Cb 752-R512B	-	.012 ⁽⁴⁾	.012 ⁽⁴⁾	.012	.010 ⁽⁵⁾	.002 ⁽⁶⁾	.002 ⁽⁶⁾	.016
Tantalum 90Ta-LOW ⁽⁷⁾	-	-	-	.012	-	-	-	.016

- NOTES (1) Minimum selected based on manufacturing consideration.
 (2) Not considered because of serious mfg. problems (warpage, distortion, extremely difficult chemically to mill).
 (3) Gages selected because of distortion due to heat treatment of thinner gages.
 (4) Poor structural resistant welds: projected application of solid state roll diffusion bonded technique.
 (5) () value indicates heat shield application.
 (6) Core material: Columbium alloy D-36 ($\rho = .286 \text{ lb/in.}^3$).
 (7) For strength requirements consider tantalum alloy T-222.

UNCLASSIFIED

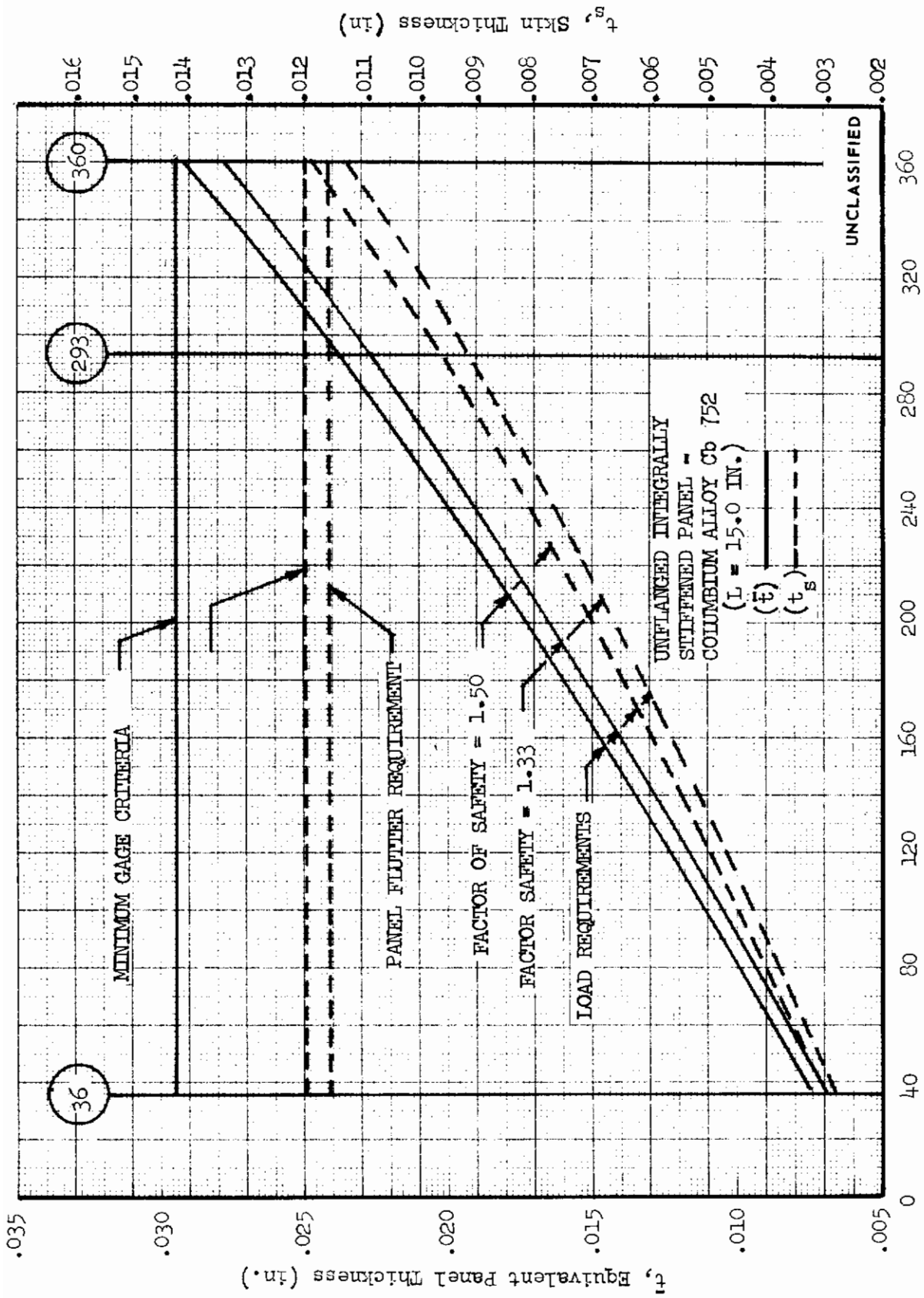


FIGURE 45 THICKNESS REQUIREMENTS FOR LOWER SURFACE PANELS (L = 15.0 INCHES)

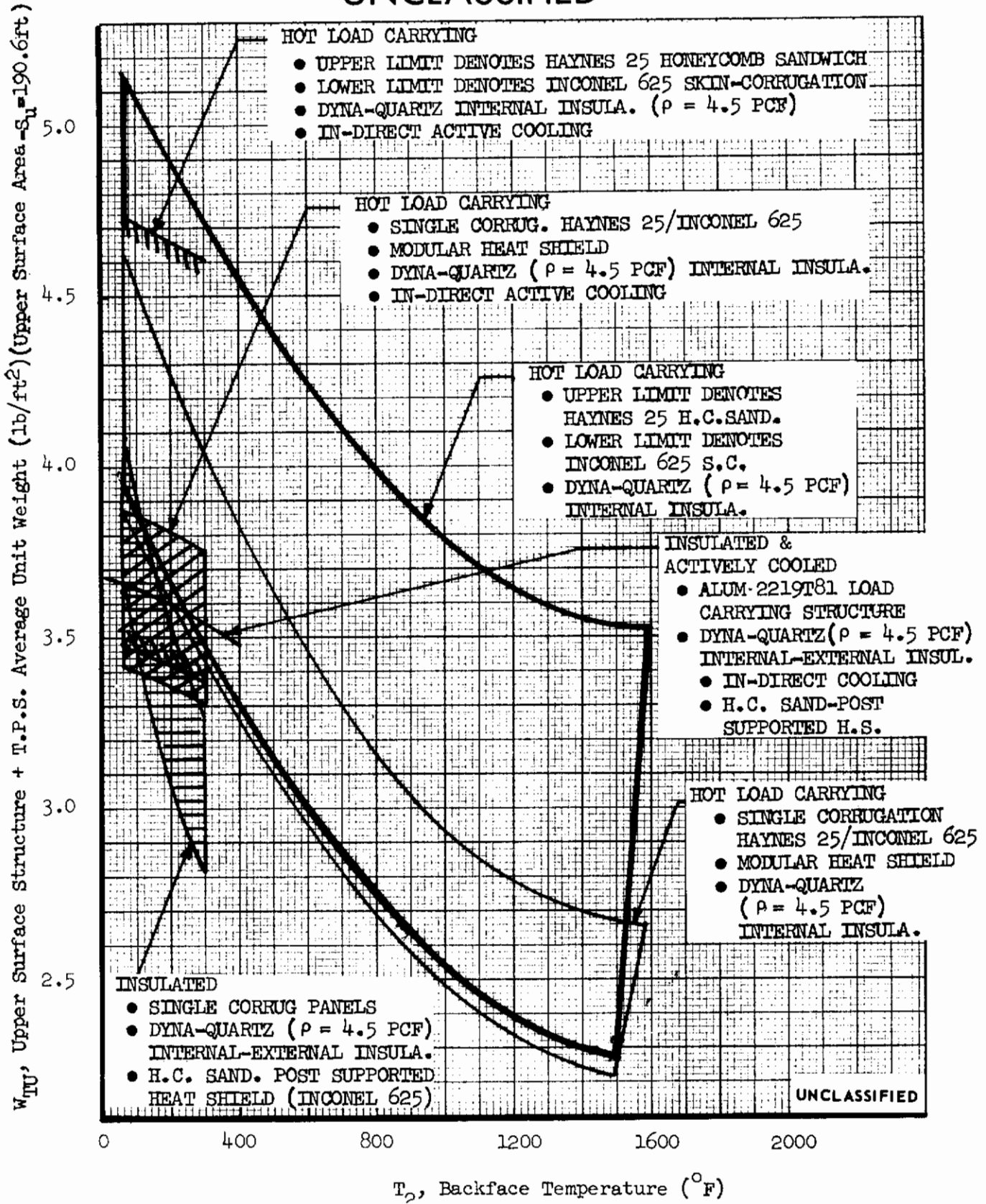


FIGURE 46 (U) UPPER SURFACE WEIGHT COMPARISON - STRUCTURE AND THERMAL PROTECTION SYSTEM FOR VARIOUS THERMO-STRUCTURAL CONCEPTS

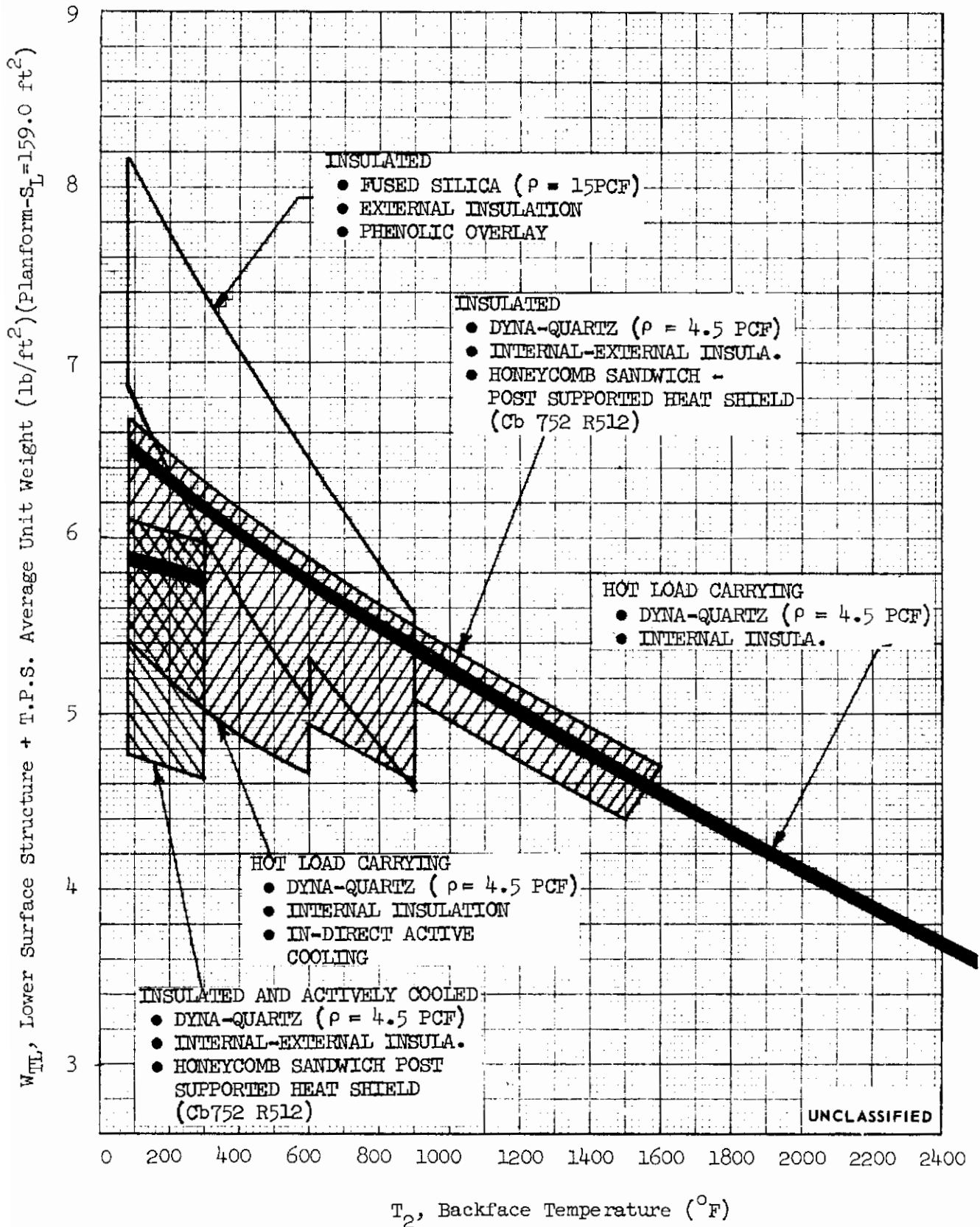


FIGURE 47 (U) LOWER SURFACE WEIGHT COMPARISON - STRUCTURE AND THERMAL PROTECTION SYSTEM FOR VARIOUS THERMO-STRUCTURAL CONCEPTS

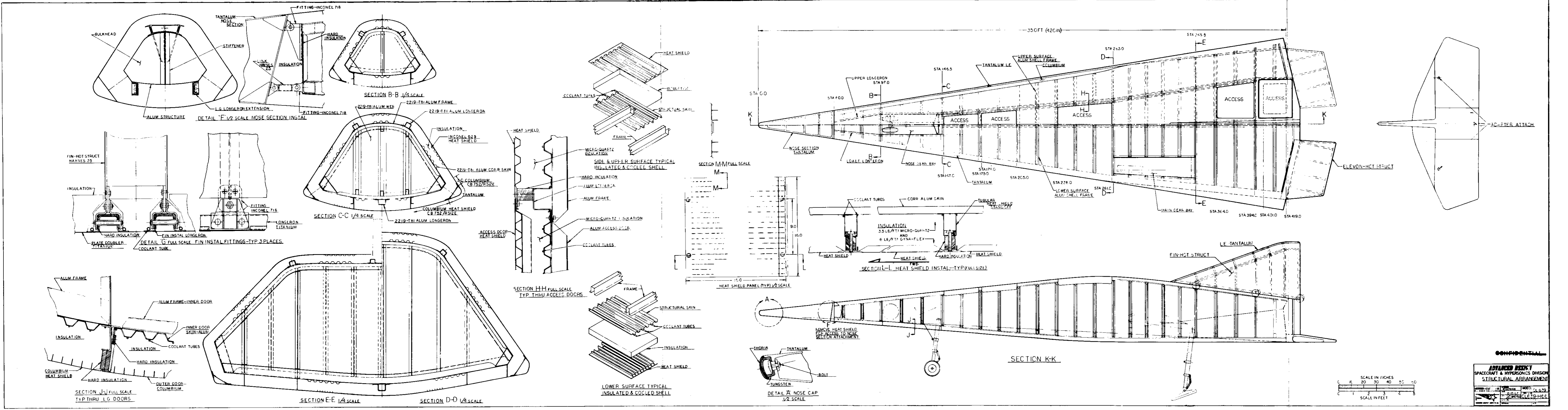
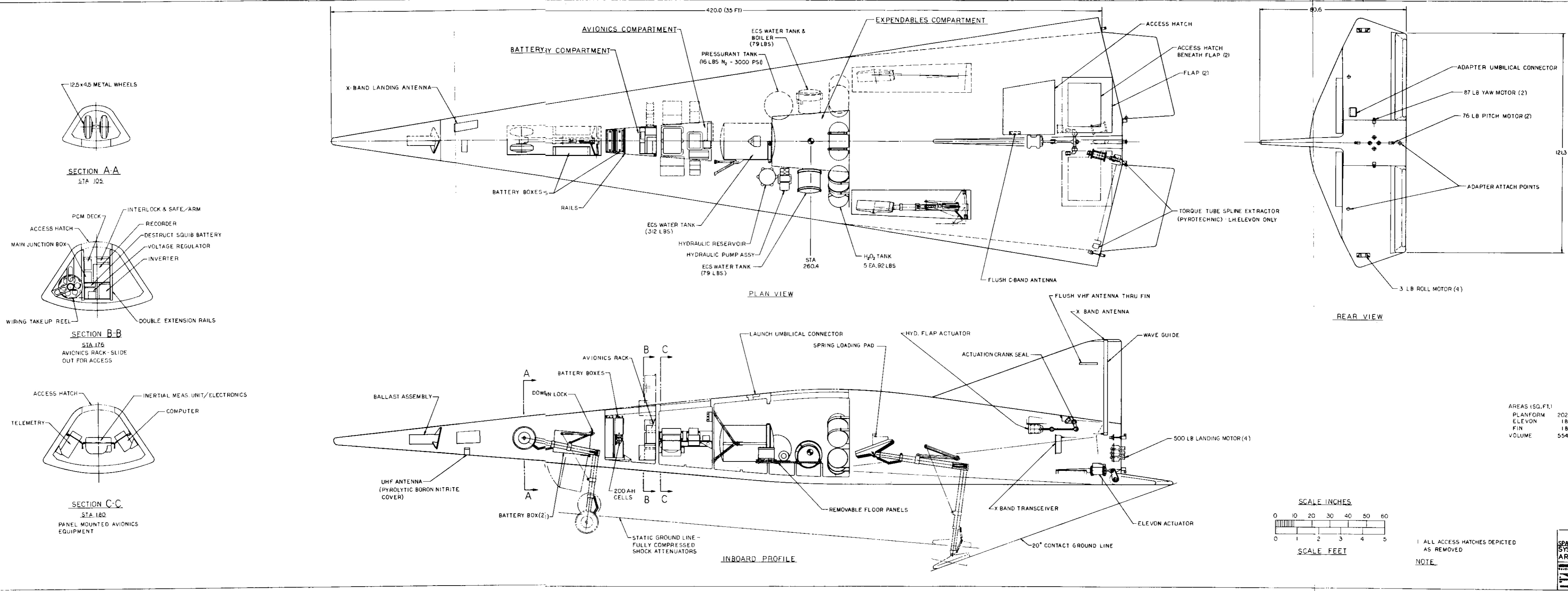
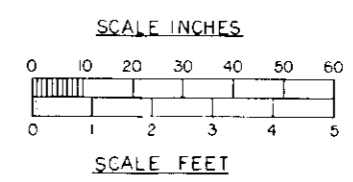


FIGURE 48 (U) MV-37 FLIGHT TEST VEHICLE STRUCTURAL ARRANGEMENT

(REVERSE SIDE IS BLANK)



AREAS (SQ. FT.)	
PLANFORM	202.7
ELEVON	18.2
FIN	18.2
VOLUME	554 CU. FT.



NOTE: ALL ACCESS HATCHES DEPICTED AS REMOVED

ADVANCED DESIGN
SPACECRAFT & HYPERSONICS DIVISION
SYSTEMS GENERAL
ARRANGEMENT

MODEL CL639
CL639-1-167

FIGURE 49 (U) BE-1 SYSTEMS GENERAL ARRANGEMENT

(REVERSE SIDE IS BLANK)

TABLE 9

(U) WEIGHT STATEMENT

STRUCTURE:	Weight (Lb)	C.G. (Sta)*
Thermal Protection	1973	258.05
Heat Shield (212 sq ft, Cb 752)	458	281
Heat Shield (343 sq ft, Inco 625)	693	287
Leading Edge (64 ft, Ta)	256	240
Nose Section (Sta 60, Ta)	160	36
Lwr Surf. Insulation (212 sq ft)	217	277
Upr Surf. Insulation (343 sq ft)	189	287
Internal Structure (2219-T81)	1018	284.90
Skins, Single Corrugation	204	285
Longerons	239	285
Frames	203	285
Nose Gear Bay and Doors	48	122
Main Gear Bay and Doors	109	316
Penalties for Access Doors (7)	40	281
Fittings - Elevons	37	419
Fittings - Body Flaps	11	394
Fittings - Vertical Fins	11	389
Gussetts and Attachments	60	285
Equipment Supports	56	235
Elevons (17.2 sq ft)	241	441.00
Elevon Seals	25	419.00
Body Flaps (11.6 sq ft)	93	412.00
Vertical Fin (34.3 sq ft)	274	397.00
Separation Ring (incl Hard Points)	65	430.00
Nose and Main Landing Gears	270	275.00
Contingency	395	294.00
EQUIPMENT: (See Table 10)	2787	247.14
BALLAST: (To 62 percent)	525	50.00
Gross Weight	7666	260.42
Less:		
Water	-418	249.00
Ammonia	- 20	226.00
Hydrogen Peroxide	-438	276.00
Minimum Landing Weight	6790	260.22
*Nose of vehicle = 0 Body reference length = 420 in.		UNCLASSIFIED

TABLE 10

(U) EQUIPMENT BREAKDOWN

	Weight (Lb)	C.G. (Sta)
GUIDANCE AND NAVIGATION SYSTEM:	69	184.00
IMU and Electronics	40	184
Computer and Rate Gyros (3)	19	184
Cabling and Connectors	10	184
FLIGHT CONTROL SYSTEM		
AERODYNAMIC CONTROL SYSTEM:	270	306.07
Hydraulic Pump, Accumulator, Reservoir	140	250
Hydraulic Actuators	70	402
Plumbing and Valves	60	325
LANDING PROPULSION SYSTEM:	50	411.80
Thrust Motors (4)	40	427
Plumbing and Valves	10	351
Propellant included in RCS	--	
AUTOPILOT SYSTEM:	50	198.00
REACTION CONTROL SYSTEM:	686	287.30
Thrust Motors	54	425
Tanks (H ₂ O ₂)	113	276
Tank (N ₂)	28	246
Hydrogen Peroxide	460	276
Nitrogen	16	246
Plumbing and Valves	15	350
DATA MANAGEMENT SYSTEM:	190	184.87
Real-Time Microwave Transmitter	14	184
Microwave Power Divider	3	184
Real Time VHF Transmitter	3	184
Delayed Time VHF Transmitter	4	184
VHF Multiplexer	2	184
PCM Deck	20	172
Subcarrier Oscillator, Sampler, and Translator	2	184
Telemetry Tape Recorder	13	172
Microwave Antenna	1	184

UNCLASSIFIED

TABLE 10

(U) EQUIPMENT BREAKDOWN (Concluded)

	Weight (Lb)	C.G. (Sta)
VHF Antenna	3	184
Instrumentation	100	184
Cabling and Connectors	25	178
TRACKING AND COMMAND SYSTEM:	86	161.20
C-Band Transponder	7	396
C-Band Diplexer	4	396
C-Band Power Divider	3	396
C-Band Antenna	1	396
Transponder - Landing	18	78
Diplexer - Landing	4	78
Power Divider - Landing	3	78
Antenna and Corner	8	78
Receiver Decoder	20	78
Antenna	1	78
Cabling, Connector, etc	17	237
ENVIRONMENTAL CONTROL SYSTEM:	748	253.86
Water	460	249
Ammonia	22	226
Ethylene - Glycol	67	285
Loop Distribution	83	285
Pump and Motor	10	226
Tanks and Supports	53	252
Heat Exchanger	53	226
ELECTRIC POWER SYSTEM:	300	147.56
Batteries	208	138
Inverter and Regulator	30	172
Umbilical and J Box	27	172
Wiring	35	155
DESTRUCT SYSTEM:	24	172.00
LANDING GEAR SYSTEM:	60	275.00
Landing Gear (included in structure)		
Controls	60	
CONTINGENCY	254	247.00
TOTAL	2787	247.14

UNCLASSIFIED

SECTION 7

(U) CONCLUSIONS

(U) A new lifting entry vehicle concept has been defined and tested through

- Parametric configuration analyses
- Parametric structural analyses
- Wind tunnel testing at $M = 1.5$ to 20
- Preliminary design

(U) The configuration has been designated FDL-5 to identify it as one of a series undergoing concurrent development by the Air Force Flight Dynamics Laboratory.

(U) The FDL-5 configuration design provides a high degree of useful volume, while maintaining high hypersonic lift-to-drag ratio. The configuration has been derived through a series of design trades involving the consideration of:

- Aerodynamic performance
- Aerodynamic stability and control
- Aerodynamic heating
- Material temperature limitations
- Usable volume
- Booster compatibility

(U) Modification of controls, base geometry and/or addition of variable geometry may be required to obtain satisfactory subsonic performance.

(U) A preliminary candidate structural concept has been defined for an unmanned hypersonic test vehicle using the FDL-5 configuration. The concept provides maximum internal volume. An insulated-and-cooled aluminum primary structure is employed, while the vehicle surface is composed mostly of radiation-cooled, coated, refractory metal and superalloy heat shields.

(U) Candidate subsystems to perform the research mission have been reviewed and a tentative selection is described.

(U) Specific conclusions related to the various technical disciplines are as follows:

7.1 (U) AERODYNAMICS

1. (C) The configuration is stable in all three axes over the Mach range from 1.5 to 20.
2. (C) Trimmed hypersonic L/D_{\max} extrapolated to reference conditions (200,000 feet altitude, 20,000 fps, 35 feet length) is 2.84 at 11 degrees angle of attack. Maximum trimmed L/D_{\max} during entry is 3.3 at Mach 12.
3. (U) Test data correlate in general with analytical predictions using tangent-cone theory on compression surfaces and Prandtl-Meyer theory on expansion surfaces at hypersonic speeds.
4. (C) Modification to the aft upper surface, base and elevon geometry will be required as a result of subsonic and transonic wind tunnel tests. Modification of these surfaces of the FDL-5 system are not expected to affect hypersonic performance.

7.2 (U) AEROTHERMODYNAMICS

1. (U) For the low-altitude reference trajectory, predicted surface temperatures are compatible with the proposed structural materials: tungsten-thoria for the nose cap, coated tantalum for leading edges, coated columbium for the lower surface, and Inconel for the upper surface. The leading-edge material must be extended approximately 4 inches beyond the leading-edge/side-panel tangency line, and portions of the forward upper surface must be fabricated from a material, such as coated columbium, which has a temperature capability exceeding that of superalloys.
2. (C) From a heating standpoint, the lower surface is the most critical. Peak centerline temperatures on this surface range from about 2000°F at station 396 to 2450°F at station 120 for the banked low altitude reference trajectory.
3. (C) For the low-altitude reference trajectory, predicted maximum temperatures on essentially the entire lower surface result from turbulent flow. For a practical range of transition Reynolds numbers, peak temperatures on the aft lower surface are not sensitive to transition criterion. Forward ramp peak temperatures, however, decrease significantly with increasing transition Reynolds number. Results of wind tunnel transition data on the FDL-5 and basic geometries indicate that heating rates based on the assumption of an instantaneous shift from laminar to turbulent flow at $Re_{\theta}/M_e = 150$ may be overly conservative.

4. (C) At the design point flight conditions, radiation equilibrium temperatures based on the AEDC heat transfer data generally agree with analytically predicted temperatures within $\pm 200^{\circ}\text{F}$ on the lower surface, and within $\pm 100^{\circ}\text{F}$ on the body side panels and aft lower compression surface.
5. (U) Increasing the vehicle wing loading from the assumed value of 35 psf results in an increase in lower surface temperature of approximately $18^{\circ}\text{F}/\text{psf}$.

7.3 (U) STRUCTURES

1. (U) The parametric structural analysis indicates that:
 - Minimum gage criteria establish structural weight requirements over most of the body shell.
 - The radiation-cooled, hot-load-carrying structural concept, without internal temperature constraint, is minimum weight.
 - The vehicle weight for a hot-load-carrying structure concept, with internal insulation and active cooling, is 2 percent more than with the use of an insulated and cooled primary load carrying aluminum alloy structure.
 - The passive insulated concept weight is competitive with that of the other concepts; however, this concept has a lower volumetric efficiency.
2. (U) Structural concept and material selections were made, and the following is recommended for the flight test vehicle:
 - Insulated and actively cooled concept, using 2219-T81 aluminum alloy for the internal primary load carrying structure (skin, frames, longerons).
 - Edge-supported heat shield panels. The lower surface uses integrally stiffened panels, made of Cb-752/R512E coated columbium alloy. The upper surface uses skin-corrugation panels, made of Inconel-625 nickel alloy. (The more commercially available and more oxidation-resistant cobalt alloy Haynes-25 may be used at a weight increase of approximately 60 lbs.)
 - Dyna-Flex ($6 \text{ lb}/\text{ft}^3$) and Micro-Quartz ($3.5 \text{ lb}/\text{ft}^3$) insulation.

7.4 (U) WEIGHT

1. (U) The estimated unmanned free flight vehicle launch weight is 7666 pounds.
2. (U) Estimated landing weight is 6790 lb, and the landing wing loading is 33.5 psf.

Confidential
~~CONFIDENTIAL~~
(THIS PAGE IS UNCLASSIFIED)

REFERENCES

1. Lockheed-California Company, Preliminary Design of Hypersonic High L/D Test Vehicles, AFFDL-TR-66-12, J. T. Lloyd et al, May 1966.

~~CONFIDENTIAL~~
(THIS PAGE IS UNCLASSIFIED)
Approved For Public Release

(REVERSE SIDE IS BLANK)

Contrails

UNCLASSIFIED

Contrails

Security Classification

DOCUMENT CONTROL DATA - R&D		
<i>(Security classification of title, body of abstract and indexing annotation must be entered when the overall report is classified)</i>		
1. ORIGINATING ACTIVITY <i>(Corporate author)</i> Lockheed Aircraft Corporation Burbank, California	2a. REPORT SECURITY CLASSIFICATION CONFIDENTIAL	2b. GROUP 4
3. REPORT TITLE PRELIMINARY DESIGN AND EXPERIMENTAL INVESTIGATION OF THE FDL-5A UNMANNED HIGH L/D SPACECRAFT Part I, Summary		
4. DESCRIPTIVE NOTES <i>(Type of report and inclusive dates)</i> Final Report (1 July 1966 through 31 March 1968)		
5. AUTHOR(S) <i>(Last name, first name, initial)</i> J. T. Lloyd		
6. REPORT DATE March 1968	7a. TOTAL NO. OF PAGES 78	7b. NO. OF REFS 1
8a. CONTRACT OR GRANT NO. Contract No. AF 33(615)-5241	9a. ORIGINATOR'S REPORT NUMBER(S) LR 21204 (PART I) IAC/619515	
b. PROJECT NO. 1366	9b. OTHER REPORT NO(S) <i>(Any other numbers that may be assigned this report)</i> AFFDL-TR-68-24-Part I	
c.		
d.		
10. AVAILABILITY/LIMITATION NOTICES This report is subject to special export controls and each transmittal to foreign governments or foreign nationals may be made only with prior approval of the Air Force Flight Dynamics Laboratory (FDMS), Wright-Patterson Air Force Base, Ohio 45433.		
11. SUPPLEMENTARY NOTES	12. SPONSORING MILITARY ACTIVITY Air Force Flight Dynamics Air Force Systems Command Wright-Patterson Air Force Base, Ohio 45433	
13. ABSTRACT (U) Conceptual design and experimental wind tunnel testing of unmanned entry research vehicles having high hypersonic lift/drag ratio and high volume are described. Analytic parametric data are presented for two lifting body classes designated HLD-35 and FDL-5. The FDL-5 is a unique configuration which is aerodynamically stabilized without outboard fins. Experimental aerodynamic and heat transfer data from the Arnold Engineering Development Center Wind Tunnels A, B, C, and F are compared with analytic data for the FDL-5. Candidate structure and subsystems are selected for performing unmanned hypersonic research with the vehicle.		

DD FORM 1473
1 JAN 64

UNCLASSIFIED

Security Classification

Approved for Public Release

Security Classification

14.	KEY WORDS	LINK A		LINK B		LINK C	
		ROLE	WT	ROLE	WT	ROLE	WT
	* Unmanned Entry Research Vehicles						
	* High Hypersonic L/D and High Volume Research Vehicles						
	* HLD-35 Configurations						
	* FDL-5 Configurations						

INSTRUCTIONS

1. ORIGINATING ACTIVITY: Enter the name and address of the contractor, subcontractor, grantee, Department of Defense activity or other organization (*corporate author*) issuing the report.

2a. REPORT SECURITY CLASSIFICATION: Enter the overall security classification of the report. Indicate whether "Restricted Data" is included. Marking is to be in accordance with appropriate security regulations.

2b. GROUP: Automatic downgrading is specified in DoD Directive 5200.10 and Armed Forces Industrial Manual. Enter the group number. Also, when applicable, show that optional markings have been used for Group 3 and Group 4 as authorized.

3. REPORT TITLE: Enter the complete report title in all capital letters. Titles in all cases should be unclassified. If a meaningful title cannot be selected without classification, show title classification in all capitals in parenthesis immediately following the title.

4. DESCRIPTIVE NOTES: If appropriate, enter the type of report, e.g., interim, progress, summary, annual, or final. Give the inclusive dates when a specific reporting period is covered.

5. AUTHOR(S): Enter the name(s) of author(s) as shown or in the report. Enter last name, first name, middle initial. If military, show rank and branch of service. The name of the principal author is an absolute minimum requirement.

6. REPORT DATE: Enter the date of the report as day, month, year, or month, year. If more than one date appears on the report, use date of publication.

7a. TOTAL NUMBER OF PAGES: The total page count should follow normal pagination procedures, i.e., enter the number of pages containing information.

7b. NUMBER OF REFERENCES: Enter the total number of references cited in the report.

8a. CONTRACT OR GRANT NUMBER: If appropriate, enter the applicable number of the contract or grant under which the report was written.

8b, 8c, & 8d. PROJECT NUMBER: Enter the appropriate military department identification, such as project number, subproject number, system numbers, task number, etc.

9a. ORIGINATOR'S REPORT NUMBER(S): Enter the official report number by which the document will be identified and controlled by the originating activity. This number must be unique to this report.

9b. OTHER REPORT NUMBER(S): If the report has been assigned any other report numbers (*either by the originator or by the sponsor*), also enter this number(s).

10. AVAILABILITY/LIMITATION NOTICES: Enter any limitations on further dissemination of the report, other than those

imposed by security classification, using standard statements such as:

- (1) "Qualified requesters may obtain copies of this report from DDC."
- (2) "Foreign announcement and dissemination of this report by DDC is not authorized."
- (3) "U. S. Government agencies may obtain copies of this report directly from DDC. Other qualified DDC users shall request through _____."
- (4) "U. S. military agencies may obtain copies of this report directly from DDC. Other qualified users shall request through _____."
- (5) "All distribution of this report is controlled. Qualified DDC users shall request through _____."

If the report has been furnished to the Office of Technical Services, Department of Commerce, for sale to the public, indicate this fact and enter the price, if known.

11. SUPPLEMENTARY NOTES: Use for additional explanatory notes.

12. SPONSORING MILITARY ACTIVITY: Enter the name of the departmental project office or laboratory sponsoring (*paying for*) the research and development. Include address.

13. ABSTRACT: Enter an abstract giving a brief and factual summary of the document indicative of the report, even though it may also appear elsewhere in the body of the technical report. If additional space is required, a continuation sheet shall be attached.

It is highly desirable that the abstract of classified reports be unclassified. Each paragraph of the abstract shall end with an indication of the military security classification of the information in the paragraph, represented as (TS), (S), (C), or (U).

There is no limitation on the length of the abstract. However, the suggested length is from 150 to 225 words.

14. KEY WORDS: Key words are technically meaningful terms or short phrases that characterize a report and may be used as index entries for cataloging the report. Key words must be selected so that no security classification is required. Identifiers, such as equipment model designation, trade name, military project code name, geographic location, may be used as key words but will be followed by an indication of technical context. The assignment of links, rules, and weights is optional.